INFORMATION TO USERS

This manuscript has been reproduced from the microfilm master. UMI films the text directly from the original or copy submitted. Thus, some thesis and dissertation copies are in typewriter face, while others may be from any type of computer printer.

The quality of this reproduction is dependent upon the quality of the copy submitted. Broken or indistinct print, colored or poor quality illustrations and photographs, print bleedthrough, substandard margins, and improper alignment can adversely affect reproduction.

In the unlikely event that the author did not send UMI a complete manuscript and there are missing pages, these will be noted. Also, if unauthorized copyright material had to be removed, a note will indicate the deletion.

Oversize materials (e.g., maps, drawings, charts) are reproduced by sectioning the original, beginning at the upper left-hand corner and continuing from left to right in equal sections with small overlaps.

ProQuest Information and Learning
300 North Zeeb Road, Ann Arbor, Mi 48106-1346 USA
800-521-0600

Mechanistic Studies of the Oxidations of Hydrocarbons by Manganese and Ruthenium Transition Metal Complexes

Jasmine R. Bryant

A dissertation submitted in partial fulfillment of the requirements for the degree of

Doctor of Philosophy

University of Washington

2002

Program Authorized to Offer Degree: Department of Chemistry

UMI Number: 3072066

UMI Microform 3072066

ProQuest Information and Learning Company
300 North Zeeb Road
P.O. Box 1346
Ann Arbor, MI 48106-1346

In presenting this dissertation in partial fulfillment of the requirements for the Doctoral degree at the University of Washington, I agree that the Library shall make its copies freely available for inspection. I further agree that extensive copying of the dissertation is allowable only for scholarly purposes, consistent with "fair use" as prescribed in the U.S. Copyright Law. Requests for copying or reproduction of this dissertation may be referred to ProQuest Information and Learning, 300 North Zeeb Road, Ann Arbor, MI 48106-1346, to whom the author has granted "the right to reproduce and sell (a) copies of the manuscript in microform and/or (b) printed copies of the manuscript made from microform."

Signature Jasmin Byfo

Date 12/9/2002

University of Washington
Graduate School

This is to certify that I have examined this copy of a doctoral dissertation by

Jasmine R. Bryant

and have found that it is complete and satisfactory in all respects,
and that any and all revisions required by the final
examining committee have been made.

Chair of Supervisory Committee:

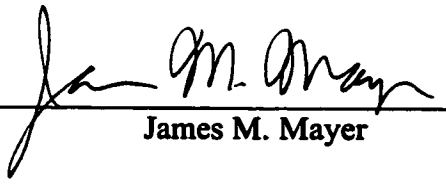

James M. Mayer

Reading Committee:

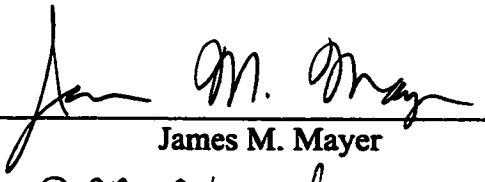

James M. Mayer

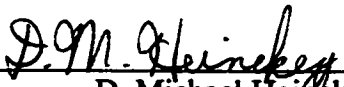

D. Michael Heinekey

Daniel Gamelin

Date: 12/9/2002

University of Washington

Abstract

Mechanistic Studies of the Oxidations of Hydrocarbons by Manganese and Ruthenium Transition Metal Complexes

Jasmine R. Bryant

Chair of the Supervisory Committee:
Professor James M. Mayer
Department of Chemistry

The oxidation of hydrocarbon C-H and O-H bonds can occur by a variety of mechanisms. These include stepwise processes such as initial electron or proton transfer, or concerted mechanisms such as hydride transfer or hydrogen-atom abstraction. Hydrocarbons containing weak C-H and O-H bonds are oxidized by $Mn(hfacac)_3$ (hfacac = hexafluoroacetylacetonate) and $[(bpy)_2(py)Ru{=}O]^{2+}$ (bpy = bipyridine and py = pyridine). $Mn(hfacac)_3$ is an easily prepared and reactive oxidant, forming stable solutions in benzene and methylene chloride. Based on an equilibrium established with tris(2,4-dibromophenyl)amine, a redox potential of 0.9 ± 0.1 V vs. $Cp_2Fe^{+/o}$ is calculated. $Mn(hfacac)_3$ oxidizes 9,10-dihydroanthracene (DHA) cleanly to anthracene with a bimolecular rate constant of 6.8×10^{-4} M^{-1} s^{-1}. $Mn(hfacac)_3$ is also capable of oxidizing xanthene, 1,4-cyclohexadiene, 2,4-di-tert-butylphenol, toluene, and *p*-methoxytoluene. Product analyses and relative rates indicate that the more electron-rich substrates react by initial electron transfer to manganese. For the less electron-rich substrates, such as 1,4-cyclohexadiene, a mechanism of hydrogen atom abstraction is suggested.

The oxidations of DHA, xanthene, and fluorene by $[(bpy)_2(py)Ru^{IV}O]^{2+}$ give mixtures of products including oxygenated and non-oxygenated compounds. The

products include those formed by organic radical dimerization, such as 9,9'-bixanthene, as well as by oxygen-atom transfer. The kinetics of these reactions and those of indene, cyclohexene, cumene, ethylbenzene, and toluene have been measured and display a clear correlation with substrate C-H bond dissociation energy. The kinetic isotope effect for the reaction of $\mathbf{Ru{=}O^{2+}}$ with DHA vs. DHA-d_4 gives $k_H/k_D \geq 35$. A mechanism of initial hydrogen-atom abstraction followed by competitive pathways of radical dimerization and trapping by the oxidant is indicated. The hydrogen-atom self-exchange rate for the transfer of $H^\bullet$ between $[(bpy)_2(py)Ru^{III}OH]^{2+}$ and $[(bpy)_2(py)Ru^{IV}O]^{2+}$ has also been measured ($k'_{HSE} = (7.6 \pm 0.4) \times 10^4\ M^{-1}\ s^{-1}$). When combined with an estimate for the DHA/HA$^\bullet$ self-exchange rate in the Marcus cross relation, this value agrees well with the observed hydrogen-atom abstraction rate. The deuterium-atom self-exchange rate is also reported for the $D^\bullet$ exchange between $[(bpy)_2(py)Ru^{III}OD]^{2+}$ and $[(bpy)_2(py)Ru^{IV}O]^{2+}$. The kinetic isotope effect for this self-exchange reaction is surprisingly near unity.

TABLE OF CONTENTS

LIST OF FIGURES

LIST OF TABLES

Acknowledgments

I would like to thank Jim Mayer for his support and guidance over the past several years. His enthusiasm and patience are much appreciated. I also want to thank the members of the Mayer lab, especially Janelle Taves, Jake Soper, Brian Bales, and Ian Rhile, for helping to pull together the many loose ends of these various projects. Other members (past and present) of the Department of Chemistry have contributed to this work, including Martin Sadilek and Jim Roe for assistance with mass spectra, Scott Lovell and Werner Kaminsky for X-ray crystallography, Bob Morley for glassblowing prowess, and members of my thesis committee and the inorganic division for guidance. My family and friends deserve my gratitude for their unyielding support. Above all, Chris Bryant has offered an unlimited amount of love, sympathy, support and constructive criticism. His patience and steadfastness have helped me to reach this goal.

Chapter 1: Oxidations of Hydrocarbons by Manganese(III) tris(hexafluoroacetylacetonate)[1]

Abstract

$Mn(hfacac)_3$ is an easily prepared and reactive oxidant (hfacac = hexafluoroacetylacetonate). It forms stable solutions in benzene and methylene chloride but is rapidly reduced in acetonitrile, DMSO, acetone, and ethers. It is reduced by ferrocene to give the Mn^{II} complex $[Cp_2Fe][Mn(hfacac)_3]$, which has been structurally characterized. $Mn(hfacac)_3$ also rapidly oxidizes 1-acetylferrocene, 1,1'-diacteylferrocene, and tris(4-bromophenyl)amine. Based on an equilibrium established with tris(2,4-dibromophenyl)amine, a redox potential of 0.9 ± 0.1 V vs. $Cp_2Fe^{+/o}$ is calculated. $Mn(hfacac)_3$ oxidizes 9,10-dihydroanthracene (DHA) cleanly to anthracene, with a bimolecular rate constant of 6.8×10^{-4} M^{-1} s^{-1} at 25 °C in benzene solution. In the presence of small amounts of water, the manganese(II) product is isolated as *cis*-$Mn(hfacac)_2(H_2O)_2$, which has also been structurally characterized. $Mn(hfacac)_3$ also oxidizes xanthene to 9,9'-bixanthene, 1,4-cyclohexadiene to benzene, and 2,4-di-*tert*-butylphenol to the phenol dimer. Toluene and substituted toluenes are oxidized to their respective tolylphenylmethanes. Product analyses and relative rates – for instance that *p*-methoxytoluene reacts much faster than toluene – indicate that the more electron rich substrates react by initial electron transfer to manganese. For the less electron rich substrates, such as 1,4-cyclohexadiene, a mechanism of initial hydrogen atom transfer to $Mn(hfacac)_3$ is suggested. The ability of $Mn(hfacac)_3$ to abstract $H^{\bullet}$ is reasonable

given its high redox potential and the basicity of $[Mn(hfacac)_3]^-$. In CH_2Cl_2 solution, oxidation of DHA is catalyzed by chloride ion.

Introduction

Oxidations of organic compounds by manganese(III) complexes have long been of interest because Mn^{III} is used as a stoichiometric oxidant in lab-scale syntheses and as a catalyst in industrial processes.[2-4] For instance, Mn^{III} is a component of the catalyst for *p*-xylene oxidation to terephthalic acid in the Amoco-Mid Century Process.[3] Further interest derives from reports that a low molecular weight manganese(III) complex is responsible for the biological degradation of lignin in woody material.[5] The heme-iron enzyme manganese peroxidase catalyzes the oxidation of Mn^{II} to Mn^{III}, which is stabilized by organic acid chelates such as oxalate, lactate, and malonate.[6] The resulting freely diffusible low molecular weight manganese complex can oxidize alkyl aromatic and phenolic substrates with weak C-H and O-H bonds, including lignin model compounds.[7]

Previous work on Mn^{III} oxidants has focused on manganese acetate, manganese pyrophosphates, manganese sulfate, manganese fluoride, and manganese acetylacetonate ($Mn(acac)_3$).[2,8] Understanding these oxidations has been complicated by the difficulty in determining the speciation of the manganese, especially the ligand environment of the reactive material. For example, manganese(III) acetate in acetic acid has been used to oxidize alcohols, phenols, aromatic ethers, and especially hydrocarbons (as in the Mid Century process), but the manganese speciation under

these conditions is complex.[3c,4]

Presented here are chemical properties and oxidation reactions of manganese(III) hexafluoroacetylacetonate, $Mn(hfacac)_3$.[9] This complex is readily prepared from Mn_2O_3 and H-hfacac. It is soluble and reactive as a well-defined molecular species in low-polarity solvents. Previous studies of Mn^{III} oxidations have indicated mechanisms of initial electron transfer or formation of dissociated ligand radicals.[10] This study indicates that $Mn(hfacac)_3$ reacts either by electron transfer or by hydrogen atom abstraction. These are reasonable pathways because $Mn(hfacac)_3$ is a strong outer-sphere oxidant (being reduced to Mn^{II}) and the reduced form $[Mn(hfacac)_3]^-$ can be protonated at a $hfacac^-$ ligand. We have previously shown that a variety of compounds which contain an oxidizing metal center and a basic ligand site can abstract hydrogen atoms from organic substrates.[8,11]

Results

Synthesis, Characterization, and Properties of $Mn(hfacac)_3$. Preparation of $Mn(hfacac)_3$ from Mn_2O_3 and six equivalents of hexafluoroacetylacetone[9,12] requires water-free solvent in order to avoid the addition of water to the fluorinated pentanedione.[13] $Mn(hfacac)_3$ is quite volatile and is readily purified by sublimation. While its X-ray structure has been reported,[12] there is little published spectroscopic data for this complex. Mass spectrometry gives the correct *m/z* and the fragmentation pattern matches those described in the literature for similar complexes.[14] ^1H NMR and

^{19}F NMR spectra in CD_2Cl_2 consist of single broad peaks at δ 10.7 ppm (^1H) and -47 ppm (^{19}F). The UV-vis spectrum contains a well-defined d→d transition at 550 nm (ε = 200 M^{-1} cm^{-1}). $Mn(hfacac)_3$ is soluble and stable in hydrocarbon and chlorinated solvents, but decomposes rapidly in acetonitrile, DMSO, THF, acetone, and ethers. Decomposition is indicated by a rapid color change from green-brown to light yellow. Since the Mn^{II} compounds in this system are yellow, decomposition is most likely a result of reduction of $Mn(hfacac)_3$ by the solvent. As a result, all oxidation reactions have been carried out in methylene chloride, hydrocarbon solvents, or in neat substrate. $Mn(hfacac)_3$ reacts with acetylacetone to give a mixture of products, including free H-hfacac (by NMR).

Ferrocene rapidly reduces $Mn(hfacac)_3$, forming the blue ferrocenium salt $[Cp_2Fe][Mn^{II}(hfacac)_3]$. ^1H NMR and UV-vis spectra of the product show the presence of Cp_2Fe^+. Electrospray ionization mass spectrometry in the negative ion mode reveals a parent ion for $[Mn^{II}(hfacac)_3]^-$ (*m/z* 676), and in the positive mode shows the characteristic pattern for Cp_2Fe^+(centered at *m/z* 186). $Mn(hfacac)_3$ is also reduced by $^nPr_4NI$, giving $[^nPr_4N][Mn^{II}(hfacac)_3]$ and iodine. The X-ray structure of $[Cp_2Fe][Mn^{II}(hfacac)_3]$ (Figure 1.1, Tables 1.1 and 1.2) shows a regular octahedral manganese complex, in contrast to the Jahn-Teller distorted d^4 $Mn(hfacac)_3$. The Mn^{II}-O bond lengths in the d^5 anion (2.158 ± 0.019 Å) are comparable to the longer distances in the distorted manganese(III) compound (2 at 2.144 ± 0.003 and 4 at 1.922 ± 0.016 Å).[12]

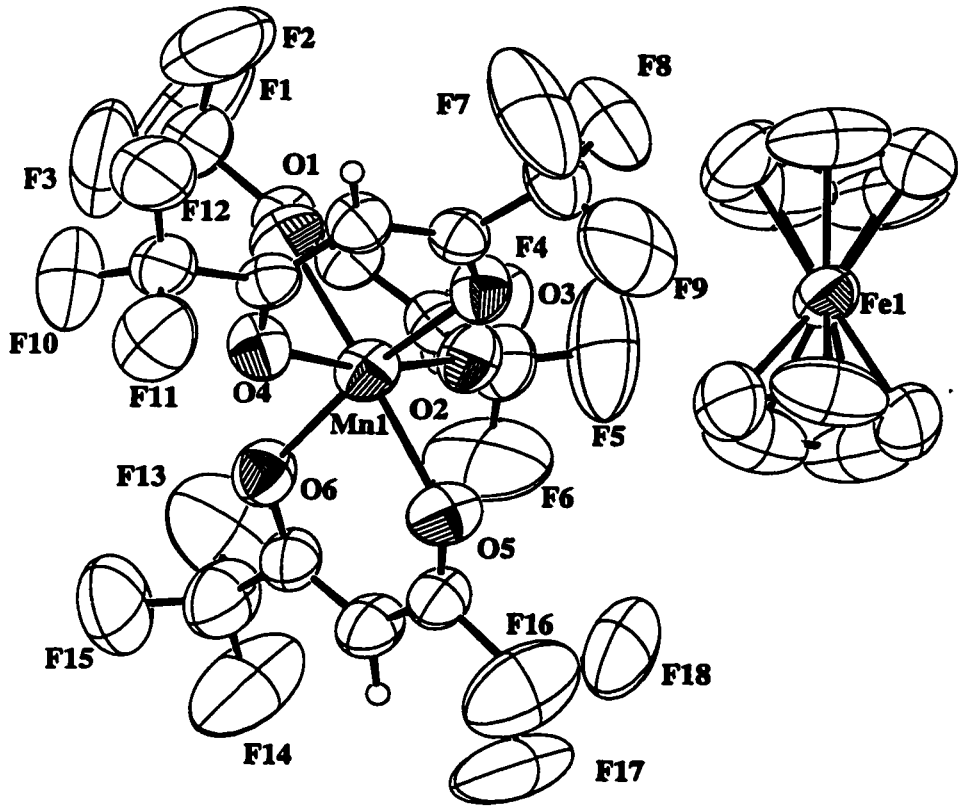

Figure 1.1. ORTEP drawing of $[Cp_2Fe][Mn(hfacac)_3]$.

Table 1.1. Crystallographic data for *cis*-$Mn(hfacac)_2(H_2O)_2$ and $[Cp_2Fe][Mn^{II}(hfacac)_3]$.

Empirical Formula	$C_{10}H_6F_{12}MnO_6$	$C_{25}H_{13}F_{18}FeMnO_6$
Formula Weight	505.09	862.14
Crystal System	Monoclinic	Monoclinic
Space Group	*C2/c* (No. 15)	$P2_1/n$ (No. 14)
Unit Cell Dimensions	$a = 21.760$ (3)	$a = 8.5403$ (3)
(Å, deg.)	$b = 8.2466$ (13)	$b = 20.3938$ (9)
	$c = 9.8746$ (7)	$c = 18.3572$ (7)
	$\beta = 96.346$ (8)	$\beta = 100.187$ (2)
Volume ($Å^3$)	1761.1 (4)	3146.9 (2)
Z	4	4
Density (calc, Mg/m^3)	1.905	1.820
Absorption Coefficient (mm^{-1})	0.898	1.008
λ (Å)	0.71070	0.71070
Crystal Size (mm)	0.21 × 0.08 × 0.04	0.35 × 0.28 × 0.20
Temperature (K)	296 (2)	296 (2)
θ Range (deg.)	2.64 – 29.35	2.25 – 30.51
Index Ranges	$-26 \le h \le 26$	$-11 \le h \le 11$
	$-10 \le k \le 10$	$-26 \le k \le 28$
	$-10 \le l \le 10$	$-25 \le l \le 25$
Reflections/ Unique	18762 / 1880	58116 / 8084
R_{int}	0.0661	0.0480
R1, wR2	0.0439, 0.1107	0.0742, 0.2599
Goodness of Fit on F^2	0.933	0.954

Table 1.2. Selected bond lengths (Å) and angles (deg) for $Mn(hfacac)_3$, $[FeCp_2][Mn(hfacac)_3]$, and $Mn(hfacac)_2(H_2O)_2$.

	$Mn(hfacac)_3$[a]	$[Mn(hfacac)_3][FeCp_2]$	$Mn(hfacac)_2(H_2O)_2$
Mn-O(1)	1.9121(25)	2.169(4)	2.162(2)
Mn-O(2)	2.1410(25)	2.168(4)	2.1400(18)
Mn-O(3)	1.9063(24)	2.144(4)	2.162(2)
Mn-O(4)	2.1469(25)	2.139(4)	2.1401(18)
Mn-O(5)	1.9372(25)	2.157(4)	2.167(2)[b]
Mn-O(6)	1.9327(24)	2.170(4)	2.167(2)[b]
O(1)-Mn-O(2)	82.23(14)	87.71(10)	82.61(7)
O(2)-Mn-O(4)	167.11(15)	177.62(10)	171.39(11)
O(3)-Mn-O(6)	171.28(15)	179.03(11)	170.06(8)[b]
O(4)-Mn-O(3)	82.89(13)	88.39(10)	82.61(7)
O(5)-Mn-O(1)	169.96(14)	178.58(10)	170.06(8)[b]
O(6)-Mn-O(5)	82.35(15)	90.26(10)	83.78(11)[b]

[a] Ref. 12. [b] O(5) and O(6) in this structure are part of water molecules, not hfacac ligands.

A redox potential has not been reported for $Mn(hfacac)_3$, but its free energy of electron attachment in the gas phase has been estimated to be -109 kcal mol^{-1} at 350 K.[15] Our attempts at electrochemical measurements have been frustrated by reactions with solvent (MeCN, DMSO) or apparently with supporting electrolyte ($^nBu_4NPF_6$ in CH_2Cl_2). The potential has therefore been estimated using reactions with ferrocene derivatives and bromoarylamines. In CH_2Cl_2, $Mn(hfacac)_3$ oxidizes ferrocene, 1-acetylferrocene (+0.27 V), 1,1'-diacetylferrocene (+0.49 V), and tris(4-

bromophenyl)amine (+0.7 V). The quoted potentials are for methylene chloride, vs. $Cp_2Fe^{+/o}$.[16] $Mn(hfacac)_3$ does not fully oxidize tris(2,4-dibromophenyl)amine, but an equilibrium is established, with $K_{eq} \cong 3 \times 10^{-5}$ by UV-vis spectroscopy. The potential for tris(2,4-dibromophenyl)amine in CH_2Cl_2 is measured at +1.2 V vs. $Cp_2Fe^{+/o}$, close to the reported value of +1.14 V vs. $Cp_2Fe^{+/o}$ in acetonitrile.[16b] Combining this potential with the observed K_{eq} gives the $Mn(hfacac)_3$ potential as 0.9 ± 0.1 V vs. $Cp_2Fe^{+/o}$ in CH_2Cl_2.

The basicity of the manganese(II) anion, $[^nPr_4N][Mn(hfacac)_3]$, has been probed in a similar manner by reaction with standard acids. No reaction is observed with lutidinium perchlorate, which has a pK_a of 14.0 in acetonitrile, but protonation is observed with *p*-toluene-sulfonic acid (pK_a of 8.01 in MeCN)[17] to give H–hfacac.

Oxidations of Organic Compounds. $Mn(hfacac)_3$ reacts with 9,10-dihydroanthracene (DHA) in benzene solution to produce anthracene in 98% yield in a matter of hours at room temperature (eq 1.1). Following the reaction by ^1H NMR spectroscopy shows the disappearance of both DHA and $Mn(hfacac)_3$, and shows the appearance of anthracene and free hexafluoroacetylacetone (H-hfacac, the protonated ligand). ^{19}F NMR spectroscopy confirms the conversion of bound $hfacac^-$ (-47 ppm) to unbound H-hfacac (-75 ppm). The H-hfacac peak has ca. 28% of the integrated intensity of the starting $Mn(hfacac)_3$. Considering the 3:1 hfacac stoichiometry in eq 1.1, the integration corresponds to an 85% yield of H-hfacac. The inorganic product of the reaction has no apparent NMR signal. UV-vis spectroscopy similarly shows the

conversion of brown-green $Mn(hfacac)_3$ to yellow manganese(II) complex(es), and the characteristic anthracene bands are readily apparent. Although no spectroscopic method allows observation of all the products, the data indicate that the bulk of the reaction follows the balanced equation written in eq 1.1.

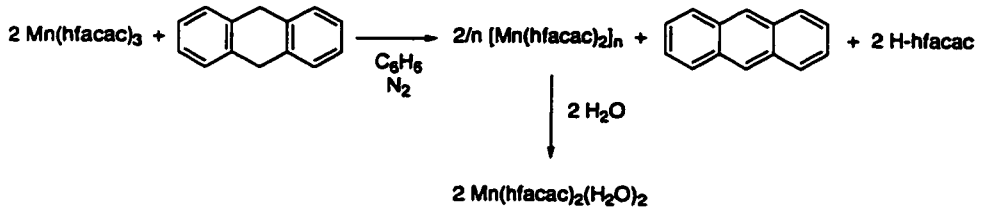

(1.1)

Aerobic reactions of $Mn(hfacac)_3$ and DHA in undried solvents give anthraquinone and anthrone (presumably by an autoxidation pathway) and precipitate yellow crystals. An X-ray crystal structure showed the yellow product to be *cis*-$Mn(hfacac)_2(H_2O)_2$ (Figure 1.2, Tables 1.1 and 1.2). This structure differs from the previously reported structure of *trans*-$[Mn(hfacac)_2(H_2O)_2]H_2O$[18] in both the number and the stereochemistry of water molecules. No precipitate is observed when the reaction is run under air/water-free conditions, even after extended periods of time. Addition of degassed water to yellow reaction solutions yields *cis*-$Mn(hfacac)_2(H_2O)_2$. The inorganic product of the reaction in eq 1.1 in the absence of water is most likely an oligomeric Mn^{II} complex, $[Mn(hfacac)_2]_n$, by analogy with trimeric $[Mn(acac)_2]_3$.[19]

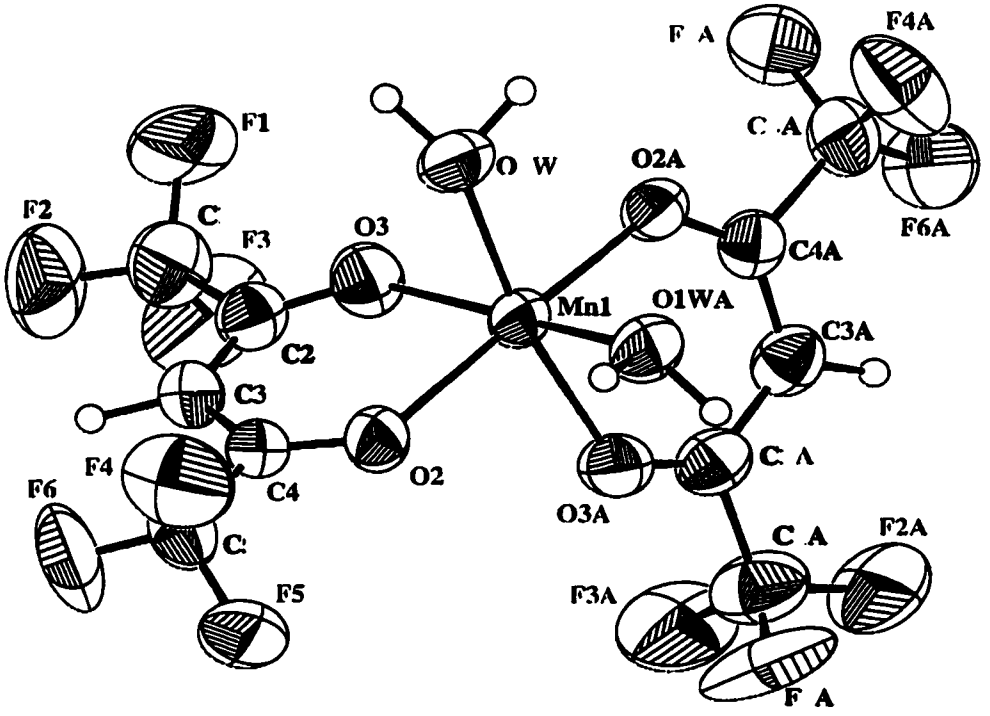

Figure 1.2. ORTEP drawing of $Mn(hfacac)_2(H_2O)_2$.

Reactions of $Mn(hfacac)_3$ with other organic substrates are similar to the DHA reaction, with conversion of green-brown Mn^{III} to yellow Mn^{II}. In benzene solution, xanthene is converted within minutes to 9,9'-bixanthene in 30(±10)% yield by GC/FID (using 9,9'-bifluorene as an integration standard; eq 1.2). The identity of 9,9'-bixanthene was indicated by GC/MS (retention time twice that of xanthene, a small M^+ and large $0.5M^+$ in the MS) and was confirmed by independent synthesis.[39]

(1.2)

1,4-Cyclohexadiene is oxidized to benzene in 82% yield over a period of days (by ^1H NMR in C_6D_6). Both reactions are considerably faster in methylene chloride (*vide infra*). 2,4-Di-*tert*-butyl phenol is oxidized to the bis(phenol) in essentially quantitative yield (by NMR) after a few minutes in C_6H_6 and 78% yield (by NMR) in CD_2Cl_2 (eq 1.3). No other products were identified; presumably the limited overoxidation (to the quinone) is a result of using 2- to 10-fold excess of the phenol. Bixanthene and the bis(phenol) result from coupling of xanthenyl and phenoxyl radicals, respectively.

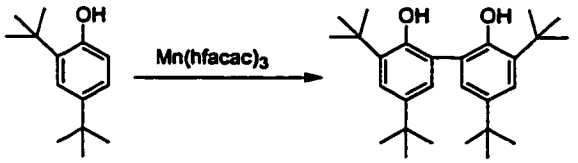

(1.3)

$Mn(hfacac)_3$ oxidizes toluene (as a 5% solution in benzene) very slowly at ambient temperatures and over a few days at 100 C. The organic products are tolylphenylmethanes, with *ortho*: *meta*: *para* = 51: trace: 48 (by GC/MS, Figure 1.3). No bibenzyl, the product of radical coupling, is observed. Tolylphenylmethanes are the result of Friedel-Crafts addition of benzyl cation to toluene,[20] as shown at the bottom of Figure 1.3. These products are often observed in metal-mediated oxidations of methylaromatics, including by Mn^{III}.[21] Oxidation of *p*-methylbenzotrifluoride

(p-$CF_3C_6H_4CH_3$) at 100 C in benzene gives only a singly $-CF_3$ substituted diarylmethane, p-$CF_3C_6H_4CH_2C_6H_5$ (Figure 1.3). This is the product of p-$CF_3C_6H_4CH_2^+$ addition to the benzene solvent, as confirmed by obtaining the d_5-substituted diarylmethane when the reaction was run in C_6D_6. p-Methoxytoluene is oxidized to coupled diarylmethane products (Figure 1.3), analogous to toluene but much faster, being complete in two weeks at ambient temperatures.

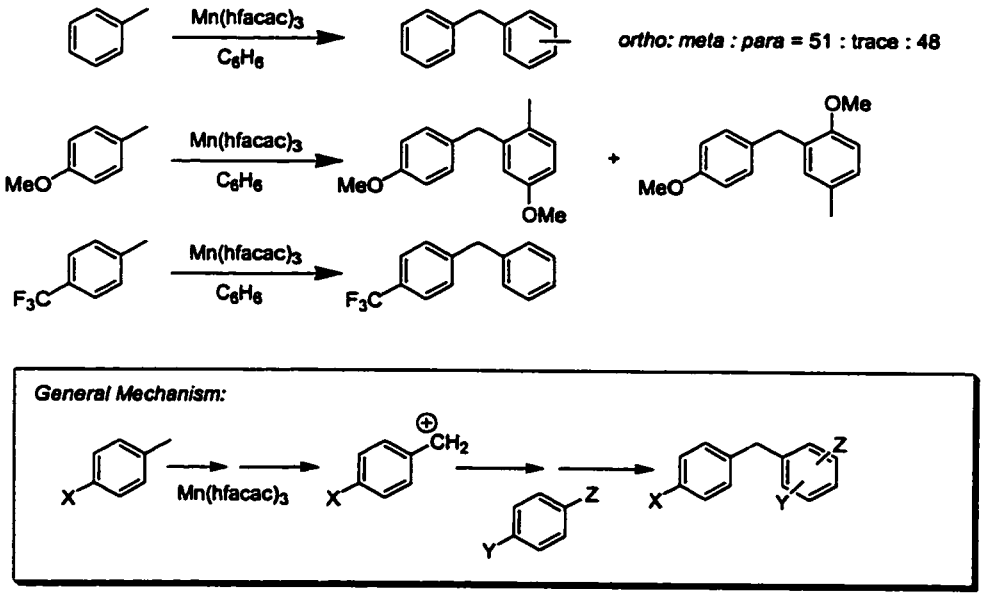

Figure 1.3. Oxidations of substituted toluenes by $Mn(hfacac)_3$.

Reacting $Mn(hfacac)_3$ with a mixture of toluene and p-methoxytoluene in benzene yielded only products from p-methoxytoluene. GC/MS of this reaction also shows a product in which a hfacac fragment is coupled to a p-methoxytoluene diarylmethane, possibly from further oxidation of the diarylmethane.[36] A similar competition reaction

between toluene and *p*-$CF_3C_6H_4CH_3$ gave ten times more toluene oxidation products than *p*-$CF_3C_6H_4CH_3$-derived products. Treatment of $Mn(hfacac)_3$ with *p*-nitrotoluene in benzene causes a color change to yellow, indicative of reduction to Mn^{II}, faster than in the reaction with toluene, but no products are observed by GC/MS or ^1H NMR. Oxidations of *p*-nitrotoluene and *p*-methylbenzotrifluoride in CH_2Cl_2 show similar bleaching of $Mn(hfacac)_3$, but again, no products are observed by GC/MS. Heating $Mn(hfacac)_3$ in neat cyclooctane causes a color change over 4 days at 100 C. Cyclooctane appears to be oxidized under these conditions, as a number of unidentified products are observed by GC/MS. No color change is observed on heating $Mn(hfacac)_3$ under similar conditions in benzene solution.

Oxidation of 1-(4-methoxyphenyl)-2,2-dimethyl-1-propanol by $Mn(hfacac)_3$ yields 4-methoxybenzaldehyde as the only product observed by GC/MS. Baciocchi and co-workers have shown that this substrate can be used as a mechanistic probe:[38] electron transfer gives the arene radical cation, which deprotonates and fragments to the benzaldehyde, while hydrogen atom abstraction leads to the ketone (Figure 1.4). The observation of the benzaldehyde product implicates an electron transfer pathway for this alkoxyaromatic compound. The analogous substrate without the methoxy group, 1-phenyl-2,2-dimethyl-1-propanol, which has not been examined as a mechanistic probe, is similarly oxidized to benzaldehyde.

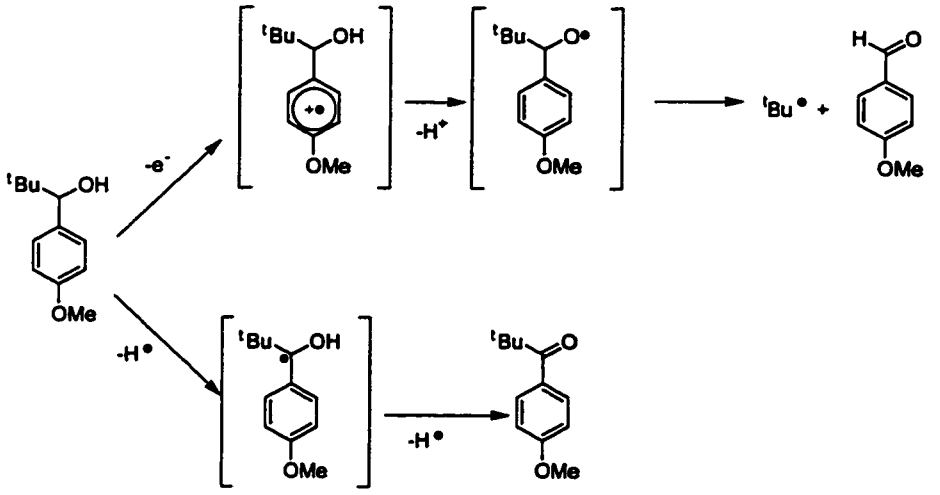

Figure 1.4. Pathways for oxidation of 1-(4-methoxyphenyl)-2,2-dimethyl-1-propanol.

Kinetics. The kinetics of $Mn(hfacac)_3$ oxidizing DHA in methylene chloride were examined in some detail. In the presence of a large excess of DHA (>100 equivalents), the decay of $[Mn(hfacac)_3]$ followed first order kinetics, but the rate constants were irreproducible. The addition of 2,6-di-*tert*-butyl pyridine, a proton scavenger, caused a marked decrease in the reaction rate, as did washing the CH_2Cl_2 solvent through basic alumina prior to use (Figure 1.5). As these observations suggested acid catalysis, a small amount of triflic acid was added to the reaction. This, unexpectedly, also resulted in a decreased rate.

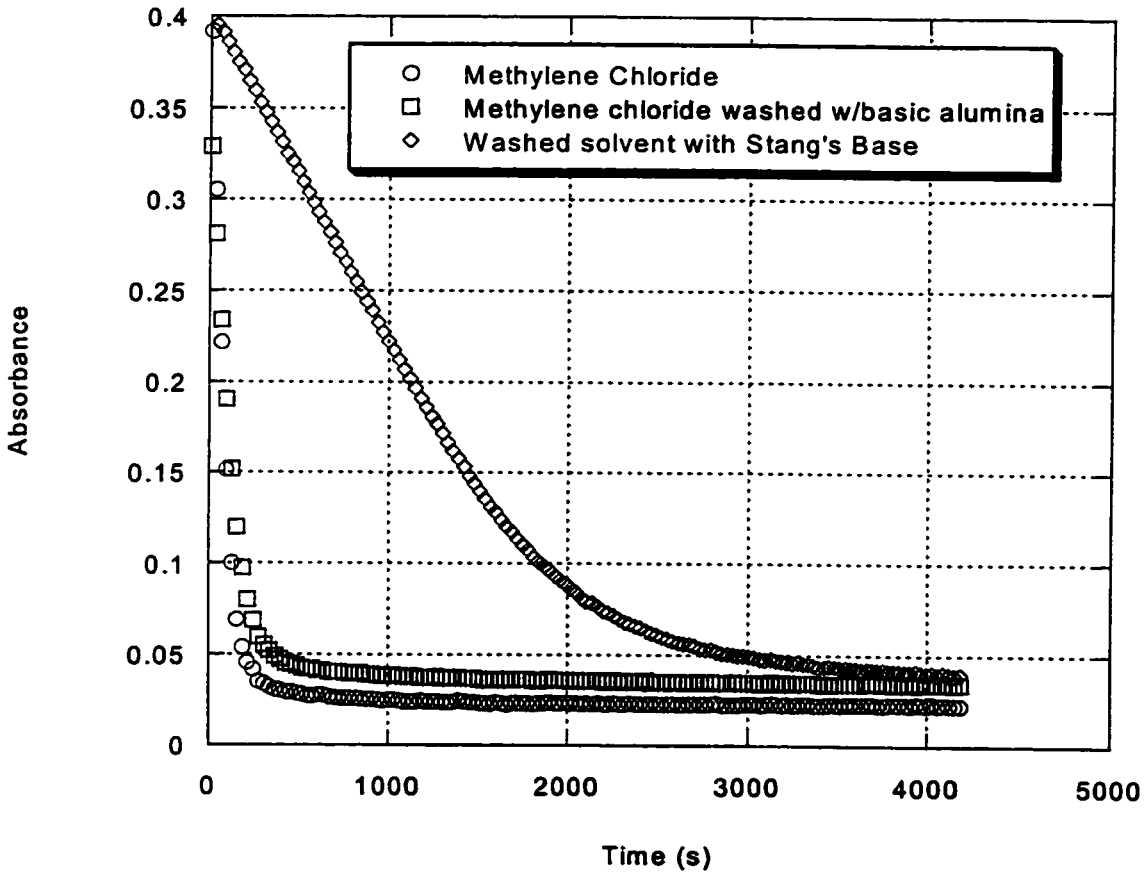

Figure 1.5. Kinetics traces in CH_2Cl_2, with solvent washed through basic alumina, and washed solvent with Stang's base added.

We believe that the origin of the irreproducibility is the presence of differing amounts of trace chloride in CH_2Cl_2 solutions.[22] Addition of chloride sources such as $^nBu_4NCl$, 2,6-di-*tert*-butylpyridinium chloride, or [PPN]Cl, results in bleaching of $Mn(hfacac)_3$ in CH_2Cl_2, both in the presence and in the absence of oxidizable substrates. This contrasts with the lack of reaction of $Mn(hfacac)_3$ with 2,6-di-*tert*-butylpyridine. Some reaction is observed, however, with $^nBu_4NPF_6$ and $[PPN]PF_6$, showing that the cations are not innocent in this system. To test for catalysis by chloride, a solution

containing $Mn(hfacac)_3$ and DHA was divided into two parts, $^nBu_4NCl$ added to one, and both reactions quenched after 3 min. Essentially quantitative conversion to anthracene and Mn^{II} was observed for the chloride-added reaction, while very little change was observed without chloride. Under these conditions, an ~1% yield of 9-chloroanthracene is also observed (detected by GC/MS and confirmed by addition of an authentic sample). The origin of the catalysis and quenching by chloride salts is not clear. This is of particular interest given the use of bromide as a co-catalyst in the Amoco-Mid Century process. Perhaps a chlorine atom or some species with reactivity like a chlorine atom is formed, analogous to the formation of Br_2^- in the Mid Century process.[3c] However, this is difficult to rationalize with the selectivity observed, for instance that DHA is oxidized in preference to $^nBu_4N^+$ and that cyclohexane is not oxidized by $Mn(hfacac)_3/Cl^-$. It appears more likely that catalysis is due to chloride binding to $Mn(hfacac)_3$.[23]

In contrast to the results in CH_2Cl_2, kinetics runs in benzene are well-behaved and reproducible. Roughly first order decay of $Mn(hfacac)_3$ is observed in the presence of excess DHA, and the pseudo-first-order rate constants are linearly related to the DHA concentration, suggesting second order kinetics with $k' = 6.8\ (\pm\ 1.5) \times 10^{-4}\ M^{-1}s^{-1}$ (Figure 1.6). Rate constants measured from 289 to 332 K yield the activation parameters $\Delta H^{\ddagger} = 14.8 \pm 1.5$ kcal mol^{-1} and $\Delta S^{\ddagger} = -24 \pm 5$ cal mol^{-1} K^{-1} (Figure 1.7). For each of the other substrates, one or two kinetic runs (3 mM Mn:120 mM substrate in benzene) showed first order decay of $Mn(hfacac)_3$ and a second order rate law was

assumed. The relative rate constants are given in Table 1.3.

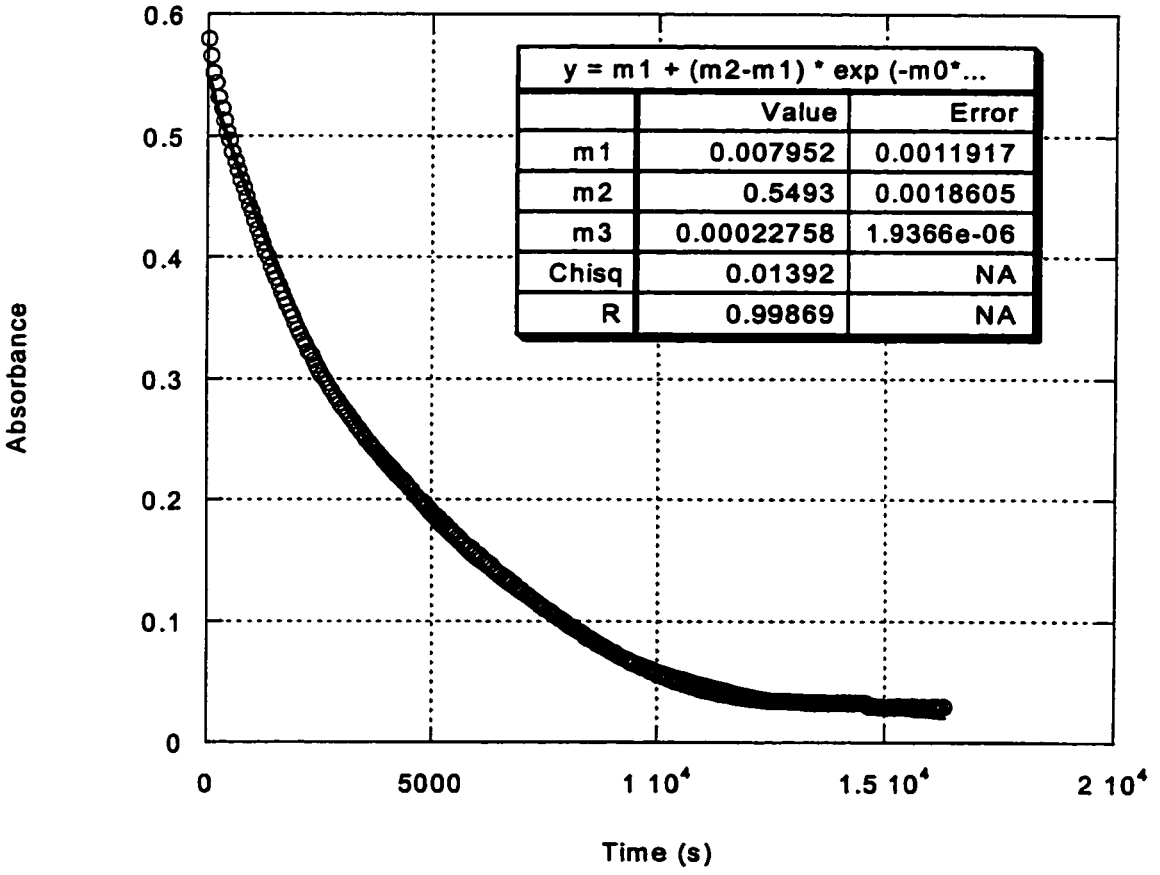

Figure 1.6. Kinetics trace in benzene (4.5 mM $Mn(hfacac)_3$:360 mM DHA).

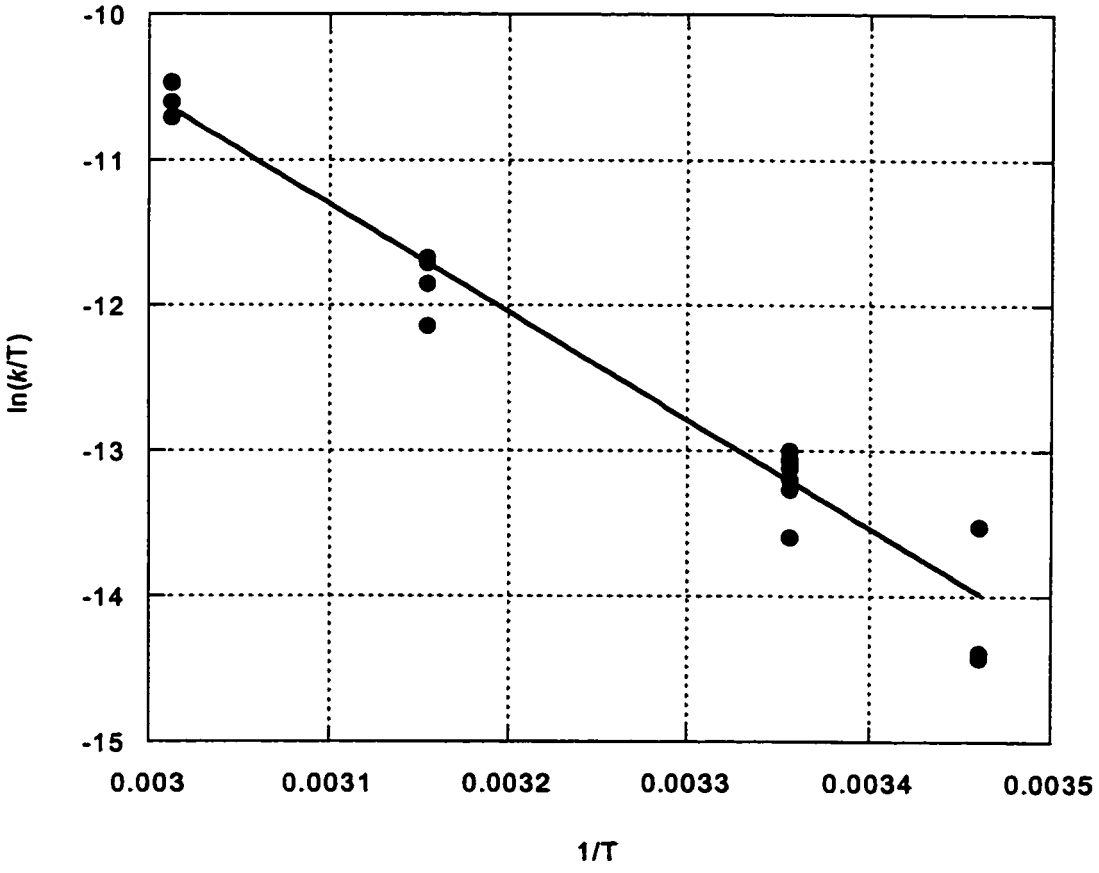

Figure 1.7. Eyring plot for the oxidation of 9,10-dihydroanthracene by $Mn(hfacac)_3$ in benzene (16 to 59 °C).

Table 1.3. Relative rate constants for oxidation by $Mn(hfacac)_3$, ionization energies, and bond dissociation energies for organic substrates.

	relative rate constant[a]	ionization energy[b]	BDE[c]
xanthene	3×10^{2}	7.65	75.5
DHA	1	8.54	78
1,4-cyclohexadiene	4×10^{-1}	8.82	77
p-$MeOC_6H_4CH_3$	3×10^{-3}	7.90	~89 [g]
$C_6H_5CH_3$	$\sim 10^{-7}$ [d]	8.83	90
p-$CF_3C_6H_4CH_3$	$\sim 10^{-8}$ [e]	~9.3 [f]	~90.5 [h]
C_6H_6	no reaction	9.24	111

[a] relative to *k*(DHA) at 298 K, 6.8×10^{-4} $M^{-1}s^{-1}$. [b] In eV, from reference 28; errors ±0.05 V or less. [c] C–H Bond Dissociation Energies, in kcal mol^{-1}, from references 30. [d] Estimated from 19% reaction after 2 months in 120mM toluene. [e] Estimated as 10 times smaller than *k*(toluene) based on a competition experiment. [f] Estimated from the IP for $C_6H_4CF_3$ [9.685 (± 0.005) eV][28] and the fact that addition of a methyl group to a benzene derivative consistently lowers the IP by ~0.4 eV.[28] [g] Estimated based on DFT calculations as 1 kcal/mol lower than toluene, see reference 30e. [h] Based on DFT calculations as 0.5 kcal/mol higher than toluene, from reference 30f.

In both benzene and CH_2Cl_2 solutions, there is evidence for catalysis of the reactions by the manganese product. To show this, a reaction of $Mn(hfacac)_3$ and excess DHA was run to completion and a second equivalent of $Mn(hfacac)_3$ was added. The rate of consumption of the second equivalent of $Mn(hfacac)_3$ was 2-3 times that of

the initial reaction (Figures 1.8 and 1.9). Such autocatalysis would normally cause substantial deviations from pseudo-first order behavior but this was not observed; perhaps the nature of the resulting manganese products varies with time. The complexities observed and the high reactivity of $Mn(hfacac)_3$ with added reagents have prevented a more in-depth kinetic study.

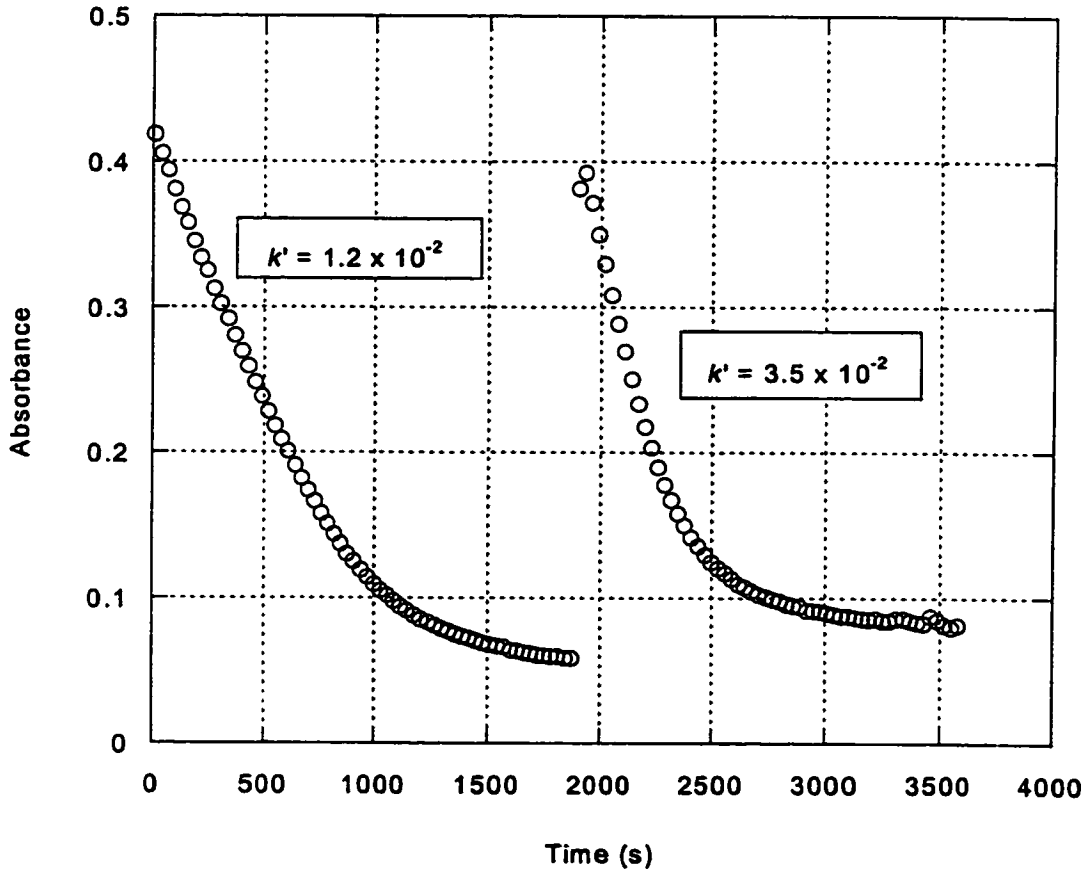

Figure 1.8. Evidence for autocatalysis in CH_2Cl_2. Original trace is 3 mM $Mn(hfacac)_3$:120 mM DHA. Second trace measured upon addition of a second equivalent of $Mn(hfacac)_3$ to give 1.8 mM $Mn(hfacac)_3$:94.8 mM DHA.

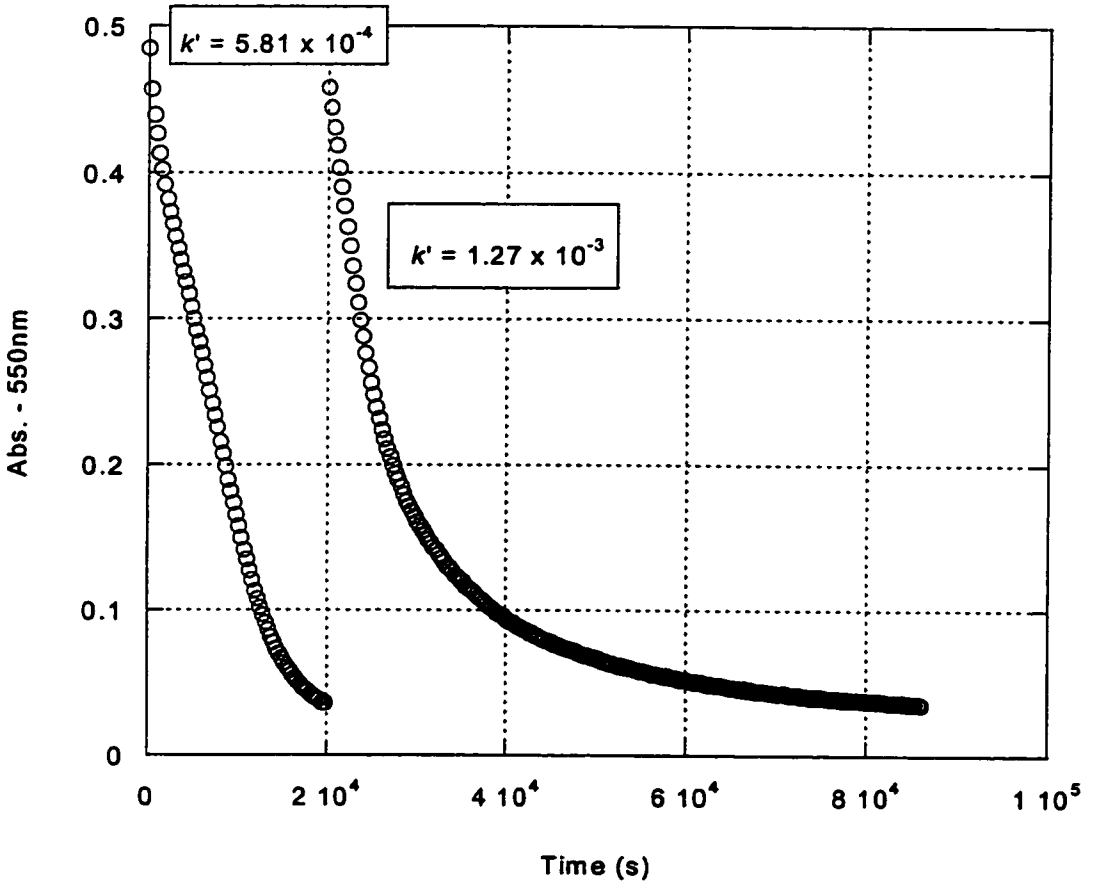

Figure 1.9. Evidence for autocatalysis in benzene. Original trace is 3.1 mM $Mn(hfacac)_3$:123.3 mM DHA. Second trace measured upon addition of a second equivalent of $Mn(hfacac)_3$ to give 2.3 mM $Mn(hfacac)_3$:92.5 mM DHA.

The kinetics of the oxidation of xanthene in benzene was also studied. A reaction with 3 mM $Mn(hfacac)_3$ and 30 mM xanthene was complete in under twenty minutes with an observed rate $k_{obs} = 5.9 \times 10^{-3}$ s^{-1} (Figure 1.10). Assuming a first-order dependence on xanthene, this gives a rate constant $k'_x = 0.197$ M^{-1} s^{-1}.

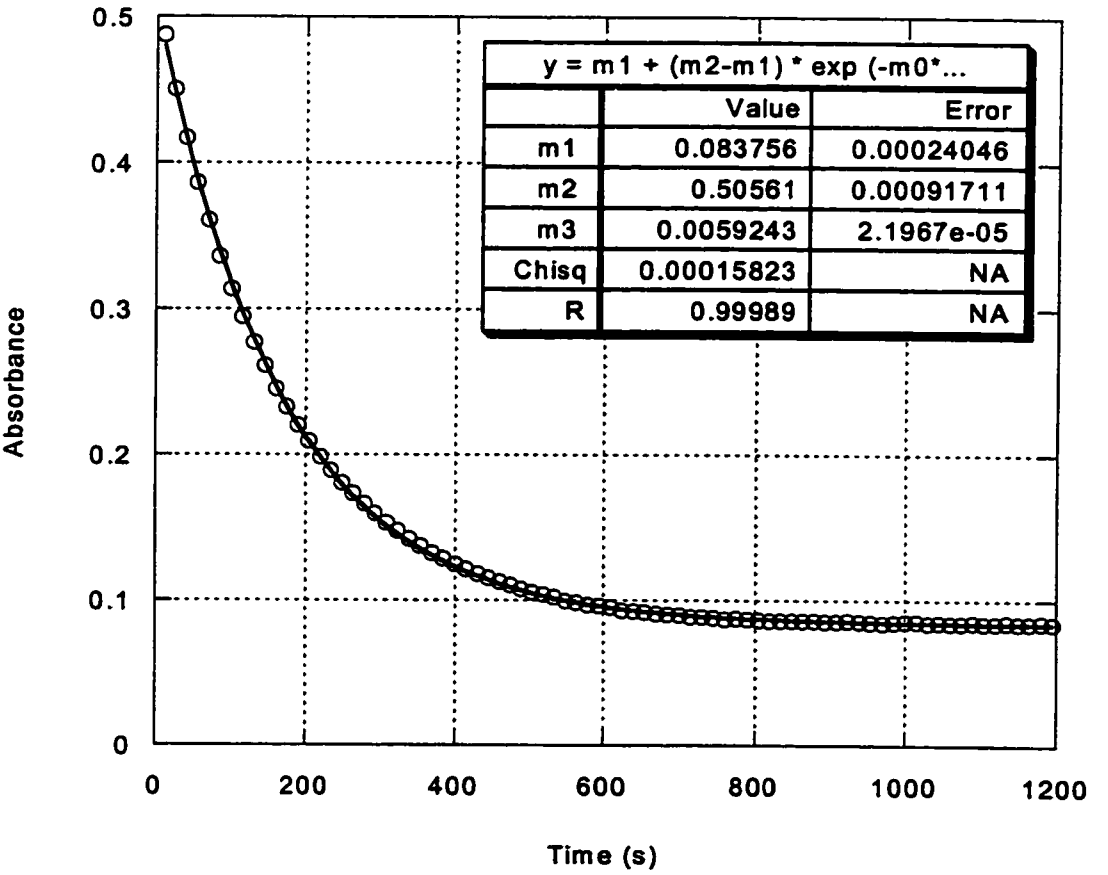

Figure 1.10. Kinetics trace in benzene (3 mM $Mn(hfacac)_3$:30 mM xanthene).

Discussion

$Mn(hfacac)_3$ is a potent oxidant, with a redox potential estimated to be +0.9 ± 0.1 V vs. $Cp_2Fe^{+/o}$ in CH_2Cl_2, equivalent to *ca.* +1.5 V vs. NHE. This is a very high potential for a neutral oxidant.[16b,24] $Mn(hfacac)_3$ could be a useful oxidizing reagent because of its ease of preparation and its solubility in nonpolar media such as hydrocarbons. We have used this solubility to study oxidations of organic compounds in benzene under conditions where the structure and speciation of the manganese

oxidant is not in question. $Mn(hfacac)_3$ undoubtedly has a distorted octahedral structure in benzene solution similar to that found in the solid state.[12] The second order kinetics for 9,10-dihydroanthracene (DHA) oxidation in this solvent implies that this molecular species is the reactive oxidant. This conclusion contrasts with the situation for "manganese(III) acetate" in acetic acid, for instance, where monomers and oligomers coexist and have different reactivities.[3c] Similarly, little is known about the structure of the organic-acid stabilized Mn^{III} complex produced by white-rot fungi to oxidize benzylic and phenolic bonds in lignin. $Mn(hfacac)_3$ thus provides a simplified model system for stoichiometric and catalytic oxidations by Mn^{III}.

The organic reactions described here all involve the oxidation of two X-H bonds (X = C, O) with the hydrogen being transferred to a ligand to form free H-hfacac. In the process, two equivalents of $Mn(hfacac)_3$ are reduced, apparently to $[Mn(hfacac)_2]_n$. The formation of bixanthene from xanthene indicates the presence of xanthenyl radicals, and the diarylmethane products from toluenes indicate the intermediacy of benzylic carbocations.[20] As shown in Figure 1.11, these intermediates could be made directly, by hydrogen atom abstraction[8,11] or hydride abstraction,[21g] or by stepwise electron and proton transfers.[21] One-step hydride transfer is very unlikely in this system, as it would require two-electron reduction of the manganese center to an unfavorable Mn^{I} complex. Initial proton transfer is also not possible since $Mn(hfacac)_3$ is not a strong base and the hydrocarbons have very low acidity. Thus, the first step in these reactions is either electron transfer or hydrogen atom transfer.[25]

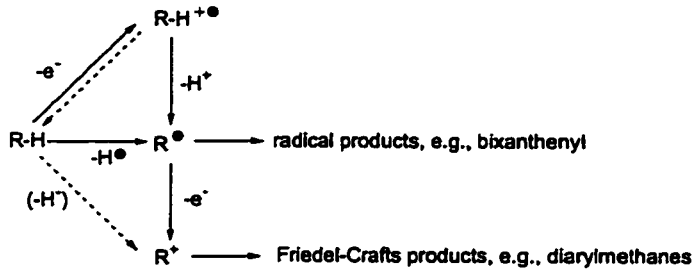

Figure 1.11. Pathways for C–H bond oxidation by $Mn(hfacac)_3$.

A pathway of initial electron transfer is indicated by the oxidation of Baciocchi's mechanistic probe, and by *p*-methoxytoluene being oxidized much faster than toluene.[26] Hydrogen atom abstractions from toluenes are not dramatically affected by substituents,[27] while the gas phase ionization energy (IE) of *p*-methoxytoluene is 0.93 eV below that of toluene (Table 1.3). Electron transfer from *p*-methoxytoluene to $Mn(hfacac)_3$ is approximately 0.5 V uphill.[29]

The rate constants in Table 1.3, however, do not simply correlate with the IE's, as would be expected for a rate limiting electron transfer pathway. 1,4-cyclohexadiene (CHD), for instance, has an IE similar to that of toluene and ~0.9 V higher than *p*-methoxytoluene, yet it reacts orders of magnitude faster than both (Table 1.3). *p*-$CF_3C_6H_4CH_3$ reacts only a factor of ten slower than toluene despite an almost 0.5 eV difference in IEs (this difference in IEs corresponds to roughly a 10^8 difference in equilibrium constants for electron transfer). It is possible that some of these reactions proceed by pre-equilibrium electron transfer followed by rate-limiting deprotonation,

but since all of the radical cations are strong acids, it is difficult to see how this would account for the, for instance, 10^5 faster rate for CHD than toluene. Pre-equilibrium electron transfer should result in an inverse-first-order rate dependence on [Mn^{II}] but addition of Mn^{II} (as [$^nPr_4N$][$Mn(hfacac)_3$]) had no appreciable effect on the reaction rate with DHA in either benzene or CH_2Cl_2. This result is, however, complicated by the tight ion pairing in these solvents. The apparent oxidation of cyclooctane also supports a hydrogen atom transfer pathway, as outersphere electron transfer from an alkane is unlikely.

The relative rate results suggest that the hydrocarbons with weak C–H bonds and high IEs most likely react by initial hydrogen atom transfer. $Mn(hfacac)_3$ could accept $H^{\bullet}$ to give [Mn^{II}(H-hfacac)$(hfacac)_2$], which would dissociate to the observed products $[Mn(hfacac)_2]_n$ and H-hfacac. It is reasonable that $Mn(hfacac)_3$ has a high affinity for $H^{\bullet}$, since it has a high redox potential and the reduced form, $[Mn(hfacac)_3]^-$ has some basicity. Our related studies of oxidizing manganese,[7,9a,31] iron,[11b] copper,[11c] and chromium complexes[11a] indicate the viability of hydrogen atom abstraction by basic ligands bound to oxidizing metal centers. An X–H bond strength can, in favorable cases, be determined from redox potential and pK_a values,[11,32] but the needed thermochemical data is not available for methylene chloride solutions and this system is complicated by the dissociation of H-hfacac.

In comparison to other Mn^{III} oxidants, $Mn(hfacac)_3$ is more reactive and is capable of oxidations under milder conditions. Its redox potential (+0.9 V vs. $Cp_2Fe^{+/o}$

in CH_2Cl_2) appears to be higher than that of $Mn(acac)_3$, ca. +0.7 V vs. $Cp_2Fe^{+/o}$ in MeCN.[33] Oxidations of *p*-methoxytoluene by "$Mn(OAc)_3$" in acetic acid are typically run at 70-100 °C.[21] Several studies of Mn^{III} reactions indicate that substrates with low IEs (8.0) are oxidized by electron transfer, but invoke alternative mechanisms for substrates with higher IE values.[34] Thermolysis of acidic solutions of manganese(III) acetate to 80 °C results in formation of carboxylmethyl radicals, $^{\bullet}CH_2CO_2H$, which are hydrogen atom abstracting agents. Malonyl radicals are formed similarly from "$Mn(OAc)_3$" and diethyl malonate. There is no evidence for the formation of hfacac$^{\bullet}$ radicals in reactions of $Mn(hfacac)_3$, and the high thermal stability of the oxidant makes this unlikely. Oxidation of hfacac$^-$ to the radical would seem much more unfavorable than for non-fluorinated ligands, yet $Mn(hfacac)_3$ appears more reactive. Carboxylmethyl, malonyl, and related radicals all add to aromatic rings and olefins competitively with hydrogen atom abstraction (a useful process[35]) but hfacac-substituted products are not, in general, observed in this system.[36] We suggest that a reasonable alternative pathway is direct hydrogen atom transfer from a weak C–H bond to a manganese-bound hfacac oxygen, giving [Mn^{II}(hfacac)$_2$(H-hfacac)] which then dissociates H–hfacac.

Conclusions

$Mn(hfacac)_3$ is an easily synthesized, hydrocarbon soluble, strong neutral oxidant (0.9 ± 0.1 V vs. $Cp_2Fe^{+/o}$). Its reactions serve as a model for the oxidations of

organic compounds by various manganese(III) complexes. In contrast to other Mn^{III} oxidations, the speciation of the manganese is well defined under the reaction conditions. $Mn(hfacac)_3$ oxidizes organic compounds that either have a low redox potential or a weak C-H or O-H bond, including 9,10-dihydroanthracene (DHA), 2,4-di-*tert*-butyl phenol, toluene, and *p*-methoxytoluene. Most of these oxidations can be performed at room temperature in benzene solution. Mechanistic studies indicate that alkoxy-aromatic compounds are oxidized by initial electron transfer, but less electron rich substrates, such as 1,4-cyclohexadiene, appear to react by initial hydrogen atom transfer to a manganese-bound hfacac oxygen.

Experimental

General Considerations. All experiments were performed under an N_2 atmosphere using standard techniques unless otherwise noted. Solvents (including deuterated solvents from Cambridge Isotope) were degassed and dried according to standard procedures.[37] Dihydroanthracene (DHA) was recrystallized twice from absolute EtOH, 2,4-di-*t*-butylphenol was sublimed, and toluene was dried over Na and vacuum transferred prior to use. Other reagents were purchased from Aldrich and used as received unless otherwise noted. 1-(4-methoxyphenyl)-2,2-dimethyl-1-propanol[38] and 9,9'-bixanthene[39] were synthesized according to literature methods.

NMR spectra were recorded on Bruker AC-200 (^1H, ^{19}F), AF-300 (^1H, ^{19}F), and AM-500 (^1H) spectrometers at ambient temperatures and are reported in ppm relative to TMS (^1H) or external $CFCl_3$ (^{19}F). UV-vis spectra were recorded on a Hewlett Packard

8453 diode array spectrophotometer and are reported as λ_{max} (nm), (ε, M^{-1} cm^{-1}). GC/MS spectra were obtained on a Hewlett Packard 5971 instrument equipped with a non-polar capillary column and a mass spectral analyzer. GC/FID spectra were obtained on a Hewlett Packard 5890 instrument equipped with a similar column. Mass spectrometric analysis for $[Cp_2Fe][Mn(hfacac)_3]$ was performed on an Esquire-LC electrospray ion trap mass spectrometer (Bruker/Hewlett-Packard). The sample was dissolved in acetonitrile and infused at a flow rate of 1μl/min. $Mn(hfacac)_3$ was analyzed on a double focusing mass spectrometer with reverse geometry (JEOL HX-110). A solid sample was introduced by a direct insertion probe (at room temperature) and ionized by electron impact (70eV). CV data were collected on a BAS CV-27.

Synthesis of $Mn^{III}(hfacac)_3$. In a modification of the literature preparation,[9] a slurry of Mn_2O_3 (1.80 g, 11.4 mmol), H-hfacac (10.5 mL, 74.1 mmol, 6.5 equiv.), and 25 mL dry *n*-hexane was heated at reflux under N_2 for 24 h. The reaction was cooled to –78° C, and the liquid decanted to isolate the dark green solid, which was further dried under dynamic vacuum. The crude product was sublimed twice under vacuum at ~65°-70° C to give 3.5 g (45%) black-green $Mn(hfacac)_3$. UV-vis (CH_2Cl_2): 276 (17,000), 550 (200). ^1H NMR (CD_2Cl_2): 10.7 (s, 3 H). ^{19}F NMR (CD_2Cl_2): -47 ppm (s). Anal. Calcd. for $C_{15}H_3F_{18}MnO_6$: C, 26.65; H, 0.44; N, 0; Fnd., C, 26.52; H, 0.49; N, 0. ESI-MS: *m/z* 676 (M^+), 469, 400, 262, 212, 139, 69.

Synthesis of $[Cp_2Fe][Mn(hfacac)_3]$. A solution of $Mn(hfacac)_3$ (0.1 g, 0.15 mmol), Cp_2Fe (20 mg, 0.11 mmol), and 10 mL pentane was stirred at room temperature

for 20 min. The blue solid was filtered and washed with additional pentane (0.05 g, 53%). X-ray quality crystals were obtained by slow diffusion of pentane into a saturated solution in CH_2Cl_2. ^1H NMR (CD_2Cl_2): 38 (br, Cp_2Fe^+; shifts upfield on addition of Cp_2Fe). UV-vis (CH_2Cl_2): 309 (660), 622 (255). ESI-MS: *m/z* 676, 207 (in the negative mode), 187, 186, 184, 155 (in the positive mode, displaying a characteristic iron isotope pattern). Anal Calcd. for $C_{25}H_{13}F_{18}FeMnO_6$: C, 34.83; H, 1.52; N, 0. Fnd.: C, 34.87; H, 1.53; N, 0. **[^{n}Pr$_4$N][Mn(hfacac)$_3$]** was prepared similarly from $Mn(hfacac)_3$ (0.2 g, 0.3 mmol), $^n Pr_4NI$ (90 mg, 0.29 mmol), and 20 mL of CH_2Cl_2. After stirring for 20 min. the CH_2Cl_2 was removed under dynamic vacuum and the yellow solid washed with pentane (0.18 g, 72%). Anal. Calcd. for $C_{27}H_{31}F_{18}MnNO_6$: C, 37.60; H, 3.62; N, 1.62. Fnd.: C, 37.78; H, 3.60; N, 1.62. UV-vis (CH_2Cl_2): 314 (~20,000).

X-ray structure determinations of Mn(hfacac)$_2$(H$_2$O)$_2$ and [Cp$_2$Fe][Mn(hfacac)$_3$]. A yellow plate of $Mn(hfacac)_2(H_2O)_2$ and a blue plate of $[Cp_2Fe][Mn(hfacac)_3]$ were mounted on glass capillaries with epoxy. Data were collected at 23 °C on a Nonius Kappa CCD diffractometer. All non-hydrogen atoms were refined anisotropically by full-matrix least-squares. Disorder in the CF_3 groups was indicated by large anisotropic displacement parameters for the F atoms. All hydrogen atoms were located from difference maps and were refined with a riding model. Data were refined using SHELXL-97 and corrected by scaling and averaging using the program SCALEPACK.

Typical procedure for organic oxidations. A solution of **xanthene** (16 mg, 90 μmol) and $Mn(hfacac)_3$ (9 μmol) in 3 mL C_6H_6 turned yellow within 15 min. Bixanthene was observed by GC/MS *m/z* 181, M^+ (at twice the retention time of xanthene), 152, 69, 39 and confirmed by comparison with an authentic sample. In an alternative procedure, a J. Young sealable NMR tube was charged with **1,4-cyclohexadiene** (0.3 μL, 3.2 μmol), C_6D_6 (1 mL), and $(Me_3Si)_2O$ (1 μL) as an internal standard. An initial ^1H NMR spectrum was acquired. The tube was brought back into the dry box and $Mn(hfacac)_3$ (4 mg, 6.4 μmol) was added and the reaction monitored by ^1H NMR. Reactions of **1-(4-methoxyphenyl)-2,2-dimethyl-1-propanol** were performed in a similar manner in both C_6D_6 and CD_2Cl_2; GC/MS showed (*m/z*): 136 (4-methoxybenzaldehyde), and 194 (starting material). Oxidations of DHA were monitored by GC/MS and ^1H NMR (as in the above procedures), and by UV-vis spectroscopy, where anthracene production was evident from its characteristic spectrum in CH_2Cl_2: 359 (8,800), 378 (8,200). Yellow crystals of **$Mn(hfacac)_2(H_2O)_2$** deposited (0.033 g, 60% yield from 0.07 g $Mn(hfacac)_3$ and 0.093 g DHA in CH_2Cl_2) upon exposure of the DHA reaction mix to air or degassed water.

Oxidation of toluene and substituted toluenes. In a typical reaction, a thick-walled glass bomb was charged with 19 mg (28 μmol) of $Mn(hfacac)_3$ and 2.8 mmol of toluene, *p*-methoxytoluene, methylbenzotrifluoride, or *p*-nitrotoluene (100 equiv.) in 5 mL of benzene. The solution sat at room temperature for several weeks. Periodically, the flask was brought into the dry box and an aliquot was removed and analyzed by

GC/MS. The *p*-methoxytoluene solution had turned yellow in 14 days and GC/MS revealed the methoxy-substituted tolylphenylmethane isomers (*m/z* 242) as well as an unidentified product (*m/z* 448 (M^+), 351, 331, 316, 301, 280, 165, 135, 105, 69). After 50 days at room temperature, the toluene and *p*-nitrotoluene flasks were heated to 100° C for ~67 hours, until the reaction mixes had turned yellow. GC/MS analysis revealed the presence of tolylphenylmethane isomers (*m/z* 182) in the toluene reaction, but no product was observed in the *p*-nitrotoluene reaction mix. The competition reactions were run under similar conditions with mixtures of toluenes. GC/MS of the methylbenzotrifluoride reaction mix revealed 4-trifluorodiphenylmethane (*m/z* 236, *m/z* 241 from reaction in C_6D_6).

Kinetics studies of the oxidation of DHA. Kinetics studies were carried out under air-free conditions in sealable quartz cuvettes with pseudo-first-order conditions of excess DHA – typically 3 mM $Mn(hfacac)_3$ and 120 or 240 mM DHA in CH_2Cl_2 or C_6H_6. Kinetic data were typically gathered at 550 nm every 10-30 s over 4,000-70,000 s. All solutions were made up and mixed in a nitrogen-filled dry box, sealed, and then transported to the spectrophotometer. Rate constants were determined at four temperatures in the range of 16 to 59 C. At least four kinetics traces were acquired at each temperature. **Product autocatalysis** was observed in both benzene and CH_2Cl_2: A typical kinetics run with a large excess of DHA was set up in C_6H_6 or CH_2Cl_2 as above. After approximately three half-lives (20000 s for C_6H_6, 750 s for CH_2Cl_2) an additional equivalent of $Mn(hfacac)_3$ was added to the cuvette and the kinetics

continued. The reaction of the second aliquot of $Mn(hfacac)_3$ was faster than the first.

Estimation of redox potential of $Mn(hfacac)_3$. UV-vis spectra were recorded for CD_2Cl_2 solutions containing 3 mM $Mn(hfacac)_3$ and either Cp_2Fe, acetylferrocene[40], 1,1'-diacetylferrocene,[41] $(4\text{-}BrC_6H_4)_3N$, or $(2,4\text{-}Br_2C_6H_3)_3N$.[42] It was assumed that $(2,4\text{-}Br_2C_6H_3)_3N$ has the same ε as $(4\text{-}BrC_6H_4)_3N$ ($\lambda_{max} = 720$ nm, $\varepsilon = 3 \times 10^4$).[43] Cyclic voltammograms of the amines were acquired from +2.0 to –1.7 V, with scan rates of 0.1 and 1.0 V/s, in CH_2Cl_2 with 0.1 M $^nBu_4NPF_6$ with a Ag/Ag^+ reference electrode and Cp_2Fe as an internal standard: $(4\text{-}BrC_6H_4)_3N$, 0.7 V, $(2,4\text{-}Br_2C_6H_3)_3N$, 1.2 V (both vs. $Cp_2Fe^{+/o}$); peak separations were comparable to that of Cp_2Fe.

Notes to Chapter 1

---

(1) Bryant, J. R.; Taves, J. E; Mayer, J. M. *Inorg. Chem.* **2002**, *41*, 2769-2776.

(2) (a) De Klein, W. J. *Organic Syntheses By Oxidation With Metal Compounds* Mijs, W. J.; de Jonge, C. R. H. I., Eds., Plenum Press: New York, 1986, 261-314. (b) Arndt, D. *Manganese Compounds as Oxidizing Agents in Organic Chemistry* Open Court: La Salle, 1981, 1-25.

(3) (a) Olah, G. A.; Molnár, Á. *Hydrocarbon Chemistry* Wiley, 1995, pp. 375ff. (b) Partenheimer, W. *Catal. Today* **1995**, *23*, 69. (c) For a recent leading reference, see: Jiao, X. D.; Metelski, P. D.; Espenson, J. H. *Inorg. Chem.* **2001**, *40*, 3228-3233.

(4) Chiswell, B.; McKensie, E. D.; Lindoy, L. F. in *Comprehensive Coordination Chemistry*; Wilkinson, G.; Gillard, R. D.; McCleverty, J. A., Eds.; Pergamon Press: Oxford, 1987: Vol. 1, 88-90.

(5) (a) Joshi, D. K.; Gold, M. H. *Biochemistry* **1994**, *33*, 10969-10976. (b) Wariishi, H.; Valli, K.; Gold, M. H. *Biochemistry* **1989**, *28*, 6017-6023. (c) Banci, L.; Ciofi-Baffoni, S.; Tien, M. *Biochemistry* **1999**, *38*, 3205-3210. (d) Wariishi, H.; Akileswaran, L.; Gold, M. H. *Biochemistry* **1988**, *27*, 5365-5370. (e) Kishi, K.; Wariishi, H.; Marquez, L.; Dunford, H. B.; Gold, M. H. *Biochemistry* **1994**, *33*, 8694-8701.

(6) Kishi, K.; Wariishi, H.; Marquez, L.; Dunford, H. B.; Gold, M. H. *Biochemistry* **1994**, *33*, 8694-8701.

(7) See, for example: (a) Valli, K.; Gold, M. H. *J. Bacteriol.* **1991**, *173*, 345-352. (b) Reddy, G. V. B.; Gelpke, M. D. S.; Gold, M. H. *J. Bacteriol.* **1998**, *180*, 5159-5164. (c) Refs. 4b, c.

(8) We have also examined hydrocarbon oxidations by manganese μ-oxo dimers: (a) Wang, K.; Mayer, J. M. *J. Am. Chem. Soc.* **1997**, *119*, 1470-1471. (b) Larsen, A. S.; Wang, K.; Lockwood, M. A.; Rice, G. L.; Won, T. J.; Lovell, S.; Sadílek, M.; Turecek, F.; Mayer, J. M. *J. Am. Chem. Soc.* **2002**, *124*, 10112-10123.

(9) Evans, S.; Hamnett, A.; Orchard, A. F.; Lloyd, D. R. *Faraday Discuss. Chem. Soc.* **1972**, *54*, 227-250.

(10) Nishino, H. *Bull. Chem. Soc. Jpn.* **1986**, 59, 1733-1739.

(11) (a) Mayer, J. M. *Acc. Chem. Res.* **1998**, *31*, 441-450. (b) Roth, J. P.; Mayer, J. M.; *Inorg. Chem.* **1999**, *38*, 2760-2761. (c) Lockwood, M. A.; Blubaugh, T. J.; Collier, A. M.; Lovell, S.; Mayer, J. M. *Angew. Chem. Int. Ed.* **1999**, *38*, 225-227.

(12) Bouwman, E.; Caulton, K. G.; Christou, G.; Folting, K.; Gasser, C.; Hendrickson, D. N.; Huffman, J. C.; Lobkovsky, E. B.; Martin, J. D.; Michel, P.; Tsai, H.; Xue, Z. *Inorg. Chem.* **1993**, *32*, 3463-3470.

(13) H_2O + H-hfacac gives the bis(*gem*-diol), 1,1,1,5,5,5-hexafluoropentane-2,2,4,4-tetraol.[12]

(14) Reichert, C.; Bancroft, G. M.; Westmore, J. B. *Can. Jour. Chem.* **1970**, *48*, 1362-1370.

(15) Sharpe, P.; Eyler, J. R.; Richardson, D. E. *Inorg. Chem.* **1990**, *29*, 2779-2787.

(16) (a) Geiger, W. E. in *Organometallic Radical Processes*; Trogler, W. C., Ed.; Elsevier Science Pub.: Amsterdam, 1990, 142-172. (b) Connelly, N. G.; Geiger, W. E. *Chem. Rev.* **1996**, *96*, 877-910.

(17) Izutsu, K. *Acid-Base Dissociation Constants in Dipolar Aprotic Solvents*, Blackwell Scientific Publications: Oxford, 1990, 21, 28.

(18) Dickman, M. H. *Acta Cryst.* **1997**, *C53*, 402-404.

(19) Cotton, F. A.; Wilkinson, G.; Murillo, C. A.; Bochmann, M. *Advanced Inorganic Chemistry*, Wiley: New York, 1999, 6th Edition, 479-482.

(20) (a) Uemura, S.; Ikeda, T.; Tanaka, S.; Okano, M. *J. Chem. Soc. Perkin 1*, **1979**, 2574-2576. (b) Darbeau, R. W.; White, E. H.; Song, F.; Darbeau, N. R.; Chou J. *J. Org. Chem.* **1999**, *64*, 5966-5978.

(21) (a) Andrulis, P. J.. Jr.; Dewar, M. J. S.; Dietz, R.; Hunt, R. L. *J. Am. Chem. Soc.* **1966**, *88*, 5473-8. (b) Uemura, S.; Tanaka, S.; Okano, M. *J. Chem. Soc. Perkin Trans. 1* **1976**, 1966-9. (c) Uemura, S.; Ikeda, T.; Tanaka, S.; Okano, M. *J. Chem. Soc. Perkin Trans. 1* **1979**, 2574-6. (d) McKillop, A.; Turrell, A. G.; Young, D. W.; Taylor, E. C. *J. Am. Chem. Soc.* **1980**, *102*, 6504-6512. (e) Necsoiu, I.; Ghenciulescu, A.; Rentea, M.; Rentea, C. N.; Nenitzescu, C. D. *Rev. Roum. Chim.* **1967**, *12*, 1503-1510. (f) King, S. T. *J. Catal.* **1991**, *131*, 215-225. (g) Lockwood, M. A; Wang, K.; Mayer, J. M. *J. Am. Chem. Soc.* **1999**, *121*, 11894-11895.

(22) We thank Professor Ronny Neumann for this suggestion (personal communication, 2000).

(23) Precedent for chloride binding to an oxidizing manganese center is found in the chlorination of alkenes by manganese acetate in the presence of chloride species. See, for example, (a) Donnelly, K. D.; Fristad, W. E.; Gellerman, B. J.; Peterson, J. R.; Selle, B. J. *Tetrahedron Lett.* **1984**, *25*, 607-610. (b) Yonemura, H.; Nishino, H.; Kurosawa, K. *Bull. Chem. Soc. Jpn.* **1986**, *59*, 3153-3159.

(24) Carborane radicals are more potent one-electron oxidants: King, B. T.; Noll, B. C.; McKinley, A. J.; Michl, J. *J. Am. Chem. Soc.* **1996**, *118*, 10902-10903.

(25) (a) It is interesting that xanthene is oxidized to bixanthene but toluene does not give bibenzyl even though (i) xanthyl and benzyl radicals must be intermediates and (ii) it is much easier to oxidize xanthyl radical to xanthyl carbocation than $PhCH_2^{\bullet}$ to $PhCH_2^{+}$.[25b] Presumably radical coupling is favored for xanthene by the much higher steady-state concentration of the xanthyl radical. If $Mn(hfacac)_3$ + RH $\rightleftharpoons$ $Mn(Hhfacac)(hfacac)_3$ + $R^{\bullet}$ were at equilibrium, the concentration of $R^{\bullet}$ would be $\sim 10^{10}$ times higher for xanthene than for toluene because of its weaker C-H bond strength. While equilibrium is unlikely, this indicates that the xanthyl radical concentration is likely to be much higher. (b) Cheng, J. -P.; Handoo, K. L.; Parker, V. D. *J. Am. Chem. Soc.* **1993**, *115*, 2655-2660; Handoo, K. L.; Cheng, J. -P.; Parker, V. D. *ibid.* 5067-5072.

(26) For leading references to other electron transfer oxidations of *p*-methoxytoluene, see: (a) Eberson, L. *J. Am. Chem. Soc.* **1983**, *105*, 3192-3199. (b) Schlesener, C. J.; Kochi, J. K. *J. Org. Chem.* **1984**, *49*, 3142-3150.

(27) Howard, J. A.; Chenier, J. H. B. *J. Am. Chem. Soc.* **1973**, *95*, 3054-3055: $^{t}BuO^{\bullet}$ abstracts $H^{\bullet}$ from *p*-$MeOC_6H_4Me$ 2.7 times faster than from toluene.

(28) http://webbook.nist.gov/chemistry accessed 14 May, 2001.

(29) Ionization potentials for the organic compounds have been used as surrogates for redox potentials, in part due to the lack of consistency in the reported electrochemical potentials. Some reported redox potentials can be found in these references: For xanthene, DHA, and p-methoxytoluene: (a) Salah, N. B.; Mhalla, F. M. *J. Electroanal. Chem.* **2000**, *485*, 42-48. For 1,4-CHD, toluene, and benzene: (b) Kochi, J. K. in *Comprehensive Organic Synthesis*; Trost, B. M., Fleming, I., Eds. Pergamon: New York, 1991, Vol. 7, 849-889. Other values for benzene, toluene, and *p*-methoxytoluene: Eberson, L. *Electron Transfer Reactions in Organic Chemistry*; Springer-Verlag: Berlin, 1987, 44.

(30) For xanthene: (a) Burkey, T. J.; Majewski, M.; Griller, D. *J. Am. Chem. Soc.* **1986**, *108*, 2218-2221. For DHA: (b) Bordwell, F. G.; Cheng, J. P.; Ji, G.; Satish, A. V.; Zhang, X. *J. Am. Chem. Soc.* **1991**, *113*, 9790-9795. For 1,4-CHD: (c) Laarhoven, L. J.; Mulder, P.; Wayner, D. D. M. *Acc. Chem. Res.* **1999**, *32*, 342-349. For toluene: (d) Bierbaum, V.; DePuy, C.; Davico, G.; Ellison, B. *Int. J. Mass Spectrom. Ion Phys.* **1996**, *156*, 109-131. For *p*-$MeOC_6H_4CH_3$: (e) Fox, T.;

Kollman, P. A. *J. Phys. Chem.* **1996**, *100*, 2950-2956. For *p*-$CF_3C_6H_4CH_3$: (f) Pratt, D. A.; Wright, J. S.; Ingold, K. U. *J. Am. Chem. Soc.* **1999**, *20*, 4877-4882. For benzene: (g) Berkowitz, J.; Ellison, G. B.; Gutman, D. *J. Phys. Chem.* **1994**, *98*, 2744-2765.

(31) Gardner, K. A.; Kuehnert, L. L.; Mayer, J. M.; *Inorg. Chem.* **1997**, *36*, 2069-2078.

(32) Mayer, J. M. Chapter 1 in *Biomimetic Oxidations Catalyzed by Transition Metal Complexes*, B. Meunier, Ed., Imperial College Press: London, **2000**. See also reference 11.

(33) Yamaguchi, K.; Sawyer, D. T. *Inorg. Chem.* **1985**, *24*, 971-976. Our electrochemistry experiments and other references indicate that redox potentials in CH_3CN and CH_2Cl_2 are similar when reported vs. $Cp_2Fe^{+/o}$.

(34) (a) Heiba, E. I.; Dessau, R. M.; Koehl, W. J., Jr. *J. Am. Chem. Soc.* **1969**, *91*, 138-145. (b) Citterio, A.; Santi, R.; Fiorani, T.; Strologo, S. *J. Org. Chem.* **1989**, *54*, 2703-2712. (c) Fristad, W. E.; Peterson, J. R.; Ernst, A. B.; Urbi, G. B. *Tetrahedron* **1986**, *42*, 3429-3442. (d) van der Ploeg, R. E.; de Korte, R. W.; Kooyman, E. C. *J. Catal.* **1968**, *10*, 52-59.

(35) Snider, B. B. *Chem. Rev.* **1996**, *96*, 339-363. See also refs. 34.

(36) The oxidation of *p*-methoxytoluene gave a product with mass corresponding to the coupling of a hfacac ligand to the aromatic ring of the substituted

diphenylmethane. It is unclear if the ligand is bound through an oxygen or a carbon. See Experimental Section for fragmentation pattern.

(37) Perrin, D. D.; Armarego, W. L. F. *Purification of Laboratory Chemicals 3rd Ed.*, Pergamon Press: New York, 1988.

(38) (a) Baciocchi, E.; Bietti, M.; Putignani, L.; Steenken, S. *J. Am. Chem. Soc.* **1996**, *118*, 5952-5960. (b) Baciocchi, E.; Bietti, M.; Lanzalunga, O. *Acc. Chem. Res.* **2000**, *33*, 243-251.

(39) Coellen, M.; Rüchardt, C. *Chem. Eur. J.* **1995**, *1*, 564-567.

(40) Mayo, D. W.; Pike, R. M.; Butcher, S. S. *Microscale Organic Laboratory*, Wiley: New York, 2nd Ed., 1989, 291-295.

(41) Schwink, L.; Knochel, P. *Chem. Eur. J.* **1998**, *4*, 950-968.

(42) Schmidt, W.; Steckhan, E. *Chem. Ber.* **1980**, *113*, 577-585.

(43) Bell, F. A.; Ledwith, A.; Sherrington, D. C. *J. Chem. Soc. (C)* **1969**, *19*, 2719-2720.

Chapter 2: Mechanistic Studies of the Oxidations of Hydrocarbons by $[Ru^{IV}(bpy)_2(py)O]^{2+}$

Abstract

The oxidations of 9,10-dihydroanthracene (DHA), xanthene, and fluorene by $[(bpy)_2(py)Ru^{IV}O]^{2+}$ give mixtures of products including oxygenated and non-oxygenated compounds. The products include those formed by organic radical dimerization, such as 9,9'-bixanthene, as well as by oxygen-atom transfer. The kinetics of these reactions have been measured and display a clear correlation with substrate C-H bond dissociation energy. The kinetic isotope effect for the reaction of $\mathbf{Ru{=}O^{2+}}$ with DHA vs. DHA-d_4 gives $k_H/k_D \geq 35 \pm 1$. A mechanism of initial hydrogen-atom abstraction followed by competitive pathways of radical dimerization and trapping by the oxidant is indicated. The hydrogen-atom self-exchange rate for the transfer of H$^\bullet$ between $[(bpy)_2(py)Ru^{III}OH]^{2+}$ and $[(bpy)_2(py)Ru^{IV}O]^{2+}$ has also been measured ($k'_{HSE} = (7.6 \pm 0.4) \times 10^4\ M^{-1}\ s^{-1}$). When combined with an estimate for the DHA/HA$^\bullet$ self-exchange rate in the Marcus cross relation, this value agrees well with the observed hydrogen atom abstraction rate. The deuterium-atom self-exchange rate is also reported for the D$^\bullet$ exchange between $[(bpy)_2(py)Ru^{III}OD]^{2+}$ and $[(bpy)_2(py)Ru^{IV}O]^{2+}$. The kinetic isotope effect for this self-exchange reaction is surprisingly near unity.

Introduction

Over the past twenty years, oxidations of substrates by $[(bpy)_2(py)Ru^{IV}O]^{2+}$ ($\mathbf{Ru{=}O^{2+}}$) have been reported in the literature.[1-4] This compound, and its closely related hydroxo and aquo counterparts, $[(bpy)_2(py)Ru^{III}OH]^{2+}$ and $[(bpy)_2(py)Ru^{II}OH_2]^{2+}$, have

been described in depth, particularly by Meyer and co-workers. The spectroscopic properties, oxidation potentials, and comproportionation/disproportionation reactions of these complexes have been extensively studied.[5] Many previous studies have proposed a variety of mechanistic pathways available to $\mathbf{Ru{=}O^{2+}}$ (and $[(bpy)_2(py)Ru^{III}OH]^{2+}$, also capable of oxidizing many of the substrates under investigation). These studies have suggested that $\mathbf{Ru{=}O^{2+}}$ can oxidize substrates via quite a variety of separate mechanisms, including hydrogen atom abstraction, proton-coupled electron transfer, oxygen atom transfer (including epoxidation), and hydride abstraction. The reactions studied have involved the oxidation of O-H bonds – H_2O_2, 2-propanol, hydroquinone, phenol, and benzyl alcohol – as well as oxidation of C-H bonds – cumene, toluene, stilbene, norbornene, styrene, cyclohexene and indene.[2,4,6,7] Recent results in our group have indicated that the previously reported mechanism of nucleophile-assisted hydride transfer for the oxidations of toluene and cumene by $\mathbf{Ru{=}O^{2+}}$ is incorrect (Chapter 3). These results have been confirmed by the Meyer laboratory and a joint publication is planned.[8] In the studies of stilbene, norbornene and styrene, primarily epoxidation products were observed, but the appearance of benzophenone and diphenylacetaldehyde in the oxidations of *cis*- and *trans*-stilbene could not be fully explained.[6] The oxidations of indene and cyclohexene have been proposed to occur by oxygen-atom insertion into the organic C-H bond.[7] Very little attention has been paid to the possibility of hydrogen-atom abstraction as a primary mechanism of the oxidation of C-H bonds by $\mathbf{Ru{=}O^{2+}}$.

The affinity of $[(bpy)_2(py)Ru^{IV}O]^{2+}$ for a hydrogen atom can be calculated using a thermodynamic cycle (eq 2.1, in H_2O with potentials vs. NHE).[9]

$$BDE = 23.06\ E^\circ + 1.37\ pK_a - C, \qquad C = -57 \pm 2\ \text{kcal/mol}$$

$$\text{where } C = \Delta H^\circ\{H\bullet(g) \rightarrow \tfrac{1}{2} H_2(g)\} - \Delta H^\circ\{H\bullet(g) \rightarrow H\bullet(aq)\} - \tfrac{1}{2} TS^\circ\{H_2(g)\} \qquad (2.1)$$

Figure 2.1 shows the various electrochemical potentials known for this system.[10] Using equation 2.1 with these values gives bond dissociation energies for **Ru=O**$^{2+}$ and **Ru-OH**$^{2+}$. **Ru=O**$^{2+}$ is a good hydrogen atom abstractor, thermodynamically, with an O-H bond dissociation enthalpy (BDE) of 84 ± 2 kcal/mol.[11,12] Addition of a hydrogen atom to **Ru=O**$^{2+}$ gives the hydroxo compound $[(bpy)_2(py)Ru^{III}OH]^{2+}$ (**Ru-OH**$^{2+}$), also capable of hydrogen atom abstraction with an O-H BDE of 82 ± 2 kcal/mol.[12] These values are higher than the hydrogen-atom affinities of both MnO_4^- (80 ± 3 kcal/mol)[9] and Fe^{III}(Hbim) (76 ± 2 kcal/mol)[14b] reported by our lab.

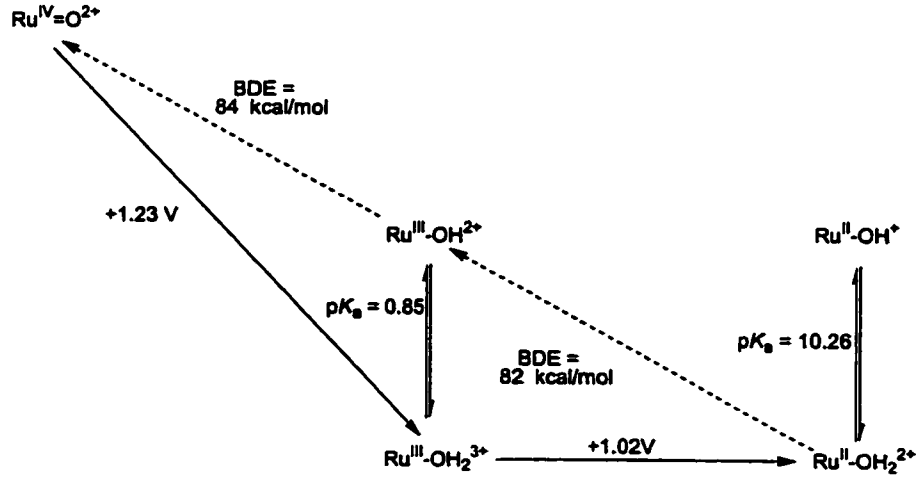

Figure 2.1. Aqueous oxidation potentials (at pH 0) and pK_as in the $[(bpy)_2(py)Ru^{IV}O]^{2+}$ system.[5a,12] Oxidation potentials were originally reported vs. SCE but are given here vs. NHE.

The addition of a hydrogen atom to **Ru-OH**$^{2+}$ gives the aquo complex

$[(bpy)_2(py)Ru^{II}OH_2]^{2+}$ (**Ru-OH_2^{2+}**). In acetonitrile, **Ru-OH_2^{2+}** undergoes solvolysis ($k_{solv} = 1.66 \times 10^{-3}$ s^{-1})[5c] to form $[(bpy)_2(py)Ru^{II}CH_3CN]^{2+}$ (**Ru-CH_3CN^{2+}**). **Ru=O^{2+}** is also known to undergo a comproportionation reaction in the presence of **Ru-OH_2^{2+}** (eq 2.2, rate constants in acetonitrile).[5c]

$$\textbf{Ru=O}^{2+} + \textbf{Ru-OH}_2^{2+} \rightleftharpoons 2\textbf{Ru-OH}^{2+} \qquad \begin{matrix} k_f = 4.07 \times 10^3\ M^{-1}\ s^{-1} \\ k_r = 80.6\ M^{-1}\ s^{-1} \end{matrix} \qquad (2.2)$$

Reported here are studies of the oxidations of 9,10-dihyroanthracene, xanthene, and fluorene by **Ru=O^{2+}**. The products of the oxidations of xanthene and fluorene include the 9,9'-bixanthene and bifluorene dimers – hallmarks of radical chemistry. While oxygenated products are observed in these oxidations, a mechanism of oxygen-atom transfer cannot fully explain the appearance of these radical dimerization products. We propose a mechanism of initial hydrogen-atom abstraction followed by competitive pathways of radical dimerization and radical trapping by the oxidant. Our investigation of these hydrocarbon oxidations displays a clear correlation between the rate of oxidation and the C-H bond dissociation energy (BDE) of the organic substrate. Previous work in the Mayer group has shown correlations between the reactivity of oxidants in hydrogen transfer reaction with thermodynamic driving force.[13]

Also reported is an extension of previous work applying the Marcus cross relation to hydrogen-atom transfer.[14] The hydrogen-atom self-exchange rate of this ruthenium system (**Ru=O^{2+}/Ru-OH^{2+}**) has been studied by dynamic ^1H NMR line-broadening.[15] A rough estimation of the calculated hydrogen-atom abstraction rate for DHA, using this value and the cross relation, is in good agreement with the experimentally determined value.

Results

Oxidations of Organic Substrates and Product Characterization. The oxidations of xanthene, 9,10-dihydroanthracene (DHA), and fluorene by **Ru=O**$^{2+}$ were carried out under nitrogen at room temperature in dry acetonitrile. Reactions were complete within minutes and a mixture of organic products were observed for each reaction. Organic products were characterized by GC/MS and quantitated using calibrated GC/FID response factors with naphthalene as an internal standard. Yields were reproducible in samples analyzed after extended periods of time (6-24 hrs.). The inorganic products were characterized by UV-vis and/or NMR spectroscopies.

DHA is oxidized rapidly (within seconds) to give a mixture of anthracene, anthrone, and anthraquinone, with anthracene as the major product (eq 2.3). The product distributions depend on the initial concentrations of oxidant and substrate (see below). Independent reactions (described below) show that **Ru=O**$^{2+}$ is capable of further oxidizing anthracene and anthrone to anthraquinone. These reactions were typically carried out with 1-2 mM **Ru=O**$^{2+}$ and 1-10 mM substrate. In order to determine the source of oxygen in the oxygenated products, additional reactions were carried out with 10 mM added $H_2{}^{18}O$. In oxidations of DHA by **Ru=O**$^{2+}$, anthraquinone shows 2% ^{18}O incorporation by GC/MS from the intensity of the $(M+2)^+$ vs. M^+ ions in comparison to reactions in which no labeled water was added. No incorporation into anthrone was detected.

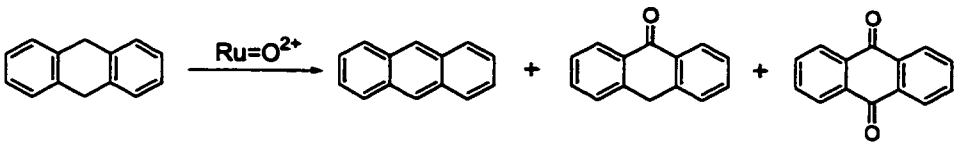

(2.3)

Xanthene reacts with **Ru=O**$^{2+}$ within seconds to give a mixture of products, as well. These reactions were carried out in the same range of concentrations as the DHA reactions and give xanthone and 9,9'-bixanthene as the only detected products (eq 2.4). Xanthone is the major product, and upon addition of 10 mM $H_2{}^{18}O$ only 2% incorporation of ^{18}O is observed.

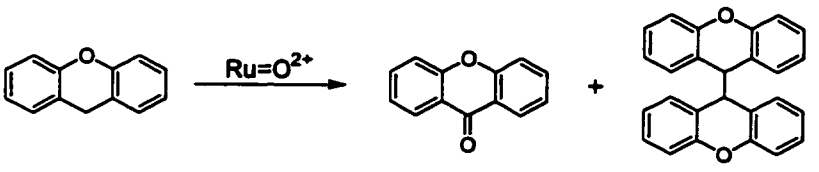

(2.4)

The reaction of **Ru=O**$^{2+}$ with fluorene is quite similar to the reaction with xanthene, but the reaction is about an order of magnitude slower (complete in about a minute in the concentration range given above for DHA and xanthene). The reaction produces fluorenone, bifluorene and very small amounts of bifluorenylidene, with fluorenone as the major product (eq 2.5). In experiments with added $H_2{}^{18}O$, <1% ^{18}O incorporation into fluorenone is observed.

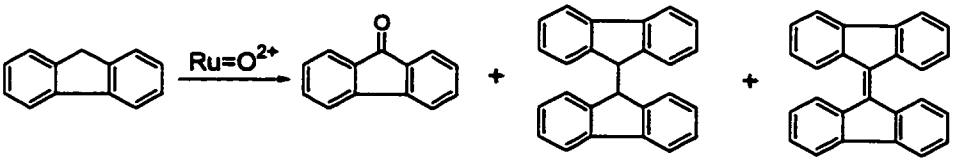

(2.5)

The initial ruthenium products of these reactions appear to be a mixture of **Ru-OH$_2$**$^{2+}$ and the known acetonitrile complex **Ru-CH$_3$CN**$^{2+}$, converting quantitatively over time to **Ru-CH$_3$CN**$^{2+}$ as the aquo complex undergoes solvolysis (k_{solv} = 1.66 × 10^{-3} s^{-1}, $t_{1/2}$ = 7 min.).[5c] After several hours, 100% conversion of **Ru=O**$^{2+}$ to **Ru-CH$_3$CN**$^{2+}$

is observed by UV-vis using the extinction coefficient for **Ru-CH_3CN^{2+}** reported by Meyer (λ_{max} 440 nm, $\varepsilon = 8160\ M^{-1}\ cm^{-1}$).[5c]

In order to determine the effect of different starting concentrations on product yields, reactions were performed with varying initial **Ru=O^{2+}** concentrations and varying initial organic substrate concentrations. For the oxidation of DHA by **Ru=O^{2+}**, product yields at various concentrations of DHA and oxidant are listed in Table 2.1. Table 2.1 also contains the amount of oxidative equivalents consumed in the reaction. This value is calculated by multiplying the concentration of the organic product by the number of **Ru=O^{2+}** equivalents required to produce it (1 equivalent for anthracene, 2 for anthrone, and 4 for anthraquinone), summing these values for all products and dividing by the initial concentration of **Ru=O^{2+}**. Yields are accurate to ± 10%. Anthrone and anthraquinone production increases with increasing oxidant concentrations, while anthracene production increases steadily with increases in the amount of DHA initially used. At high substrate to oxidant ratios (10:1), no anthraquinone is detected (<~0.05mM). Less than quantitative consumption of oxidative equivalents may be due, in part, to the slow decomposition of **Ru=O^{2+}** during storage and in solution – possibly to the μ-oxo dimer $[(bpy)_2(py)Ru^{III}\text{-}O\text{-}Ru^{III}(py)(bpy)_2]^{4+}$.[5c]

Table 2.1. Yields of products formed from the reaction of $Ru{=}O^{2+}$ with DHA.

$[Ru{=}O^{2+}]$:[DHA] (mM)	[Anthrone] produced (mM) (% of oxidant)	[Anthraquinone] produced (mM) (% of oxidant)	[Anthracene] produced (mM) (% of oxidant)	Total % oxidant
1:1	0.06 (12)	0.06 (24)	0.39 (39)	75
1:2	0.11 (22)	0.05 (20)	0.55 (55)	97
1:4	0.09 (18)	0.03 (12)	0.70 (70)	100
1:10	0.09 (18)	<0.01 (<4%)	0.87 (87)	105
2:4	0.17 (17)	0.11 (22)	1.10 (55)	94
4:4	0.30 (15)	0.30 (30)	1.33 (33)	78

In the reactions of $Ru{=}O^{2+}$ with xanthene at varied xanthene concentrations, the yield of 9,9'-bixanthene increased with increasing xanthene concentration, while xanthone production remained essentially constant (see Table 2.2). With increasing concentrations of the oxidant, bixanthene and xanthone are produced in increasing amounts. The reasons for the lower values of total oxidant consumed are not clear. Presumably further oxidation of bixanthene may play a role, but this was not investigated independently.

Table 2.2. Yields of products formed from the reaction of $Ru{=}O^{2+}$ with xanthene. The number of $Ru{=}O^{2+}$ equivalents required to produce each product are 2 for xanthone and 1 for bixanthene.

[$Ru{=}O^{2+}$]:[Xanthene] (mM)	[Xanthone] produced (mM) (% of oxidant)	[Bixanthene] produced (mM) (% of oxidant)	Total % oxidant
1:1	0.36 (72)	0.013 (1.3)	73.3
1:2	0.35 (70)	0.019 (1.9)	71.9
1:4	0.31 (62)	0.025 (2.5)	64.5
1:10	0.38 (76)	0.036 (3.6)	79.6
2:4	0.66 (66)	0.045 (2.3)	68.3
4:4	1.31 (65.5)	0.045 (1.1)	66.6

The product yields from reactions of fluorene with $Ru{=}O^{2+}$ at various concentrations are presented in Table 2.3. In these reactions, bifluorene production increases with increasing fluorene concentration while fluorenone production increases with increasing oxidant concentration. Again, the less than quantitative conversion based on initial oxidant concentration may be a result of further oxidation of the bifluorene. This is supported by the observation of bifluorenylidene, but the amounts produced were too small to accurately quantify.

Table 2.3. Yields of products formed from the reaction of $Ru{=}O^{2+}$ with fluorene. The number of $Ru{=}O^{2+}$ equivalents required to produce each product are 1 for bifluorene and 2 for fluorenone.

[$Ru{=}O^{2+}$]:[Fluorene] (mM)	[Fluorenone] produced (mM) (% of oxidant)	[Bifluorene] produced (mM) (% of oxidant)	Total % oxidant
1:1	0.37 (74)	0.011 (1.1)	76.8
1:2	0.33 (66)	0.014 (1.4)	67.4
1:4	0.31 (62)	0.017 (1.7)	63.7
1:10	0.33 (66)	0.023 (2.3)	68.3
2:4	0.63 (66)	0.027 (1.4)	67.4
4:4	1.25 (63)	0.027 (0.7)	63.7

The reactions of $Ru{=}O^{2+}$ with anthracene and anthrone were investigated as well. At 2 mM $Ru{=}O^{2+}$ and 4mM anthracene, 0.47 mM anthraquinone is produced (71% of $Ru{=}O^{2+}$ equivalents). This reaction occurs at a greatly reduced rate in comparison to the oxidation of DHA (30 minutes at room temperature for anthracene vs. 5 seconds for DHA). The Ru product of this reaction appears to be only $Ru\text{-}CH_3CN^{2+}$ as no $Ru\text{-}OH_2^{2+}$ is observed by UV-vis, consistent with the timescale of the reaction being longer than that for solvolysis. Anthrone is oxidized by $Ru{=}O^{2+}$ quantitatively to anthraquinone (determined by GC/FID) in seconds to give a mixture of $Ru\text{-}OH_2^{2+}$ and $Ru\text{-}CH_3CN^{2+}$ (by UV-vis).

Kinetics. The kinetics of the reactions of $Ru{=}O^{2+}$ with DHA, anthracene, xanthene, fluorene, indene, cyclohexene, ethylbenzene and toluene were measured under pseudo-first order conditions (with the organic substrate in excess) in acetonitrile. The reactions were carried out at room temperature under an inert atmosphere and the appearance of Ru^{II} ($Ru\text{-}OH_2^{2+}$ and $Ru\text{-}CH_3CN^{2+}$) products was monitored by changes

in the UV-vis. Reactions with DHA, xanthene, fluorene, cyclohexene and indene required stopped-flow measurements as these were typically complete in a few seconds to a few minutes. Anthracene, ethylbenzene and toluene kinetics were measured on a diode array UV-vis spectrophotometer over 30 minutes to several hours. Reactions with toluene and ethylbenzene required several hours to reach completion, even with 2500-fold excess substrate (0.5 M). **Ru=O**$^{2+}$ is known to decompose slowly in acetonitrile (over 24 hours or more),[5c] but not appreciably during the timescale of kinetics measurements. Kinetics traces were fitted with SPECFIT, a global analysis software package, using a multi-exponential fit. The rapid reactions with DHA, xanthene and indene could be fit with a biexponential model A $\rightarrow$ B, B $\rightarrow$ C. The slower reaction of **Ru=O**$^{2+}$ with fluorene required an additional step and was fitted with the model A $\rightarrow$ B, B $\rightarrow$ C, C $\rightarrow$ D. The calculated spectra returned by SPECFIT in the kinetic modeling of these reactions (see Figures 2.2-2.4), are consistent with the process **Ru=O**$^{2+}$ $\rightarrow$ Ru^{III}-species $\rightarrow$ Ru^{II} (a mixture of **Ru-OH$_2$**$^{2+}$ and **Ru-CH$_3$CN**$^{2+}$). The returned spectra are in good agreement with the known spectra of these complexes (Figure 2.5). The Ru^{III}-species is most likely **Ru-OH**$^{2+}$ or Ru-bound organic complexes. The ligand environment around the Ru^{III} species is not known, but the spectrum is consistent with previously reported spectra for Ru^{III} species.[5c] For example, the UV-vis spectrum of **Ru-OH**$^{2+}$ in water has a λ_{max} at 364 nm[5a] and 380 nm in CH_3CN, with very little absorbance in the 420-480 nm range.[5c] The final spectra of these reactions are consistent with a mixture of Ru^{II} species – **Ru-OH$_2$**$^{2+}$ and **Ru-CH$_3$CN**$^{2+}$ (and perhaps Ru-(O=X)). Ru^{II} species have a characteristic MLCT at ~450 nm. This is evident in the observed spectra for **Ru-OH$_2$**$^{2+}$ and **Ru-CH$_3$CN**$^{2+}$, as well as in the spectra returned by SPECFIT for the mixtures of products at the end of the

reactions. The xanthene reaction shows some of this characteristic absorbance in the returned spectrum for the end of the first phase of the reaction (A $\rightarrow$ B). In this rapid reaction, the spectrum returned for B is most likely a mixture of Ru^{III} and Ru^{II} species.

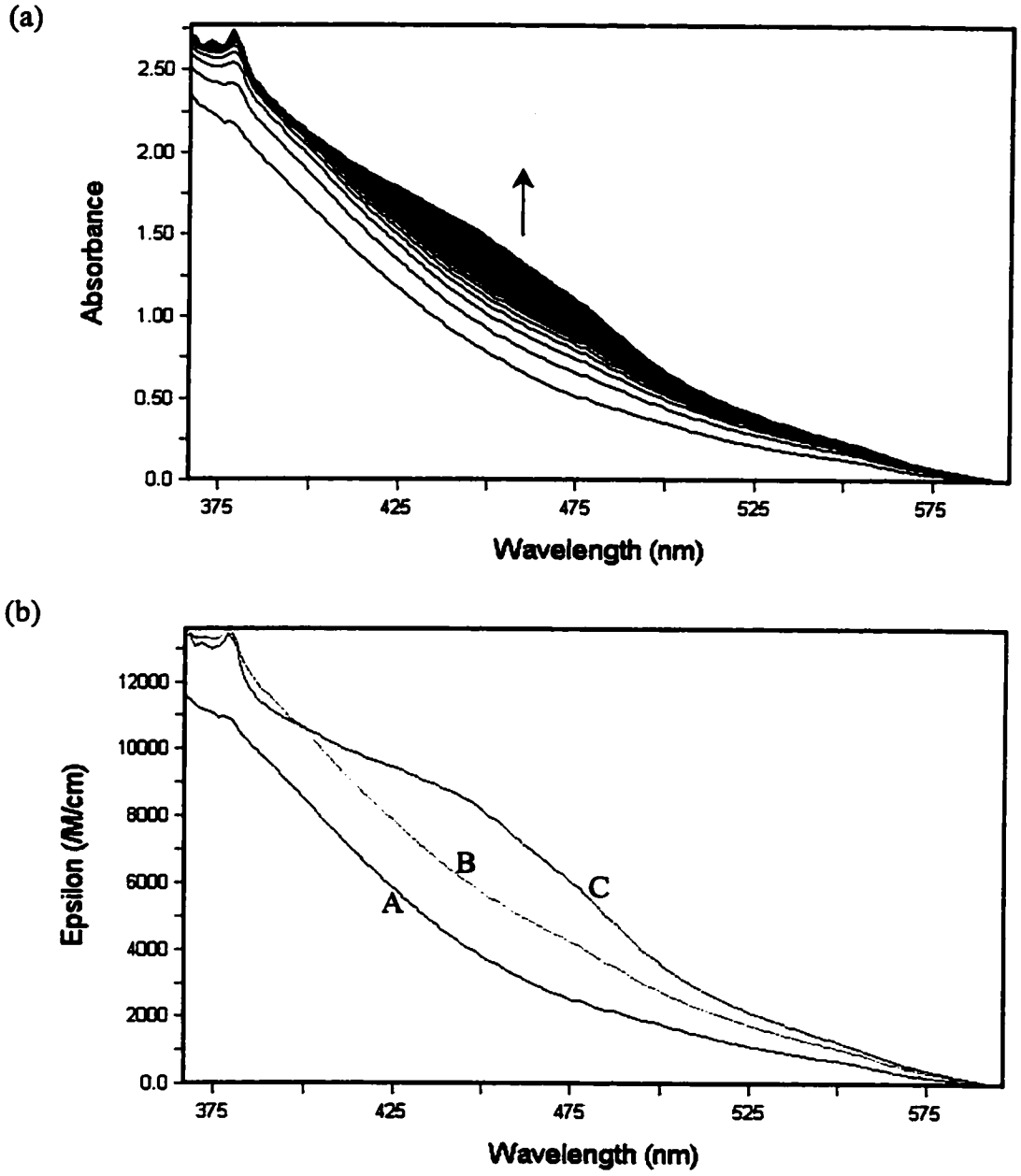

Figure 2.2. a) Spectral changes observed for the reaction of 0.2 mM $Ru{=}O^{2+}$ with 6 mM DHA over 30 s. b) Calculated spectra returned by SPECFIT for the phases A → B and B → C. c) Single wavelength trace of the data at 385.5 nm with SPECFIT fit.

(c)

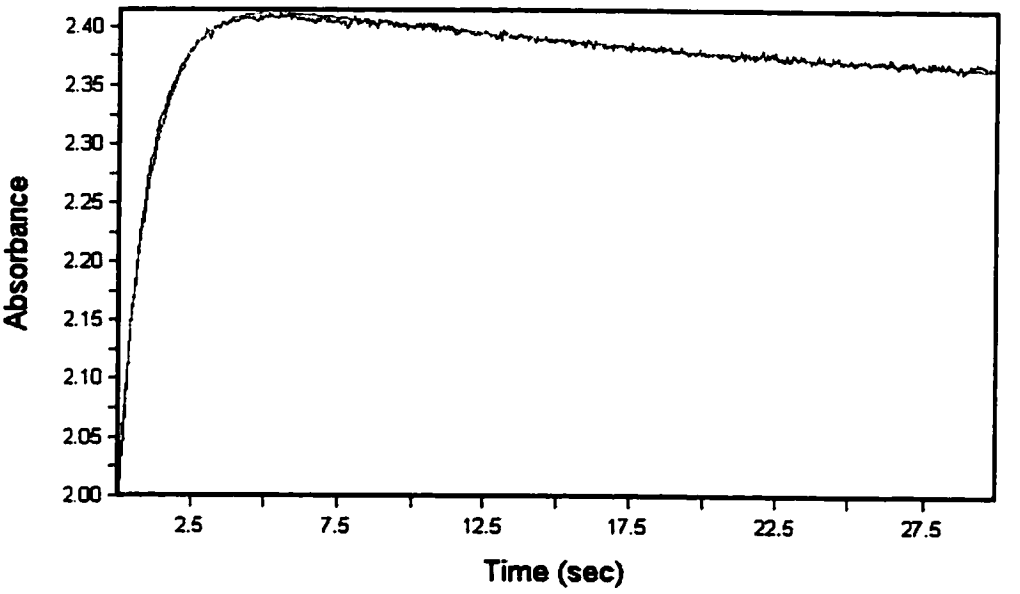

Figure 2.2 continued.

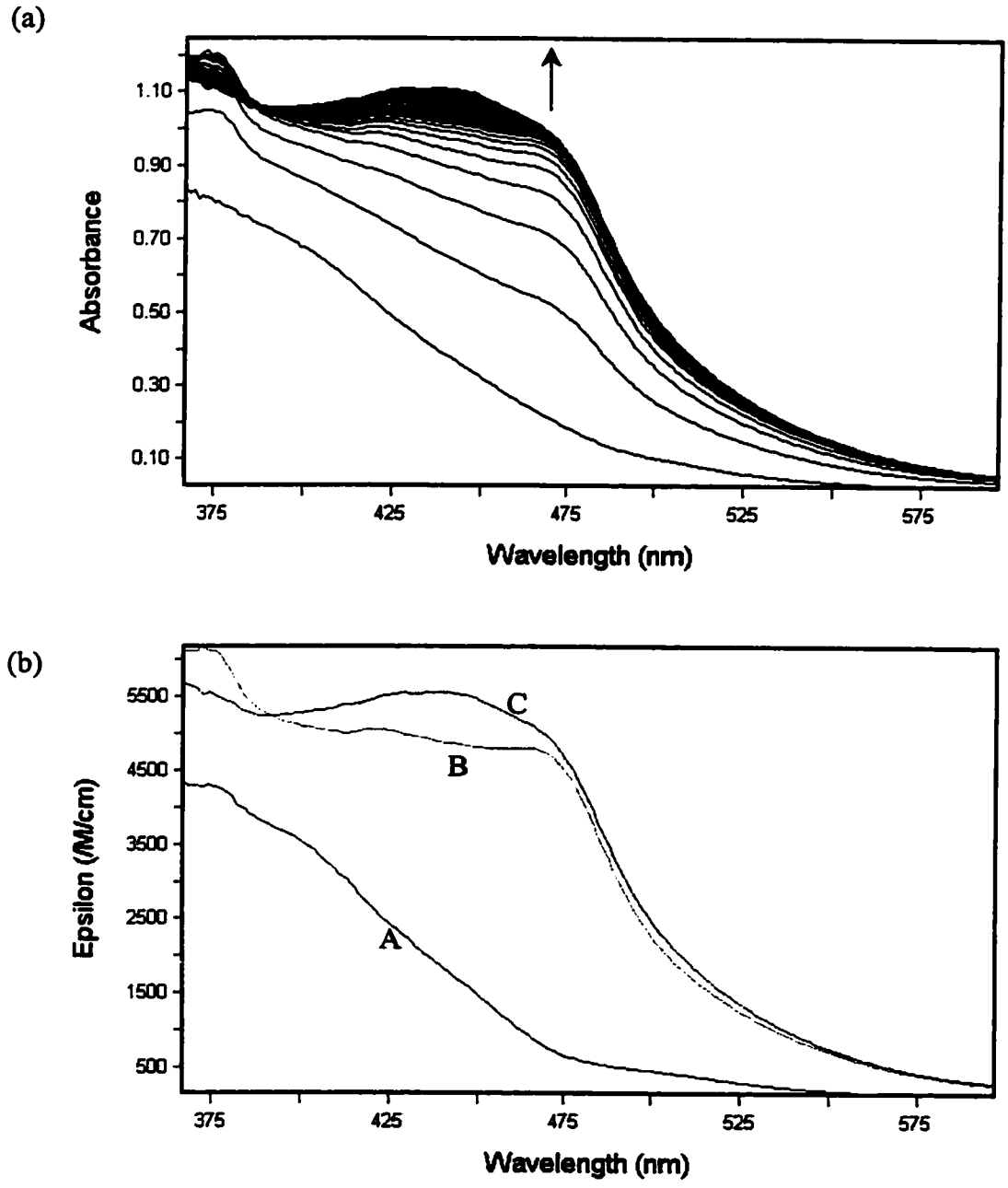

Figure 2.3. a) Spectral changes observed for the reaction of 0.2 mM **Ru=O**$^{2+}$ with 20 mM xanthene over 3 s (1000 scans/s). b) Calculated spectra returned by SPECFIT for the phases A → B and B → C. c) Trace of the data at 385.5 nm with SPECFIT fit.

(c)

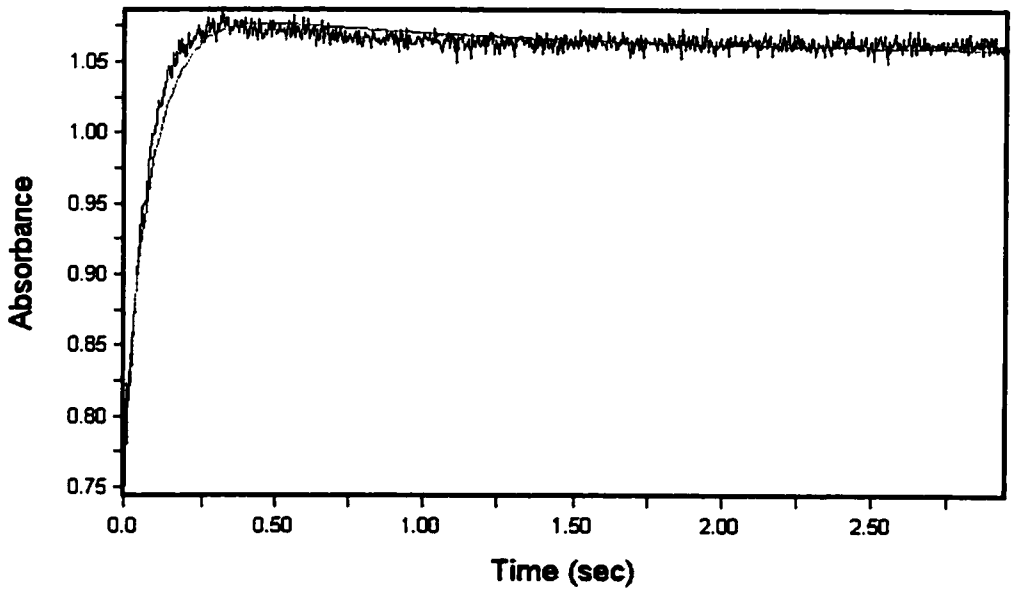

Figure 2.3 continued.

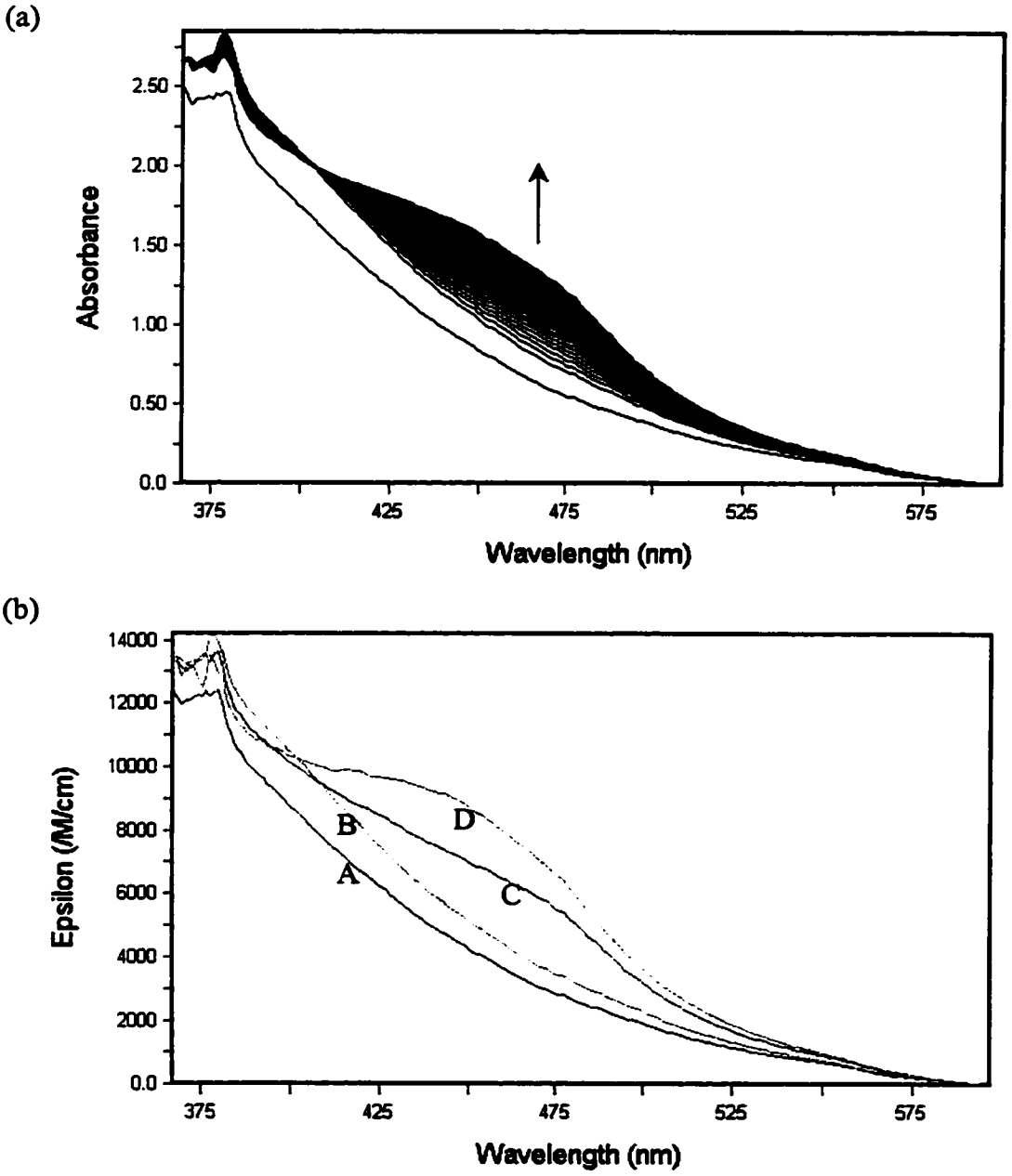

Figure 2.4. a) Spectral changes observed for the reaction of 0.2 mM $\mathbf{Ru{=}O^{2+}}$ with 40 mM fluorene over 120 s (21 scans/s). b) Calculated spectra returned by SPECFIT for the phases A → B, B → C and C → D. c) Trace of the data at 385.5 nm with SPECFIT fit.

(c)

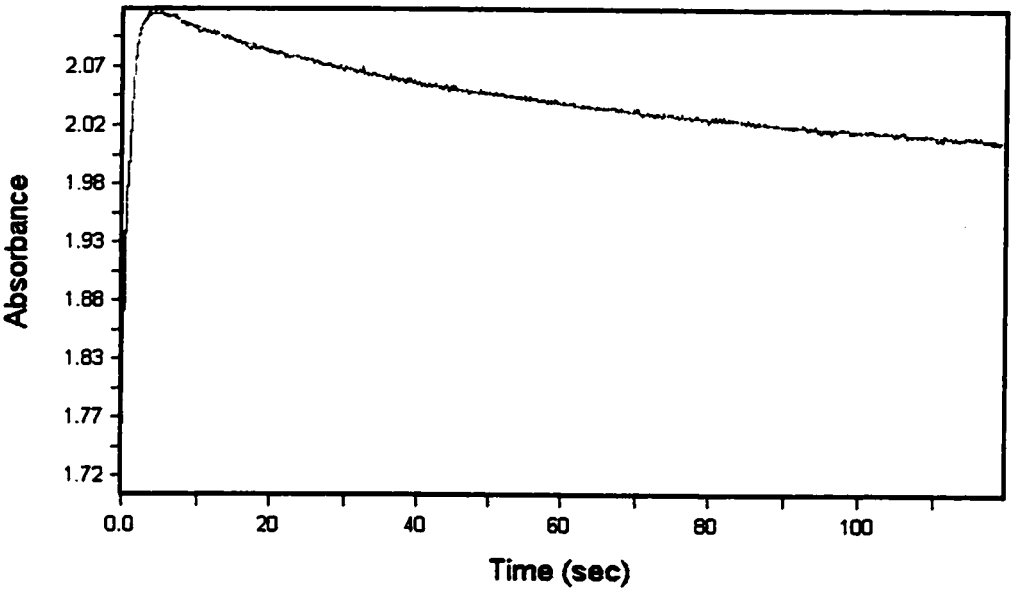

Figure 2.4 continued.

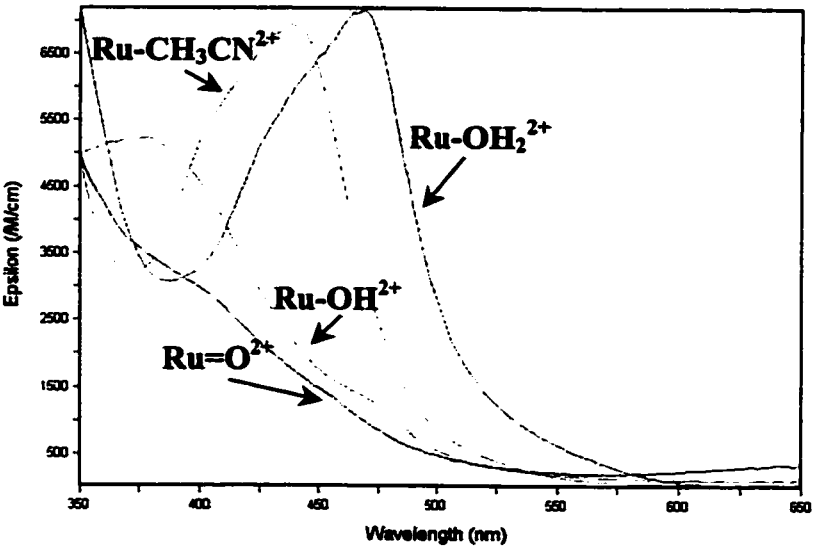

Figure 2.5. Observed spectra for **Ru=O^{2+}**, **Ru-OH^{2+}**, **Ru-OH$_2$$^{2+}$**, and **Ru-CH$_3$CN^{2+}**. **Ru-OH^{2+}** is produced by mixing a 1:1 ratio of **Ru=O^{2+}** with **Ru-OH$_2$$^{2+}$**. A small amount of **Ru-OH$_2$$^{2+}$** is present in the spectrum.

These kinetic models give first-order rate constants for the fast, initial phase of the reactions. A plot of k_{obs}(A → B) vs. [DHA] is linear (Figure 2.6) and yields a second order rate constant, $k'_{DHA} = 125 \pm 8\ M^{-1}\ s^{-1}$. The rate of the slow phase (B → C) does not correlate with DHA concentration and varies from 0.027 s^{-1} to 0.79 s^{-1} (average k_{obs}(B → C) = 0.066 s^{-1}). Reactions with xanthene were treated in the same manner (Figure 2.6) and gave a second order rate constant $k'_X = 577 \pm 13\ M^{-1}\ s^{-1}$. The second, slow phase (B → C) has observed rates that vary from 0.19 s^{-1} to 1.66 s^{-1}. Fluorene reactions were fitted with the kinetic model A → B, B → C, C → D. A plot of k_{obs}(A → B) vs. [Fluorene] (Figure 2.6) yields a second order rate constant $k'_F = 21.9 \pm 1.8\ M^{-1}\ s^{-1}$. As in the reactions above, the rate of the B → C phase does not appear to correlate with initial fluorene concentration. It does, however, appear to be slower than that of the rates observed in the DHA and xanthene reactions, varying from 0.014 s^{-1} to 0.065 s^{-1}. The C → D phase is similar in rate to the solvolysis of **Ru-OH_2^{2+}** to for **Ru-CH_3CN^{2+}**. The observed C → D rate is $2.8 \times 10^{-3}\ s^{-1}$ (varying from $5.8 \times 10^{-5}\ s^{-1}$ to $7.8 \times 10^{-3}\ s^{-1}$), not far from the reported solvolysis rate of $1.66 \times 10^{-3}\ s^{-1}$.[5c] Kinetic fits of single wavelength traces of these reactions at short times give good agreement with the rates for the A → B phase returned by SPECFIT.

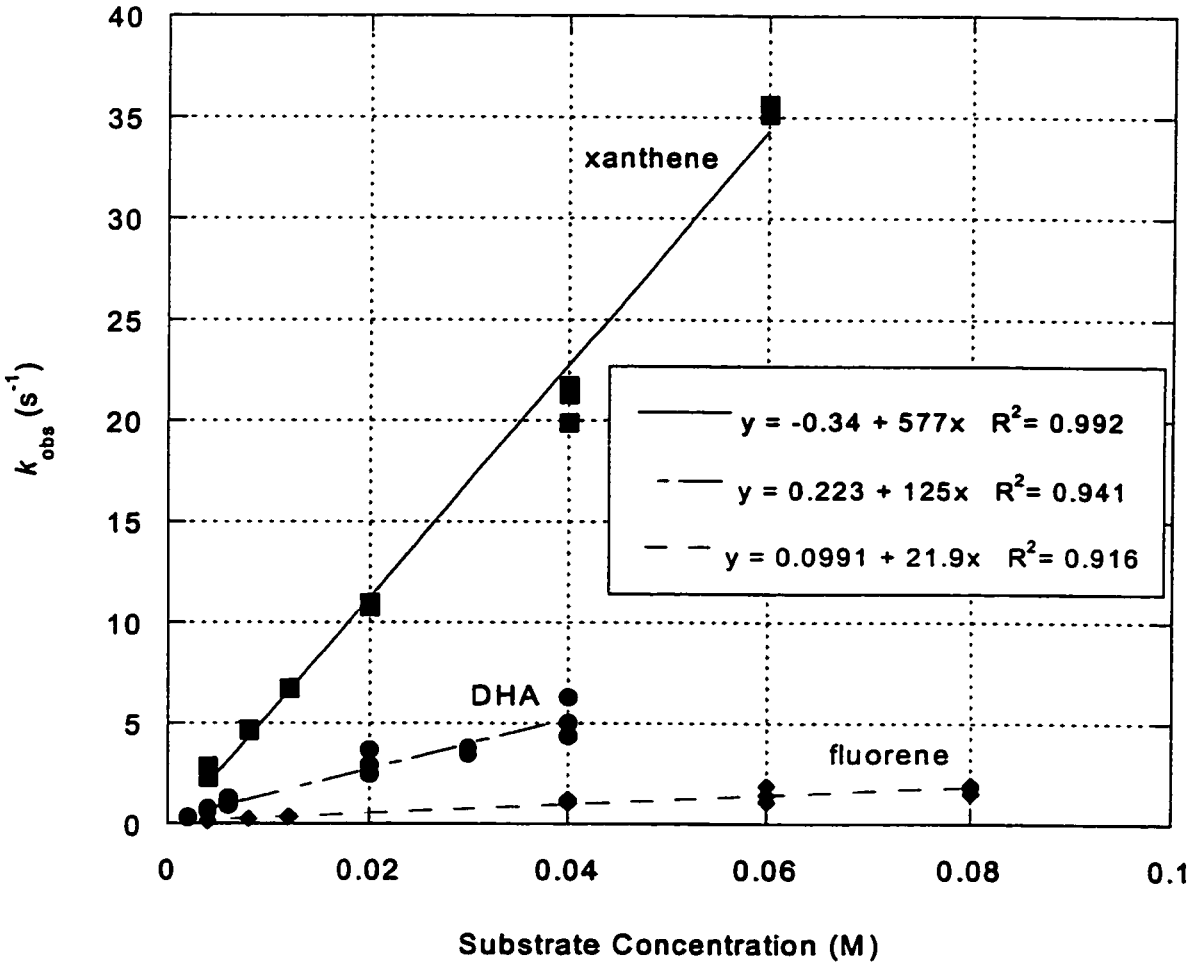

Figure 2.6. Plot of k_{obs} vs. concentration for reactions of $\mathbf{Ru{=}O^{2+}}$ with xanthene, DHA, and fluorene.

All three oxidation reactions display first order dependence of the A → B phase on the organic substrate and follow the rate law

$$\text{Rate} = k[\text{RH}][\text{Ru}^{\text{IV}}] = k_{obs}[\text{Ru}^{\text{IV}}] \qquad (2.6)$$

evidenced by the fact that graphs of log(k_{obs}) vs. log[substrate] are linear with a slope near unity and intercepts equal to logk' (Figure 2.6).

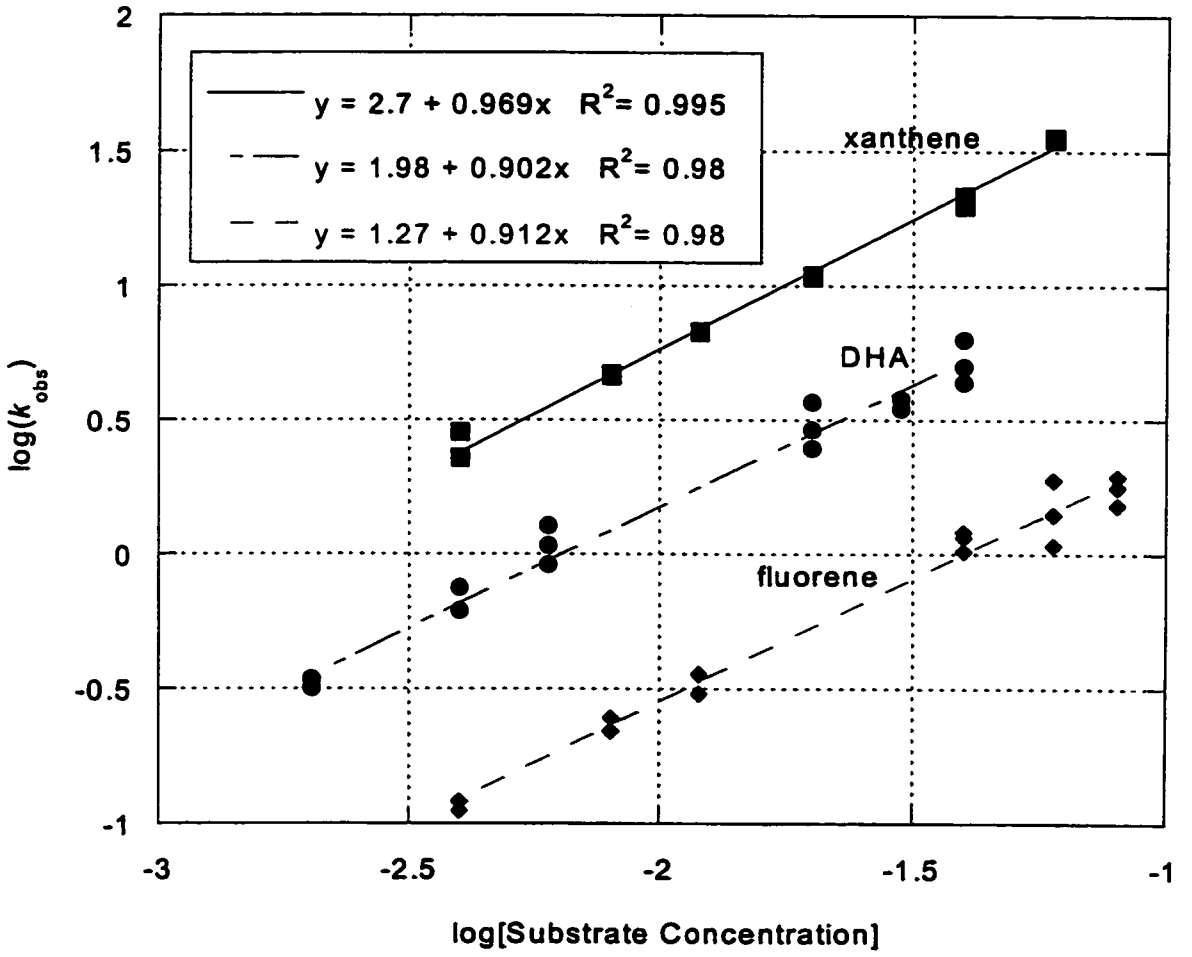

Figure 2.7. Plot of log(k_{obs}) vs. log(substrate concentration) for reactions of **Ru=O**$^{2+}$ with xanthene, DHA, and fluorene.

The rates of oxidation of toluene, ethylbenzene, cyclohexene and indene were measured at several concentrations. The reactions were analyzed in the same manner as the xanthene and DHA reactions. Toluene is oxidized over a period of hours at k'_{tol} = (6.4 ± 0.6) × 10^{-3} M^{-1} s^{-1}. This value is in marked contrast to the previously reported

oxidation rate of 5×10^{-5} M^{-1} s^{-1} for the oxidation of toluene by **Ru=O**$^{2+}$.[4b] This is not unreasonable since the reaction reported by Meyer was done in air-saturated solutions and many of the results reported in the original paper have been difficult to reproduce by our group and Meyer's (a joint publication is planned for the reinvestigation of the oxidation of cumene by **Ru=O**$^{2+}$).[8] The oxidation of toluene gives benzaldehyde (and possibly benzoic acid, though it was not observed by GC/FID or GC/MS). Ethylbenzene is also oxidized slowly (several hours) at $k'_{EB} = (2.2 \pm 0.2) \times 10^{-2}$ M^{-1} s^{-1}. Cyclohexene is oxidized over several minutes at $k'_{CH} = (9.2 \pm 1.2) \times 10^{-1}$ M^{-1} s^{-1}. Indene is oxidized on the stopped-flow time scale (seconds) at $k'_{ind} = 10.8 \pm 1$ M^{-1} s^{-1} to give indenone as the only product (by GC/MS). This rate constant is identical, within the error limits, to the value reported by Meyer and coworkers.[7] Meyer reports a second-order rate constant of 5.74 ± 0.4 M^{-1} s^{-1} which takes into account a stoichiometric factor of 2 for the oxidation of indene to indenone by **Ru=O**$^{2+}$. A summary of rate constants (for A→B, the initial, fast phase) is presented in Table 2.4.

Table 2.4. Rate constants for the oxidation of organic substrates by **Ru=O**$^{2+}$. Rate constants are for the initial phase, A → B.

Substrate	Oxidation Rate Constant (M^{-1} s^{-1})
Xanthene	5.77×10^{2}
DHA	1.25×10^{2}
Fluorene	2.19×10^{1}
Indene	1.08×10^{1}
Cyclohexene	9.2×10^{-1}
Anthracene	2.7×10^{-1}
Ethylbenzene	2.2×10^{-2}
Toluene	6.4×10^{-3}

Activation parameters were measured for the oxidation of xanthene by **Ru=O**$^{2+}$ over a temperature range of 278 to 318 K. A plot of ln(k/T) vs. 1/T (Figure 2.8) yields $\Delta H^{\ddagger} = 4.9 \pm 1.0$ kcal mol^{-1} and $\Delta S^{\ddagger} = -30 \pm 5$ cal mol^{-1} K^{-1}. These values are similar in magnitude to those reported for other C-H bond oxidations by **Ru=O**$^{2+}$. For example, the oxidation of cyclohexene to 2-cyclohexen-1-one has activation parameters of $\Delta H^{\ddagger} = 7.4 \pm 0.1$ kcal mol^{-1} and $\Delta S^{\ddagger} = -34 \pm 3.4$ cal mol^{-1} K^{-1}.[7] The oxidation of *trans*-stilbene to *trans*-stilbene oxide by **Ru=O**$^{2+}$ has reported activation parameters of $\Delta H^{\ddagger} = 4.4 \pm 0.1$ kcal mol^{-1} and $\Delta S^{\ddagger} = -46 \pm 0.4$ cal mol^{-1} K^{-1}.[7]

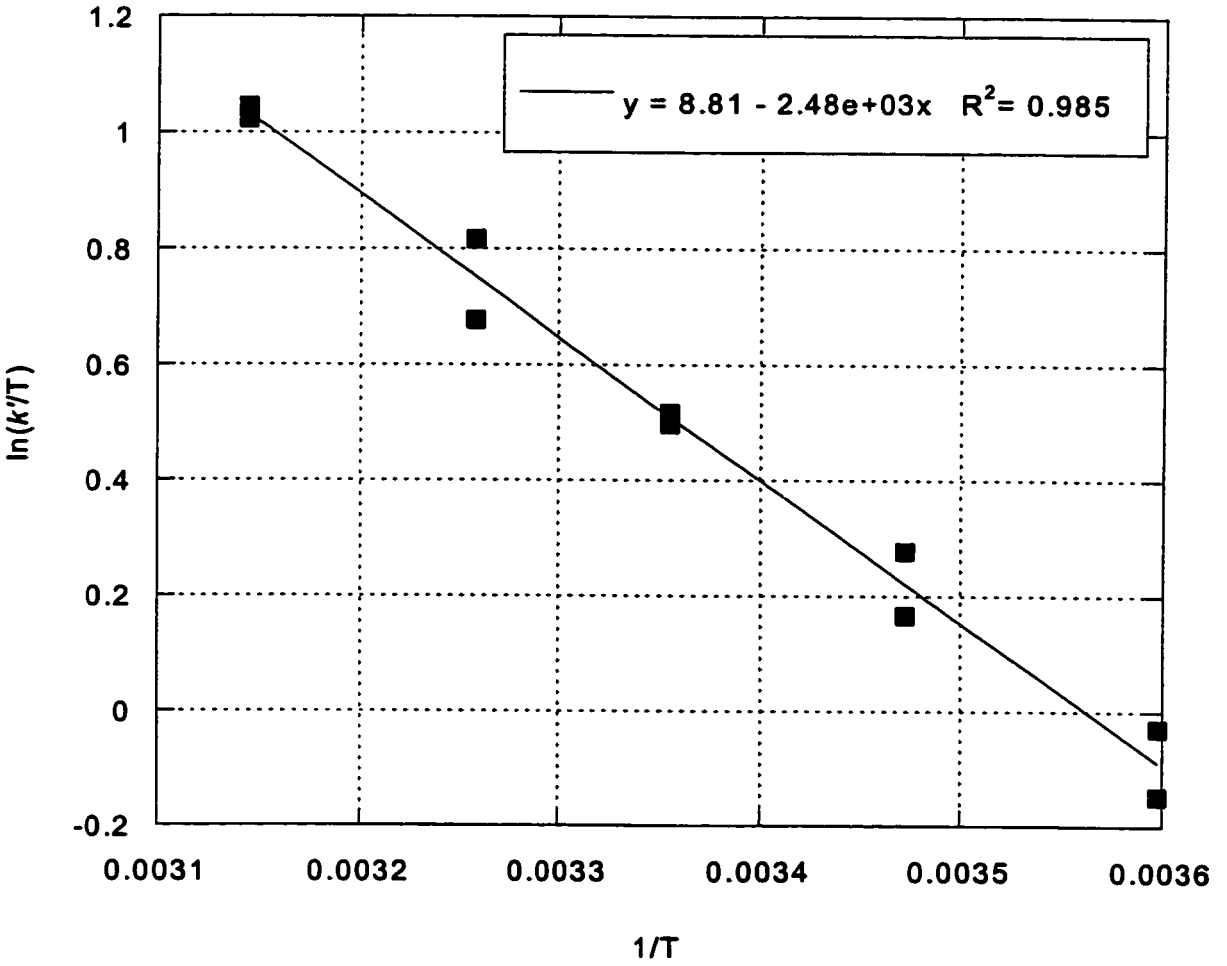

Figure 2.8. Eyring plot for the oxidation of xanthene by **Ru=O**$^{2+}$ (5-45 °C).

In order to check for the possible intermediacy of radicals in these reactions, the kinetics of the oxidation of xanthene by **Ru=O**$^{2+}$ in O_2-saturated solutions were also measured. Measurements were carried out in the stopped flow with 0.2 mM **Ru=O**$^{2+}$ and 20-60 mM xanthene. Data were analyzed as described above and gave a first-order rate constant $k'_{xan,O2}$ (A→B) = 340 ± 30 M^{-1} s^{-1}. This is a decrease in rate by almost half from the reaction rate under N_2 of k'_{xan} = 577 ± 13 M^{-1} s^{-1}.

The deuterium isotope effect for the oxidation of DHA versus DHA-d_4 was

measured over a range of concentrations and analyzed in a manner similar to that of the oxidation of DHA. The DHA-d_4 showed 98-99% deuterium enrichment by ^{1}H NMR. Reactions were complete within seconds, but were slower than the rate of oxidation of unlabeled DHA with an average $k'_{DHA\text{-}d4} = 3.6 \pm 0.4\ M^{-1}\ s^{-1}$. This gives a deuterium isotope effect for the oxidation of DHA $k_H/k_D = 35 \pm 1$. Because of this large value, the 1-2% residual H contributes to the reactivity of the DHA-d_4. Taking this into account (but ignoring secondary isotope effects), the actual k_H/k_D is between 50 (calculated for 1% residual H) and 100 (for 2% residual H).[16] A large deuterium isotope effect of $k_H/k_D = 21 \pm 1$ for the oxidation of cyclohexene by **Ru=O**$^{2+}$ has been reported.[7]

The reactions of **Ru=O**$^{2+}$ with anthracene and anthrone were measured in order to determine their roles as possible intermediates. The kinetics of the oxidation of anthracene are less complicated (spectroscopically) than the oxidations of DHA, xanthene, or fluorene, and can be fitted with a simple A → B model. Only one Ru product is evident in the UV-vis spectrum of this reaction, consistent with **Ru-CH$_3$CN**$^{2+}$ (Figure 2.9).

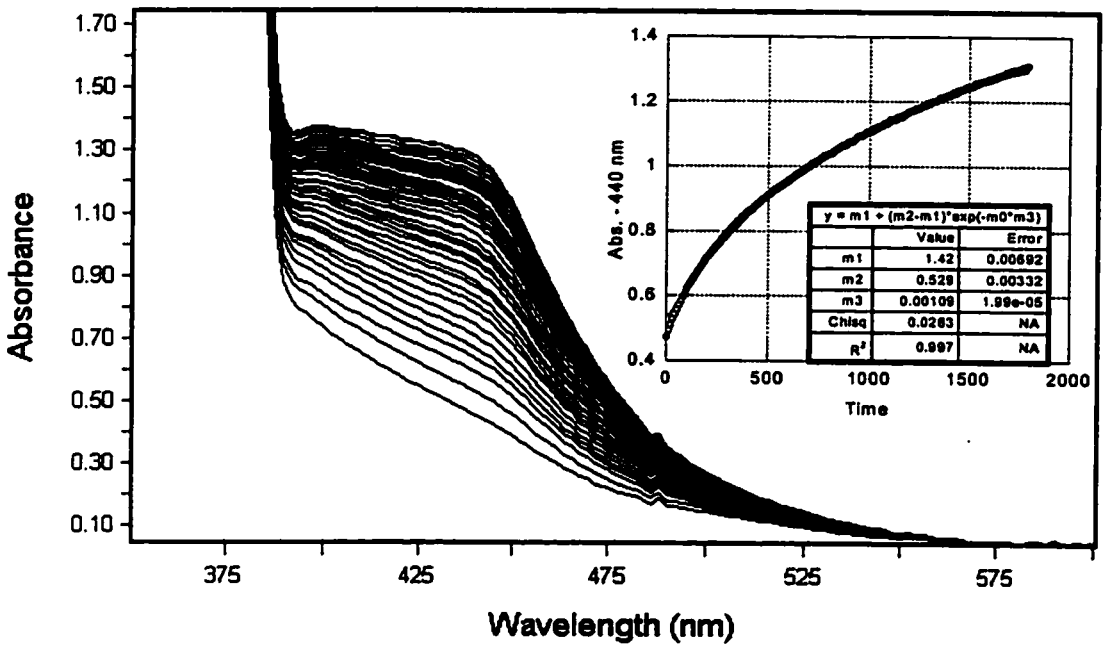

Figure 2.9. Stacked plot of the oxidation of anthracene – 0.2 mM **Ru=O**$^{2+}$:4 mM anthracene with inset of kinetics data from the reaction monitored at 440 nm.

Monitoring at 440 nm (λ_{max} for **Ru-CH$_3$CN**$^{2+}$) results in an observed rate, $k_{obs} = (1.09 \pm 0.02) \times 10^{-3}$ ($k'_{anth} = 0.27 \pm 0.03$ M^{-1} s^{-1}). See Table 2.4 for a list of rate constants. The oxidation of anthrone by **Ru=O**$^{2+}$ is quite rapid – complete within the mixing delay of the stopped-flow instrument. Assuming a first-order dependence on anthrone concentration, a lower limit for the rate constant of oxidation can be determined. Assuming three half-lives of the reaction are complete in the first 0.003 s of the reaction, the first order rate constant $k'_{anthrone} > \sim 10^5$ M^{-1} s^{-1}.

Self-Exchange Rates. The hydrogen-atom self-exchange rate for **Ru=O**$^{2+}$/**RuOH**$^{2+}$ was measured by dynamic NMR methods.[15] Addition of **Ru-OH$_2$**$^{2+}$ to a solution of **Ru=O**$^{2+}$ results in the formation of **Ru-OH**$^{2+}$ via the comproportionation/disproportionation reaction given in equation 2.2. The presence of

Ru-OH^{2+} results in the broadening of the proton resonances for the pyridyl ligands of **Ru=O^{2+}** because of the self-exchange reaction (Figure 2.10a and b).

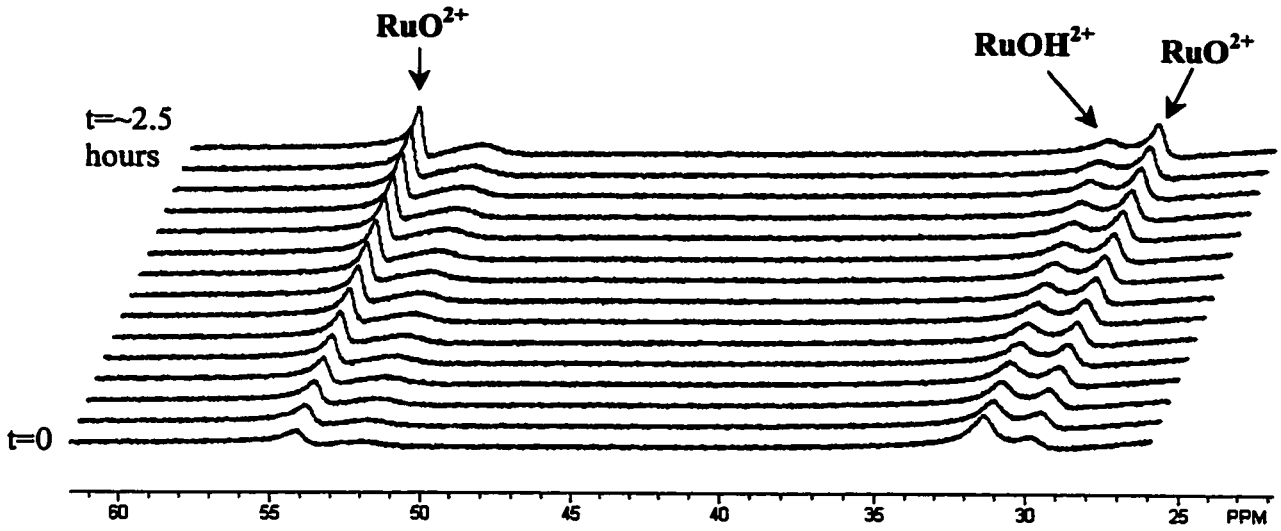

Figure 2.10a. Stack plot of the spectra obtained from the **Ru=O^{2+}/Ru-OH^{2+}** self-exchange experiments.

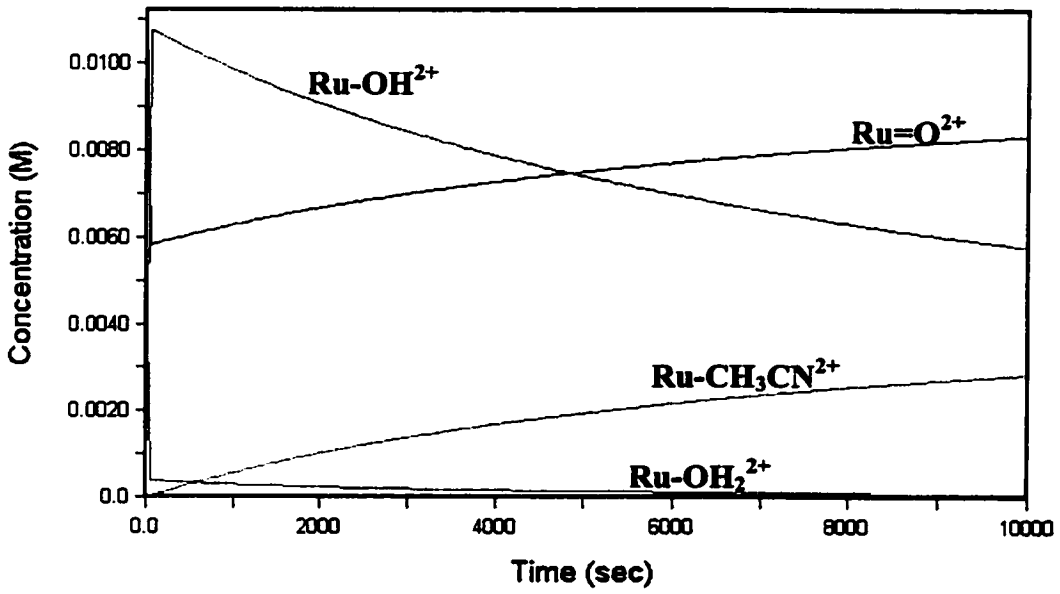

Figure 2.10b. Calculated concentration curve for the NMR tube self-exchange reaction based on initial concentrations of 11.2 mM **Ru=O**$^{2+}$ and 5.8 mM Ru-OH_2^{2+}.

As **Ru-OH_2**$^{2+}$ undergoes solvolysis in the CD_3CN solvent, the equilibrium shifts, the amount of **Ru-OH**$^{2+}$ decreases, and the line widths sharpen. Using an internal standard, the concentration of **Ru-OH**$^{2+}$ can be determined at various times. As a result, a range of concentrations of **Ru-OH**$^{2+}$ can be obtained over time in only one NMR tube. A plot of the increase in line width ($\pi\Delta W$) for two different resonances versus [**Ru-OH**$^{2+}$] is linear. These observations indicate that **Ru=O**$^{2+}$ and **Ru-OH**$^{2+}$ undergo chemical exchange on the NMR time-scale. This process is a net hydrogen-atom self-exchange (proton-coupled electron transfer), as these complexes differ only by H$^{\bullet}$. The slope of the line for two runs with different batches of Ru starting materials and measured at two different proton resonances yields an average self-exchange rate constant of k'_{HSE} = (7.6 ± 0.4) × 10^4 M^{-1} s^{-1} (Figure 2.11).

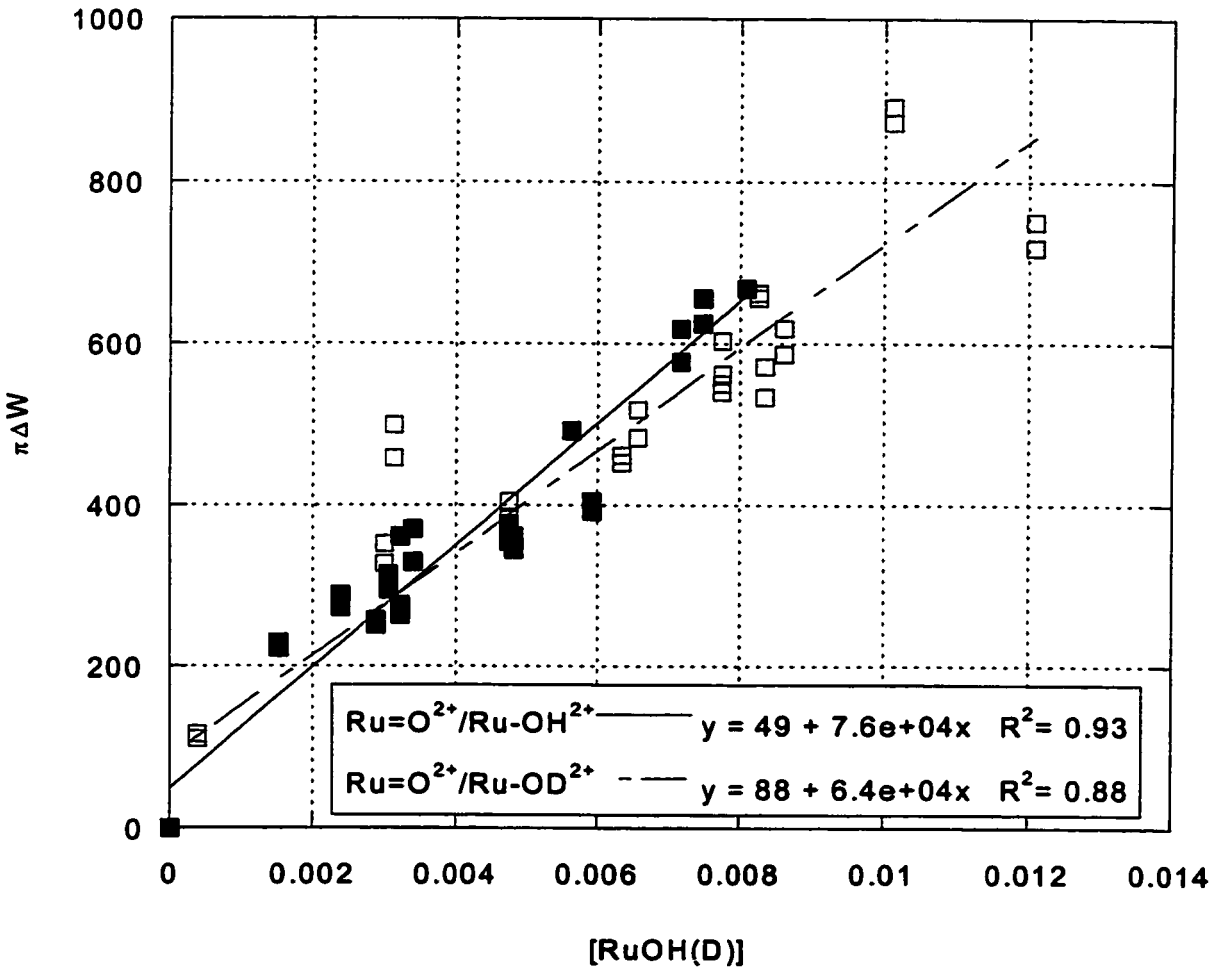

Figure 2.11. Graph of $\pi\Delta W$ vs. [RuOH(D)] for the hydrogen-atom (■) and deuterium-atom (□) self-exchanges for all runs (2 of each).

The same procedure was carried out with the addition of **Ru-OD$_2^{2+}$** in order to determine the deuterium-atom self-exchange rate. **Ru-OD$_2^{2+}$** was synthesized from [(bpy)$_2$(py)RuCl]PF$_6$ following the literature procedure[5b] for the synthesis of **Ru-OH$_2^{2+}$**, but substituting D_2O for water in all cases. Only one batch of **Ru-OD$_2^{2+}$** was synthesized and it was stored in a vial in the dry box between experiments. The integral

for H_2O in the CD_3CN reaction solution remained constant throughout the experiment indicating nearly quantitative D_2O incorporation into the starting material (solvolysis of **Ru-OH$_2^{2+}$** by CD_3CN increases the amount of free H_2O in the sample). The CD_3CN used in the experiment was dried thoroughly over CaH_2 and P_2O_5 and the NMR indicated only a small amount (<0.5 mM) of H_2O present in the solvent. A plot of the increase in line width ($\pi\Delta W$) for two different resonances versus [**Ru-OD^{2+}**] is linear and gives a self-exchange rate constant of $k'_{DSE} = (6.4 \pm 0.4) \times 10^4\ M^{-1}\ s^{-1}$ (Figure 2.11). This gives a self-exchange isotope effect $k'_{HSE}/k'_{DSE} = 1.2 \pm 0.1$.

Discussion

Overview of the Reactions. $[(bpy)_2(py)Ru^{IV}O]^{2+}$ is an extensively studied oxidant that is known to oxidize a wide variety of substrates.[4,6,7] The possibility of hydrogen-atom abstraction as a possible mechanism for C-H bond oxidation by **Ru=O^{2+}** has been overlooked in many mechanistic studies of this oxidant. Furthermore, mechanisms of hydride transfer and oxygen-atom insertion have not fully explained all of the experimental evidence available in these reactions. This study of a wide range of hydrocarbons with oxidizable C-H bonds has perhaps shed more mechanistic light on this versatile oxidant.

In this system, the presence of both oxygen and non-oxygen added products indicates two possible pathways for the oxidation of these organic substrates – an oxygen-atom transfer and a net hydrogen-atom abstraction. The addition of an oxygen atom to the organic substrate may involve oxidation of the substrate followed by addition of water and subsequent proton loss, oxygen-atom transfer directly from the metal, or the involvement of O_2. Since the reactions presented here are carried out in

the absence of atmospheric O_2, the only sources of oxygen are water and the metal complex, **Ru=O**$^{2+}$. No incorporation of ^{18}O is observed when $H_2{}^{18}O$ is added to the reaction solutions, indicating that **Ru=O**$^{2+}$ is the only source of oxygen atoms. In this system, the resulting organic product from oxygen-atom transfer is the ketone – xanthone, fluorenone, anthrone, anthraquinone, and indenone. Net hydrogen-atom abstraction may be accomplished as removal of a proton and an electron simultaneously (hydrogen-atom abstraction), or stepwise. In this case, the organic products are dimers – 9,9'-bixanthene and bifluorene – or in the case of DHA, the fully aromatic anthracene.

Mechanistic Considerations. The presence of dimerization products in the oxidations of xanthene and fluorene (as 9,9'-bixanthene and bifluorene) by **Ru=O**$^{2+}$ indicates the intermediacy of radicals in these processes. This intermediacy is further supported by the change in the rate of oxidation of xanthene in oxygen-saturated solutions, a classic test for the presence of radical intermediates. The large deuterium isotope effect for the oxidation of DHA-d_4 ($k_H/k_D \geq 35 \pm 1$) indicates that C-H bond breaking is an important part of the rate-limiting step. These data, combined with the observance of Ru^{III} species as the inorganic intermediates, consistent with an initial one electron oxidation step, all point to a mechanism of initial hydrogen-atom abstraction. The appearance of oxygenated compounds as products of the reactions, however, must also be accounted for. Previous work has suggested **Ru=O**$^{2+}$ insertion into the substrate C-H bond as the mode of oxygenation for some substrates (cyclohexene and indene).[1,7] In this system, however, the presence of products that do not undergo O-atom transfer argues against C-H insertion as the only mechanism of oxidation. The most likely explanation for the oxygenated products, and the only one supported by all the experimental data – such as the dependence of product distributions on oxidant and

substrate initial concentrations – is that of trapping of the organic radical by the oxidant – a process that is competitive with radical-radical dimerization. Trapping by the oxidant is further supported by the results of labeling studies.

The comproportionation/disproportionation equilibrium reaction given in equation 2.3 is most likely not a kinetically important source of **Ru-OH**$^{2+}$ at high concentrations of DHA and xanthene – at these concentrations $t_{1/2}$(oxidation) < $t_{1/2}$(comproportionation). For example, at 40 mM DHA and 0.2 mM **Ru=O**$^{2+}$, the $t_{1/2}$ for the A → B phase of the oxidation is 0.13 s while the $t_{1/2}$ for comproportionation (the formation of **Ru-OH**$^{2+}$ by the reaction of **Ru=O**$^{2+}$ with **Ru-OH$_2$**$^{2+}$ formed from the oxidation of DHA) is 0.85 s.

For the oxidations of xanthene, fluorene, DHA, cyclohexene, ethylbenzene, toluene and indene, a mechanism of initial hydrogen-atom abstraction followed by radical dimerization or trapping of the radical by the oxidant (either **Ru=O**$^{2+}$ or **Ru-OH**$^{2+}$) is proposed (Figure 2.12).

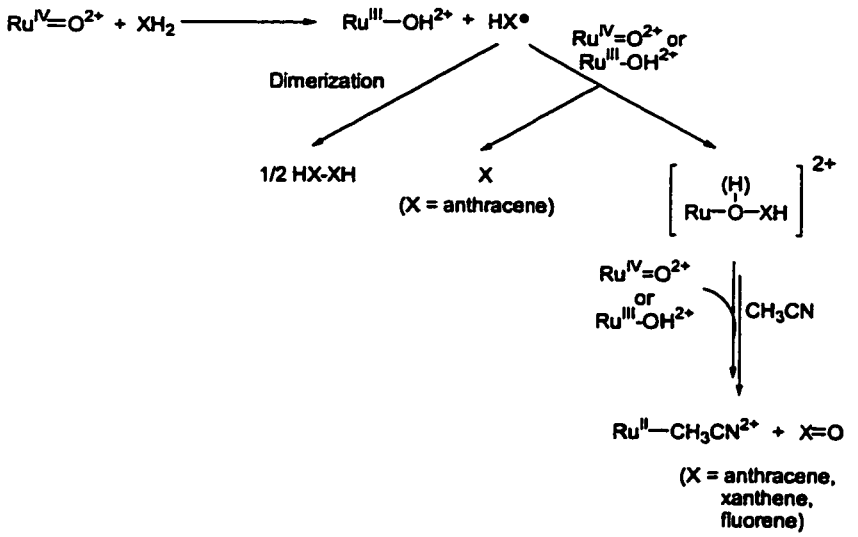

Figure 2.12. General pathways for the oxidation of DHA, xanthene, and fluorene by **Ru=O^{2+}**.

The oxidation products observed represent the bifurcation of reaction pathways after initial hydrogen atom removal generates the organic radical. This is consistent with the product ratio dependence on starting concentrations of oxidant and substrate. At high substrate concentrations (relative to **Ru=O^{2+}**), radical dimerization is competitive with trapping by the oxidant and subsequent oxygen-atom transfer. At higher **Ru=O^{2+}** concentrations, however, the encounter of the radical with **Ru=O^{2+}** or **Ru-OH^{2+}** followed by O-atom transfer is more likely, yielding higher ketone production relative to dimerization products. The trapping of the organic radical by **Ru=O^{2+}** or **Ru-OH^{2+}** must be a relatively rapid step to compete with radical dimerization processes, as these are known to occur at ~10^9 M^{-1} s^{-1},[17] but these radicals are in much lower concentration compared to that of the oxidant. Subsequent steps may be much slower. Oxidation of the organic substrate by **Ru-OH^{2+}** to generate **Ru-OH$_2^{2+}$** would likely be slower than

oxidation by $\mathbf{Ru{=}O^{2+}}$. Further oxidation of the Ru-trapped organic is required as no alcohol products or intermediates are observed. Furthermore, the organic product must be released from the Ru, most likely through a slow solvolysis process, to give the final Ru^{II} products observed ($\mathbf{Ru\text{-}OH_2^{2+}}$ and $\mathbf{Ru\text{-}CH_3CN^{2+}}$).

Using this model of initial hydrogen-atom abstraction followed by competitive dimerization/trapping, the rate constant for the initial, rapid phases of each reaction can be assigned as the hydrogen-atom abstraction step. This assignment is supported by the excellent correlation of these rates with the C-H bond dissociation energies of the organic substrates (Figure 2.13, see Table 2.6).

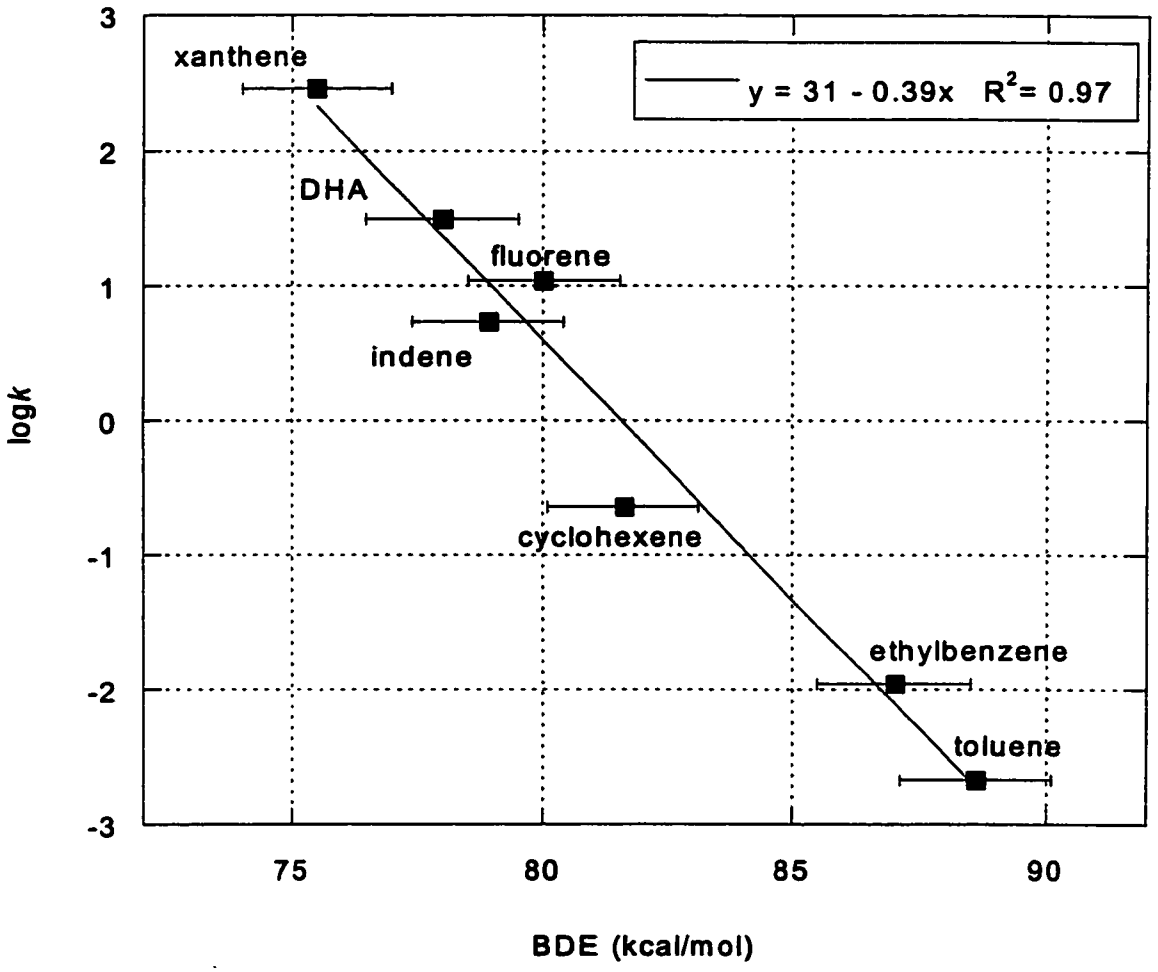

Figure 2.13. Plot of log *k* for the oxidation of each substrate vs. BDE (Table 2.6). Rate constants are statistically corrected for the number of oxidizable hydrogens, but not for the stoichiometry of the reaction due to the varying number of Ru equivalents necessary for each product.

The slower phases observed in the kinetic measurements of these reactions correspond to the further oxidation of the Ru-bound organic complexes and/or solvolysis processes. For example, DHA, xanthene and fluorene oxidations display a second, slow phase (B

→ C) with observed values that are highly variable. This phase describes a variety of possible reactions: the oxidation of Ru^{III}-bound organics by **Ru=O**$^{2+}$ or **Ru-OH**$^{2+}$, the oxidation of free organics by **Ru-OH**$^{2+}$, and the solvolysis of Ru-bound products. In the oxidation of fluorene, this phase is followed by a slower phase that is most likely the solvolysis of **Ru-OH$_2$**$^{2+}$ to **Ru-CH$_3$CN**$^{2+}$.

The rate of trapping of the organic radical by the oxidant (versus the dimerization rate) can be estimated using a SPECFIT simulation of the xanthene and fluorene reactions. The dimerization of xanthenyl and fluorenyl radicals is known to occur at ~10^9 M^{-1} s^{-1} (5.8×10^9 for fluorene).[17] Using the model given in Figure 2.14, a trapping rate (for trapping by **Ru=O**$^{2+}$ and **Ru-OH**$^{2+}$) of 5×10^6 s^{-1} for xanthene and 1×10^6 s^{-1} for fluorene gave reasonable agreement with experimentally determined final concentrations of products, reproducing most of the trends observed (Table 2.5).

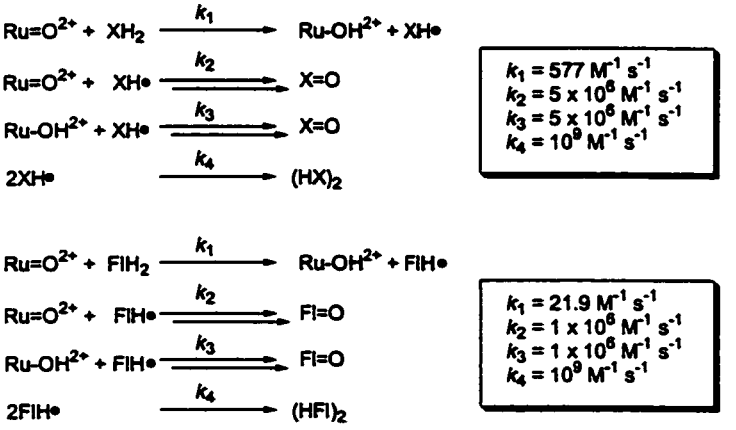

Figure 2.14. Model used for the calculation of trapping versus dimerization rates for the reaction of **Ru=O**$^{2+}$ with xanthene (XH_2) and fluorene (FlH_2).

Table 2.5. Experimental and calculated product concentrations using the model in Figure 2.14 for reactions of **Ru=O**$^{2+}$ with xanthene and fluorene. $(HX)_2$ represents the organic dimers 9,9'-bixanthene and bifluorene. X=O represents the ketone products xanthone and fluorenone.

[**Ru=O**$^{2+}$]:[XH_2] (mM)	$(HX)_2$ exp. (mM)	$(HX)_2$ calc. (mM)	X=O exp. (mM)	X=O calc. (mM)
xanthene - 1:1	0.013	0.010	0.36	0.38
1:2	0.019	0.010	0.35	0.38
1:4	0.025	0.021	0.31	0.38
1:10	0.036	0.043	0.38	0.36
2:4	0.045	0.017	0.66	0.76
4:4	0.045	0.020	1.31	1.55
fluorene - 1:1	0.011	0.006	0.37	0.49
1:2	0.014	0.014	0.33	0.49
1:4	0.017	0.026	0.31	0.47
1:10	0.023	0.053	0.33	0.45
2:4	0.027	0.027	0.63	0.97
4:4	0.027	0.025	1.25	1.97

Dihydroanthracene is oxidized rapidly by **Ru=O**$^{2+}$ ($k'_{DHA} = 125 \pm 8\ M^{-1} s^{-1}$) to give anthracene, anthrone and anthraquinone. The rate of oxidation of DHA is intermediate to those of xanthene and fluorene, consistent with its intermediate C-H bond strength of 78 kcal/mol (Table 2.6).[11a] Again, the products represent the branching of pathways following a fast initial phase. In the oxidation of DHA by **Ru=O**$^{2+}$ no dimers are observed, but there is a comproportionation reaction known to occur with hydroanthracene radicals ($2HA^{\bullet} \rightarrow A + DHA$, $k'_{disp} \sim 10^9\ M^{-1} s^{-1}$).[17] Furthermore, the reaction of **Ru=O**$^{2+}$ or **Ru-OH**$^{2+}$ with $HA^{\bullet}$ to give anthracene is likely to be very fast as the H-$A^{\bullet}$ bond is very weak (see below). The role of the removal of a hydrogen atom in the rate-determining step of the oxidation of DHA is supported by the large deuterium isotope effect observed in this system ($k_H/k_D \geq 35$). Isotope effects of

this magnitude are often attributed to tunneling and have been observed in other oxidations by **Ru=O**$^{2+}$.[18] The only other isotope effected reported for a C-H bond oxidation by **Ru=O**$^{2+}$ is for the oxidation of cyclohexene ($k_H/k_D = 21 \pm 1$).[7]

The oxidation of DHA to anthrone and anthraquinone is not a step-wise process involving the oxidation of anthracene. The rate of oxidation of anthracene by **Ru=O**$^{2+}$ ($k'_{Anth} = 0.273 \pm 0.005\ M^{-1}\ s^{-1}$) is not rapid enough to account for the amount of anthrone and anthraquinone produced in the reaction. A SPECFIT simulation of the reactions in which anthrone and anthraquinone are produced solely from the oxidation of anthracene subsequent to DHA oxidation predicts anthracene as the only detectable product at 2 mM **Ru=O**$^{2+}$ and 4 mM DHA (the simulation predicts less than 1 μM concentration of oxygenated products). Actual products observed under these conditions are 1.10 mM anthracene, 0.17 mM anthrone, and 0.11 mM anthraquinone. Anthrone and anthraquinone must be produced via a pathway separate from the formation of anthracene. Furthermore, the presence of anthrone and anthraquinone as products indicate that anthraquinone is produced competitively with anthrone, not directly from it. The very rapid reaction of **Ru=O**$^{2+}$ with anthrone ($k' > \sim 10^4$) would lead to complete consumption of anthrone by **Ru=O**$^{2+}$ on the time-scale of the reaction. The addition of the second oxygen to anthrone may occur while the anthrone is bound to Ru (during the B → C phase of the reaction), while there is still **Ru=O**$^{2+}$ present.

The oxidation of anthracene does not proceed by the same mechanism as the oxidation of DHA, xanthene, fluorene, toluene and indene. The apparent conversion of **Ru=O**$^{2+}$ directly to **Ru-CH$_3$CN**$^{2+}$ supports a two electron oxidation and argues against the involvement of **Ru-OH**$^{2+}$ as the one-electron oxidation intermediate, but may also be due to solvolysis of **Ru-OH$_2$**$^{2+}$ on the same time scale of the reaction. The C-H bond

dissociation energies of anthracene are much higher so there are no readily oxidized C-H bonds. The role of $\mathbf{Ru{=}O^{2+}}$ as an electrophile in the oxidation of anthracene is possible, as in the oxidations of triphenylphosphine[19,3a] and dimethylsulfoxide.[3b]

Reactivity vs. Thermodynamic Driving Force. In each oxidation reaction, the initial, fast phase is linearly dependent on the concentration of organic substrate. With the exception of anthracene (which is oxidized by a different mechanism), these rate constants correlate well with substrate C-H bond dissociation enthalpies (Figure 2.13), consistent with this step being a hydrogen atom abstraction. Oxidation rates do not correlate well with ionization energy (ionization energies for the organic compounds have been listed instead of oxidation potentials due to inconsistency in many reported electrochemical potentials), arguing against rate-determining electron transfer as the initial step of the reaction (Table 2.6).

Table 2.6. Oxidation Rate Constants, Ionization Energies, Oxidation Potentials, and Bond Dissociation Energies for Organic Substrates.

Substrate	Ionization Energy (eV)[a]	pK_a[b]	BDE[c] (kcal/mol)	Oxidation Rate Constant (M^{-1} s^{-1})
Xanthene	7.65	41.0	75.5	5.77×10^2
DHA	8.54	41.1	78	1.25×10^2
Indene	8.14	20.1	78.9	1.08×10^1
Fluorene	7.91	33.6	80	2.19×10^1
Cyclohexene	8.95		81.6[f]	9.2×10^{-1}
Ethylbenzene	8.77		87[f]	2.2×10^{-2}
Toluene	8.828		90[e]	6.4×10^{-3}
Anthracene	7.44		~111[d]	2.7×10^{-1}

[a] See ref. 20. [b] Values measured in DMSO[21] and extrapolated to CH_3CN using the equation p$K_{a(C\text{-}H)}$ (CH_3CN) = 11 + p$K_{a(C\text{-}H)}$ (DMSO).[22] [c] From ref. 21. [d] Based on DFT calculation, see ref. 23. [e] From ref. 24. [f] From ref. 25.

Ru=O^{2+} is also known to be a poor outer-sphere electron-transfer agent, further arguing against a mechanism of initial electron transfer.[5a,12] Nor do the rates appear to correlate with the pK_as of the organic substrates, ruling out initial, rate-determining proton loss and subsequent electron transfer. This is further supported by the weak basicity of **Ru=O**$^{2+}$ – it is not protonated in aqueous solutions between pH 0 and 7.[19]

An initial hydrogen atom removal step would generate the organic radical which can then undergo one of two subsequent steps – trapping by the oxidant subsequent oxygen atom transfer or, in the cases of xanthene and fluorene, radical dimerization to form bixanthene or bifluorene. In the case of DHA, the hydroanthracenyl radical may undergo an additional hydrogen-atom abstraction to form anthracene or disproportionation of two hdyroanthracenyl radicals (HA$^{\bullet}$) to form anthracene and

DHA. Subsequent hydrogen-atom abstraction (from $HA^{\bullet}$) should be rapid as the C-H bond strength for $H\text{-}A^{\bullet}$ is calculated to be 43 kcal/mol.[26] Assuming that the correlation of bond strength with hydrogen-atom abstraction holds over this range, the hydrogen removal should occur near the diffusion limit. This rate constant is competitive with the rate constant for disproportionation, but the observed rate would be much larger due to the greater concentration of Ru present ($\sim 10^{-4}$ M).

The rate of oxidation of DHA by $\mathbf{Ru{=}O^{2+}}$ is quite rapid – consistent with the ~7 kcal/mol driving force for this reaction. In previous studies of oxidation rate versus thermodynamic driving force, good correlation has been observed for a variety of oxidants (including $\mathbf{Ru{=}O^{2+}}$) and over a range of bond dissociation energies (Figure 2.15).[27]

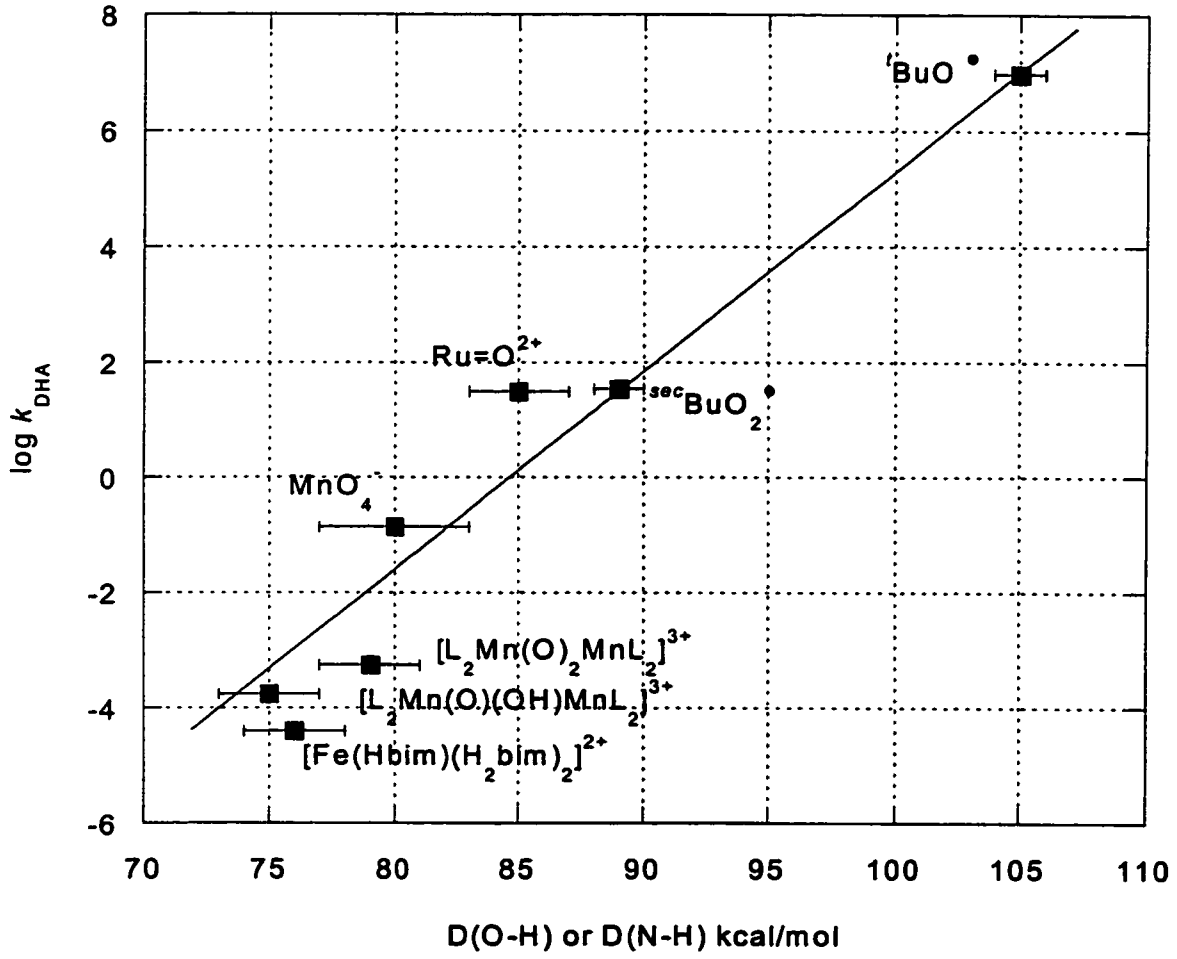

Figure 2.15. A plot of log*k* (the rate constant for H-atom abstraction from DHA (per hydrogen)) vs. the strength of the X-H bond formed by the oxidant. The straight line is drawn through the two oxygen radical points.

Self-Exchange Rates. In an extension of previous studies in our lab of H-atom transfer reactions,[14a] we have found that the rate constant for the oxidation of DHA by **Ru=O^{2+}** also follows the Marcus cross relation. The hydrogen-atom self-exchange rate constant measured for the **Ru=O^{2+}/Ru-OH^{2+}** system is quite rapid with k'_{HSE} = 7.6 ×

10^4 M^{-1} s^{-1}. This rate constant is about 10 times faster than the second-order rate constant found by Meyer and co-workers for the comproportionation reaction of **Ru=O**$^{2+}$ with **Ru-OH$_2$**$^{2+}$ to yield 2**Ru-OH**$^{2+}$ given in eq 2.2 ($k_f = 4.07 \times 10^3$ M^{-1} s^{-1}).[5c] This comproportionation is almost a self-exchange reaction (with ΔG = -2.3 kcal/mol, close to $\Delta G = 0$ for a self-exchange reaction) and it is the net transfer of a hydrogen atom. The **Ru=O**$^{2+}$/**Ru-OH**$^{2+}$ self-exchange rate constant is also ~10 times faster than the H$^\bullet$ transfer rate constant found for the iron-bi-imidazoline system previously studied by our lab (5.8×10^3 M^{-1} s^{-1}).[14] This is consistent with the Ru rate being slightly faster than predicted in Figure 2.12, while the iron number is slightly slower.

The value shows reasonably good correlation with our application of Marcus Theory to hydrogen-atom transfer using the Marcus cross relation. The Marcus cross relation (eq 2.7) allows the calculation of a reaction rate constant given two self-exchange rates, an equilibrium constant derived from the thermodynamic driving force, and a frequency factor (typically close to unity). The self-exchange rate for DHA/HA$^\bullet$ is not known, but can be estimated from our previous studies with the iron-bi-imidazoline system.[14]

$$k_{xy} = \sqrt{k_{xx} k_{yy} K_{xy} f_{xy}} \qquad (2.7)$$

Using $k_{xy} = 3.9 \times 10^{-5}$ M^{-1} s^{-1} (the hydrogen-atom abstraction rate constant reported for the oxidation of DHA by **Fe^{III}(Hbim)** at 30 °C.[14c]), $k_{xx} = 9.7 \times 10^2$ M^{-1} s^{-1} (the self-exchange rate constant per hydrogen atom for **Fe^{III}(Hbim)/Fe^{II}(H$_2$bim)**[14a]), $K_{xy} = 0.034$ (the equilibrium constant based on the difference in bond dissociation energies between **Fe^{III}(Hbim)** and DHA), and $f_{xy} = 1$ (the frequency factor)[28] a value for k_{yy} (the self-exchange rate for DHA/HA$^\bullet$) can be calculated. These values result in a very small self-exchange rate constant estimate for DHA/HA$^\bullet$ ($k_{yy} = 5 \times 10^{-11}$ M^{-1} s^{-1}).

Substituting this value for DHA into eq 2.7 with the values for the $\mathbf{Ru{=}O^{2+}/Ru\text{-}OH^{2+}}$ system reported here gives a predicted DHA oxidation rate of 0.5 M^{-1} s^{-1},[29] in somewhat reasonable agreement with the experimental value of 125 M^{-1} s^{-1} given the amount of error involved in many of these reported values. Our previous study of observed and calculated rate constants for hydrogen-atom transfer reactions have shown agreement within about an order of magnitude.[14a]

The surprising result of this self-exchange study, however, is the apparent lack of an isotope effect for this reaction. The observed $k'_{HSE}/k'_{DSE} = 1.2 \pm 0.1$ is essentially unity. This is quite different from the kinetic isotope effect of 14.6 ± 0.7 reported by Meyer for the comproportionation reaction in eq 2.2 (with 1% w/v solutions of H_2O vs. D_2O in CH_3CN).[5c] It is not clear, at this point, why some reactions show large isotope effects and some do not.

Conclusions

The mechanism that most consistently explains the results presented here involves initial hydrogen-atom abstraction from the substrate to give the organic radical. This radical can be trapped by the oxidant to undergo oxygen-atom transfer and subsequent oxidation and product release or it can encounter another radical to form dimerization products (for xanthene and fluorene) or undergo additional hydrogen-atom abstraction (as in the case of DHA). See Figure 2.12 for a summary of these pathways.

The self-exchange rate constant measured for the transfer of a net hydrogen atom between $\mathbf{Ru\text{-}OH^{2+}}$ and $\mathbf{Ru{=}O^{2+}}$ is similar in magnitude to previous self-exchange measurements for other oxidants. When used in the Marcus cross relation with an estimate for the self-exchange rate for DHA/HA$^{\bullet}$, good correlation between

experimental and calculated rates for the oxidation of DHA is observed.

Experimental Section

General Considerations. All experiments were performed under an N_2 atmosphere using standard techniques unless otherwise noted. Solvents (including deuterated solvents from Cambridge Isotope) were degassed and dried according to standard procedures.[30] Acetonitrile (low-water brand) was purchased from Burdick and Jackson and dispensed from a stainless steel keg plumbed directly into the dry box. Deuterated acetonitrile (CD_3CN) was stirred over CaH_2 for two days, vacuum transferred to P_2O_5 and stirred for four hours. It was then transferred back to CaH_2, stirred for 30 minutes, and transferred to a sealable flask prior to use. Dihydroanthracene (DHA) was recrystallized twice from absolute ethanol. Other reagents were purchased from Aldrich and used as received unless otherwise noted. $Ru(bpy)_2Cl_2$ and $[Ru(bpy)_2(py)Cl](PF_6)$ were synthesized according to literature methods.[5a,31] $[Ru(bpy)_2(py)(OH_2)](PF_6)_2$ and $[Ru(bpy)_2(py)O](PF_6)_2$ were synthesized by modified literature procedures. The same procedure for the synthesis of $[Ru(bpy)_2(py)(OH_2)](ClO_4)_2$ was followed,[5b] except that a saturated solution of KPF_6 in water was used to precipitate the product. A procedure similar to the one used to synthesize $[Ru(bpy)_2(py)^{18}O](ClO_4)_2$ was used[4a] to produce $[Ru(bpy)_2(py)O](PF_6)_2$. Liquid Br_2 was added in a very small amount to the dissolved $\mathbf{Ru\text{-}OH_2^{2+}}$ and the resulting solution was purged with N_2 for several minutes. The solution was cooled and 1-2 mL of saturated KPF_6 in water was added to precipitate the product. $\mathbf{Ru\text{-}OD_2^{2+}}$ was synthesized in a manner identical to that used for the synthesis of $\mathbf{Ru\text{-}OH_2^{2+}}$ except that D_2O replaced H_2O at all points in the synthesis from $[Ru(bpy)_2(py)Cl](PF_6)$. $\mathbf{Ru{=}O^{2+}}$,

Ru-OH^{2+}, **Ru-OH$_2^{2+}$**, **Ru-OD$_2^{2+}$** and **Ru-CH$_3$CN^{2+}** were characterized by NMR and UV-vis spectroscopies.[5a,b] DHA-d_4 was synthesized by a previous member of the lab by exchange of protons with sodium dimsylate-d_5 in DMSO-d_6.[32]

NMR spectra were recorded on Bruker AC-200, AF-300, and DRX-500 spectrometers at ambient temperatures and are reported in ppm relative to TMS (^{1}H). UV-vis spectra were recorded on a Hewlett Packard 8453 diode array spectrophotometer and are reported as λ_{max} (nm), (ε, M^{-1} cm^{-1}). UV-vis kinetics measurements were carried out on an OLIS stopped-flow apparatus with a rapid scanning monochromator. GC/MS spectra were obtained on a Hewlett Packard 5971 instrument equipped with a non-polar capillary column and a mass spectral analyzer. GC/FID spectra were obtained on a Hewlett Packard 5890 instrument equipped with a similar column. Yields of organic products were quantified using response factors and confirmed by the addition of authentic samples.

Typical Procedure for Organic Oxidations. A solution of **xanthene** (4 mg, 20 μmol) and **Ru=O^{2+}** (5 μmol) in 5 mL acetonitrile turned orange within 5 min. 9,9'-Bixanthene was observed by GC/MS *m/z* 181, M^+ (at twice the retention time of xanthene), 152, 69, 39.[33] Xanthone was observed at *m/z* 196, 168, 139. Oxidation of **fluorene** was performed in a similar manner and bifluorene (*m/z* 330, 165), bifluorenylidene (*m/z* 328), and fluorenone (*m/z* 180, 152) were detected by GC/MS. Oxidations of **DHA** were monitored by GC/MS and by UV-vis spectroscopy, where anthracene production was evident from its characteristic spectrum in CH_3CN: 359 (8,800), 378 (8,200) after removal of the Ru^{II} product by passing the solution through a silica pipette column. Anthracene was quantitated by UV-vis and by GC/FID response factors. Anthraquinone production was also observed by GC/MS (*m/z* 208, 180, 152).

The oxidation of anthracene, anthrone, indene, cyclohexene, ethylbenzene and toluene were carried out under similar conditions and products were identified by GC/MS.

^{18}O-labeling studies were conducted under the same conditions as above, but with 10mM added $H_2{}^{18}O$. The amount of ^{18}O incorporation was measured by comparing the M^+:$(M+2)^+$ peak intensity ratios for products formed in the presence of $H_2{}^{18}O$ to those formed in the absence of $H_2{}^{18}O$.

Kinetic Studies. Kinetic data were typically gathered over a range of 350 to 650 nm every 0.001 to 0.5 s over 1-1000 s. These stopped-flow reactions of **Ru=O**$^{2+}$ with xanthene, fluorene and DHA were carried out with 0.2 mM **Ru=O**$^{2+}$ and 2-80 mM substrate in CH_3CN. Solutions were made up in an N_2-filled dry box immediately prior to use. Kinetic data were analyzed using the global analysis software package SPECFIT (Spectrum Software Associates, Marlborough, MA).

Kinetics studies with xanthene in O_2-saturated solution were carried in the stopped-flow instrument. Acetonitrile was sparged with O_2 prior to mixing with the reagents. Data were collected and analyzed in the same manner as in the kinetics studies of xanthene under inert atmosphere.

Kinetic studies with anthracene were carried out in sealable cuvettes fitted with Teflon Kontes valves. Solutions were made up and transferred to the cuvette in a nitrogen-filled dry box and then transported to the spectrophotometer. Kinetics were monitored every 2s for 600s.

Self-Exchange Measurements. The self-exchange rates for **Ru=O**$^{2+}$/**Ru-OH**$^{2+}$ and **Ru=O**$^{2+}$/**Ru-OD**$^{2+}$ were measured by dynamic line broadening. A solution of 0.0045 g **Ru=O**$^{2+}$ (5.6 μmol), 0.0023 g **Ru-OH$_2$**$^{2+}$ (2.9 μmol) and 1 mL hexamethyldisiloxane (as an internal standard) in 0.5 mL CD_3CN was prepared in a

sealable NMR tube. ^{1}H-NMR spectra were acquired every 10 minutes for 3-4 hours. Linewidths for **Ru=O^{2+}** were measured at δ 53.1 and –31.0 ppm by fitting to Lorentzian functions using the commercially available NUTS software (Acorn NMR). Values for ΔW were obtained by subtracting the natural linewidths for **Ru=O^{2+}** in the absence of **Ru-OH^{2+}** from the values obtained by Lorentzian fitting.

Notes to Chapter 2

(1) a) Gilbert, J.; Roecker, L.; Meyer, T. J. *Inorg. Chem.* **1987**, *26*, 1126-1132. b) Seok, W. K.; Dobson, J. C.; Meyer, T. J. *Inorg. Chem.* **1988**, *27*, 3-5. c) Meyer, T. J. *J. Electrochem. Soc. 1984, 131*, 221c.

(2) Binstead, R. A.; McGuire, M. E.; Dovletoglou, A.; Seok, W. K.; Roecker, L. E.; Meyer, T. J. *J. Am. Chem. Soc.* **1992**, *114*, 173-186.

(3) a) Moyer, B. A.; Sipe, K.; Meyer, T. J. *Inorg. Chem.* **1981**, *20*, 1475-1480. b) Roecker, L.; Dobson, J. C.; Vining, W. J.; Meyer, T. J. *Inorg. Chem.* **1987**, *26*, 779-781. c) Reference 1b.

(4) a) Thompson, M. S.; Meyer, T. J. *J. Am. Chem. Soc.* **1982**, *104*, 4106-4115. b) Thompson, M. S.; Meyer, T. J. *J. Am. Chem. Soc.* **1982**, *104*, 5070-5076. c) Roecker, L.; Meyer, T. J. *J. Am. Chem. Soc.* **1987**, *109*, 746-754.

(5) a) Moyer, B. A.; Meyer, T. J. *Inorg. Chem.* **1981**, *20*, 436-444. b) Dobson, J. C.; Helms, J. H.; Doppelt, P.; Sullivan, B. P.; Hatfield, W. E.; Meyer, T. J. *Inorg. Chem.* **1989**, *28*, 2200-2204. c) Binstead, R. A.; Stultz, L. K.; Meyer, T. J. *Inorg. Chem.* **1995**, *34*, 546-551.

(6) Stultz, L. K.; Binstead, R. A.; Reynolds, M. S.; Meyer, T. J. *J. Am. Chem. Soc.* **1995**, *117*, 2520-2532.

(7) Stultz, L. K.; Huynh, M. H. V.; Binstead, R. A.; Curry, M.; Meyer, T. J. *J. Am. Chem. Soc.* **2000**, *122*, 5984-5996.

(8) Curry, M; Huynh, M. H. V.; Stultz, L. K.; Binstead, R. A.; Meyer, T. J.; Bryant, J. R.; Mayer, J. M. *manuscript in preparation.*

(9) Gardner, K. A.; Kuehnert, L. L.; Mayer, J. M. *Inorg. Chem.* **1997**, *36*, 2069-2078. This equation is for values in H_2O and oxidation potentials vs. NHE.

(10) Lebeau, E. L.; Binstead, R. A.; Meyer, T. J. *J. Am. Chem. Soc.* **2001**, *123*, 10535-10544.

(11) BDE's are calculated using a thermodynamic cycle. For leading references, see: a) Bordwell, F. G.; Cheng, J.-P.; Ji, G.-Z.; Satish, A. V.; Zhang, X. *J. Am. Chem. Soc.* **1991**, *113*, 9790-9795. b) Bordwell, F. G.; Cheng, J.-P.; Harrelson, J. A., Jr. *J. Am. Chem. Soc.* **1988**, *110*, 1229-1231. c) Zhang, X.-M.; Bordwell, F. G.; *J. Am. Chem. Soc.* **1992**, *114*, 7458-7462. d) Parker, V. D. *J. Am. Chem. Soc.* **1992**, *114*, 7458-7462; and correction: Parker, V. D. *J. Am. Chem. Soc.* **1993**, *115*, 1201.

(12) Bond dissociation enthalpies are calculated using oxidation potentials at pH=0 given in reference 10.

(13) Mayer, J. M. *Acc. Chem. Res.* **1998**, *31*, 441-450.

(14) a) Roth, J. P.; Yoder, J. C.; Won, T.-J.; Mayer, J. M. *Science* **2001**, *294*, 2524-2526. b) Roth, J. P.; Lovell, S.; Mayer, J. M. *J. Am. Chem. Soc.* **2000**, *122*, 5486-5498. c) Roth, J. P.; Mayer, J. M. *Inorg. Chem.* **1999**, *38*, 2760-2761 and references therein. In this section, **Fe^{II}(H$_2$bim)** refers to the fully protonated iron tris-2,2'-biimidazoline. **Fe^{III}(Hbim)** refers to the same complex minus one hydrogen atom (a proton and an electron) — Fe(Hbim)(H_2bim)$_2$.

(15) Sandström, J. *Dynamic NMR Spectroscopy*; Academic Press: New York, 1982.

(16) For a discussion of the effect of residual H on observed k_H/k_D, see: Sorokin, A.; Robert, A.; Meunier, B. *J. Am. Chem. Soc.* **1993**, *115*, 7293-7299.

(17) Arends, I. W. C. E.; Mulder, P.; Clark, K. B.; Wayner, D. D. M. *J. Phys. Chem.* **1995**, *99*, 8182-8189.

(18) a) Gilbert, J. A.; Gersten, S. W.; Meyer, T. J. *J. Am. Chem. Soc.* **1982**, *104*, 6872-6873. b) Binstead, R. A.; Meyer, T. J. *J. Am. Chem. Soc.* **1987**, *109*, 3287-3297. c) References 1a and 3b.

(19) Moyer, B. A.; Meyer, T. J. *J. Am. Chem. Soc.* **1978**, *100*, 3601-3603.

(20) http://webbook.nist.gov/chemistry accessed 18 Sept. 2002.

(21) a) Reference 11a. b) Bordwell, F. G. *Acc. Chem. Res.* **1988**, *21*, 456-463 and references therein.

(22) Wayner, D. D. M.; Parker, V. D. *Acc. Chem. Res.* **1993**, *26*, 287-294.

(23) Barckholtz, C.; Barckholtz, T. A.; Hadad, C. M. *J. Am. Chem. Soc.* **1999**, *121*, 491-500.

(24) Bierbaum, V.; DePuy, C.; Davico, G.; Ellison, B. *Int. J. Mass Spectrom. Ion Phys.* **1996**, *156*, 109-131.

(25) Denisov, E. T.; Denisova, T. G. *Handbook of Antioxidants*, 2nd Ed., CRC Press: Boca Raton, 2000, pp. 21-36.

(26) The C-H bond strength in $HA^{\bullet}$ can be calculated from the bond dissociation energies of H_2 and DHA and the heat of hydrogenation of anthracene given in Cox, J. D.; Pilcher, G. *Thermochemistry of Organic and Organometallic Compounds*; Academic Press: New York, 1970. D(H-H) for H_2 is 104.2 kcal/mol, ΔH for DHA $\rightarrow$ anthracene + H_2 is 17 kcal/mol, and D(C-H) for $HA^{\bullet} + H \rightarrow$ DHA is 78

kcal/mol. Summing to get $HA^{\bullet} \rightarrow$ anthracene + H is (104 + 17 – 78) = 43 kcal/mol.

(27) Larsen, A. S.; Wang, K.; Lockwood, M. A.; Rice, G. L.; Won, T.-J.; Lovell, S.; Sadilek, M.; Turecek, F.; Mayer, J. M *J. Am. Chem. Soc.* **2002**, *124*, 10112-10123.

(28) Marcus, R. A.; Sutin, N. *Biochim. Biophys. Acta* **1985**, *811*, 265-322.

(29) This value is calculated using a frequency factor value of 0.51 from the equation given in reference 28: $\ln f_{xy}=[¼(\ln K_{xy})^2]/[\ln(k_{xx}k_{yy}/Z^2)]$ using $Z = 10^9$ as suggested by Nelsen, S. F.; Ismagilov, R. F.; Chem, L.-J.; Brandt, J. L.; Chen, X.; Pladziewicz, J. R. *J. Am. Chem. Soc.* **1996**, *118*, 1555-1556. Using this value for Z (rather than 10^{11}) is suggested by the authors for reactions where K_{xy} is very different from 1. Using $Z = 10^{11}$ gives $f_{xy} = 0.56$, not a very large difference.

(30) Perrin, D. D.; Armarego, W. L. F. *Purification of Laboratory Chemicals 3rd Ed.*, Pergamon Press: New York, 1988.

(31) Sullivan, B. P.; Salmon, D. J.; Meyer, T. J. *Inorg. Chem.*, **1978**, *17*, 3334-3341.

(32) Bailey, R. J.; Card, P. J.; Schechter, H. *J. Am. Chem. Soc.* **1983**, *105*, 6096-6103.

(33) Bryant, J. R.; Taves, J. E.; Mayer, J. M. *Inorg. Chem.* **2002**, *10*, 2769-2776.

Chapter 3: Mechanistic Study of the Oxidation of Cumene by $[(bpy)_2(py)RuO]^{2+}$

Abstract

The oxidation of cumene by $[(bpy)_2(py)Ru^{IV}O]^{2+}$ was originally thought to proceed by a mechanism of initial hydride transfer. Reported here is a detailed study of the kinetics of this oxidation and its organic oxidation products. The organic products of the oxidation, α-methylstyrene, cumyl alcohol, and acetophenone, were not reported in the original study and lend insight into the mechanism of oxidation. In a plot of oxidation rate vs. C-H bond dissociation energy, the oxidation of cumene correlates well with other C-H bond oxidations by $[(bpy)_2(py)Ru^{IV}O]^{2+}$. This correlation, as well as the observed products, have led us to propose a mechanism of initial hydrogen-atom abstraction.

Introduction

In 1982, Thompson and Meyer reported on their study of the mechanism of oxidation of alkylaromatics by $[(trpy)(bpy)Ru^{IV}O]^{2+}$ and $[(bpy)_2(py)Ru^{IV}O]^{2+}$ (trpy = 2,2',2"-terpyridine, bpy = 2,2'-bipyridine, py = pyridine).[1] The study focused primarily on the oxidations of 4-isopropyl-, methyl-, and ethyl-benzoate ions by $[(trpy)(bpy)RuO]^{2+}$ in aqueous solution. The study was extended to oxidations of toluene and cumene by $[(bpy)_2(py)RuO]^{2+}$ in acetonitrile – the change in oxidant necessitated by the rapid decomposition of $[(trpy)(bpy)RuO]^{2+}$ in CH_3CN. Meyer and

coworkers concluded that these oxidations proceeded by a $2e^-$ process most accurately described as hydride abstraction by $[(bpy)_2(py)RuO]^{2+}$ (Figure 3.1). In a desire to test the applicability of a Marcus-type treatment to the process of hydride transfer, the Mayer group became interested in this novel termolecular pathway.

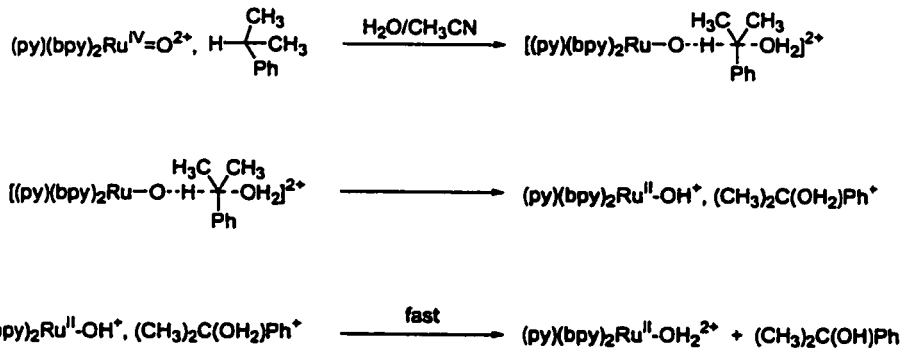

Figure 3.1. The mechanism proposed by Meyer and coworkers for the oxidation of cumene by $[(bpy)_2(py)RuO]^{2+}$ in acetonitrile.

The proposed mechanism involved initial hydride transfer with concomitant stabilization of the cation by solvent water. A similar mechanism has been suggested by the Mayer group for the oxidation of toluene by aqueous permanganate.[2] The Meyer proposal was based primarily on the aqueous oxidation results, but were supported by an apparent dependence of the rate of oxidation on the concentration of added nucleophiles – water, *tert*-butanol, and lithium bromide in acetonitrile (Figure 3.2).

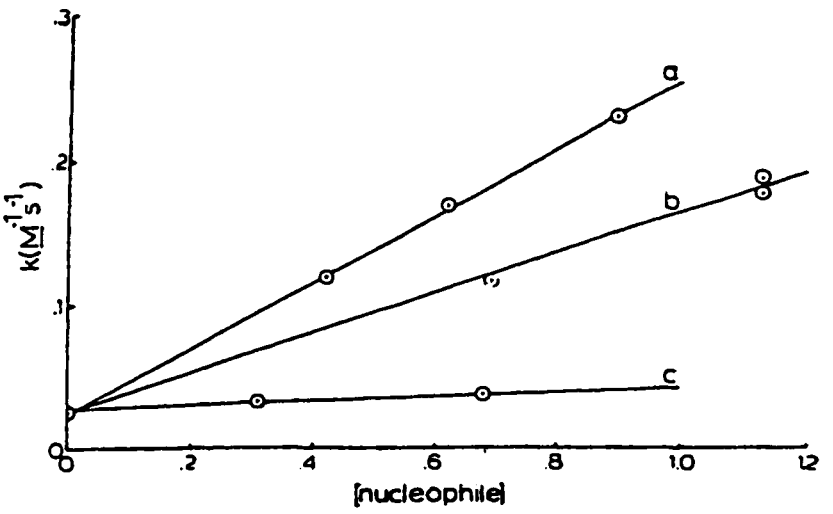

Figure 3.2. Figure 3 given in reference 1: Variation of observed rate constants at 24.3° C for the oxidation of cumene by $Ru(bpy)_2(py)O^{2+}$ in acetonitrile plotted as a function of added nucleophiles concentration: (a) water, (b) tert-butyl alcohol, (c) lithium bromide.[1]

There were some unusual features of this proposed mechanism, however, that stimulated further investigation by our lab. Thompson and Meyer suggested an S_N2-like mechanism for the oxidation of the benzylic hydrogen in cumene ($C_6H_5CH(CH_3)_2$). This oxidation occurs at a tertiary carbon – unlikely for an S_N2 reaction.[3] The authors invoked this mechanism to explain the observation of a third-order rate law – first order in ruthenium, cumene, and entering nucleophile. Their observations of rates, however, indicated a trend opposite of what one would expect for nucleophilic substitution: water > *t*-butyl alcohol > bromide.[4] After initial investigations by the Mayer laboratory were unable to reproduce the data reported in the original paper, we learned from Meyer

that they had difficulty repeating the results in subsequent investigations, as well. A joint publication of our findings here is in preparation.[5] Our recent results for the oxidation of cumene have led us to a mechanistic proposal involving initial hydrogen-atom abstraction.

Results

Oxidation of Cumene. The oxidation of cumene by $[(bpy)_2(py)Ru^{IV}=O]^{2+}$ (**Ru=O**$^{2+}$) was carried out in acetonitrile under a variety of conditions – at varied concentrations of added cumene and under N_2, O_2 and air. **Ru=O**$^{2+}$ concentrations were held constant at 1 mM and cumene concentrations were varied from 2 to 50 mM. An additional reaction at 2 mM **Ru=O**$^{2+}$:4 mM cumene was done, as well. Reactions are complete at room temperature in several hours. On this time scale, the only Ru product is **Ru-CH$_3$CN**$^{2+}$, due to the slow solvolysis of **Ru-OH$_2$**$^{2+}$ ($k_{solv} = 1.66 \times 10^{-3}$).[6] The organic products are cumyl alcohol, α-methylstyrene, and acetophenone, as well as trace amounts of 2-phenylpropionaldehyde and 2-phenylpropenal (eq 3.1). These products were identified by GC/MS, confirmed by the addition of authentic samples (except in the case of 2-phenylpropenal), and quantitated by GC/FID using calibrated response factors.

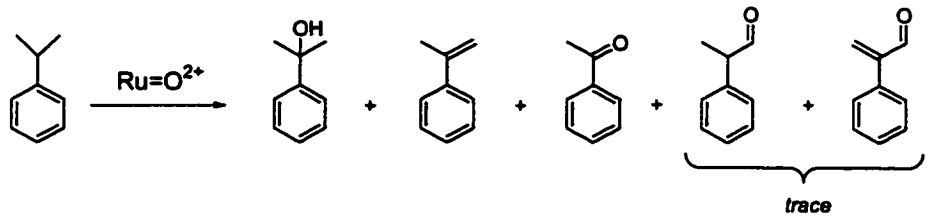

(3.1)

Product yields from the reactions of **Ru=O^{2+}** with cumene are given in Table 3.1. Yields were measured approximately 20 hours after the solutions were mixed and again after ~5 days. Reaction solutions were stored in the dry box in the interim. The initially observed concentrations of α-methylstyrene and acetophenone remained essentially constant (within error), while the amount of cumyl alcohol increases with increasing cumene concentration. In some samples, the amounts of cumyl alcohol and α-methylstyrene tend to decrease over time and the yield of acetophenone increases. At high cumene concentration (50 mM), the amounts of α-methylstyrene and cumyl alcohol are unchanged after several days. The yield of oxidation products observed typically accounts for 50-99% of oxidative equivalents, but this value is difficult to quantitate due to the number of organic products.

Table 3.1. Product yields from the oxidation of cumene by 1 mM **Ru=O^{2+}** at various cumene concentrations (under N_2). A reaction at 2 mM **Ru=O^{2+}** is also included.

[Ru=O^{2+}]:[cumene] (mM)	[α-methylstyrene] (mM)	[acetophenone] (mM)	[cumyl alcohol] (mM)
1:2	0.10	0.07	0.16
After 5 days	0.02	0.09	0.14
1:10	0.07	0.10	0.22
After 5 days	0.08	0.12	0.17
1:50	0.11	0.09	0.24
After 5 days	0.11	0.11	0.24
2:4	0.18	0.25	0.92

In order to determine whether the presence of O_2 affected the product ratios, reactions were performed at identical oxidant and substrate concentrations under N_2 (dry box), O_2 (saturated solutions) and air (benchtop). Results are presented in Table 3.2.

Table 3.2. Product yields from the oxidation of 2 mM cumene by 1 mM Ru=O^{2+} under N_2, O_2, and air.

[Ru=O^{2+}]:[cumene] (Conditions)	[α-methylstyrene] (mM)	[acetophenone] (mM)	[cumyl alcohol] (mM)
1:2 – N_2	0.09	0.05	0.13
After 5 days	0.05	0.06	0.12
1:2 – Air	-	0.22	0.12
After 5 days	0.02	0.21	0.11
1:2 – O_2	-	0.14	0.08
After 5 days	0.01	0.13	0.08

Reactions done in the presence of O_2 produced little to no detectable amounts of α-methylstyrene, roughly constant amounts of cumyl alchohol, and increased amounts of

acetophenone. Over time, the growth of α-methylstyrene in O_2-containing reaction solutions is observed.

The oxidation of cumene was also attempted in the presence of 10 mM and 200 mM $H_2{}^{18}O$ (with 2 mM **Ru=O**$^{2+}$ and 4 mM cumene). The amount of ^{18}O incorporation into the oxygenated products was quantitated by GC/MS. At 10 mM $H_2{}^{18}O$, 9% ^{18}O incorporation into cumyl alcohol and <1% incorporation into acetophenone is observed. At 200 mM $H_2{}^{18}O$, these values are 20% and 2% incorporation, respectively. Previous workers have reported that the oxygen in **Ru=O**$^{2+}$ does not exchange with ^{18}O in water over the time scale of these reactions.[7]

Oxidation of Cumene in the Presence of Nucleophiles. In an attempt to look for nucleophilically substituted products of the oxidation of 9.4 mM cumene by 4.7 mM **Ru=O**$^{2+}$, reactions were run in the presence of a 27.8 mM added nucleophile – lithium bromide, water, or *t*-butanol. Products were analyzed by GC/MS. All products were observed to be identical in composition to the products observed for the oxidation of cumene with no added nucleophiles present. No substituted products were detected.

Oxidation of Other Organics. To determine if some products were the results of over-oxidation of cumene, oxidations of α-methylstyrene, 2-phenylpropionaldehyde and cumyl alcohol by **Ru=O**$^{2+}$ were attempted. Reactions were performed at 1-2 mM **Ru=O**$^{2+}$ and 2-4 mM substrate with 2mM naphthalene as an internal GC/FID standard. Cumyl alcohol reacts slowly (hours) with **Ru=O**$^{2+}$ to give α-methylstyrene (a yield of 120% vs. initial **Ru=O**$^{2+}$, consuming 60% of the initial cumyl alcohol). This is most

likely an acid-catalyzed dehydration. The final Ru product (observed by UV-vis) is consistent with a mixture of **Ru-CH_3CN^{2+}** and the previously reported μ-oxo-dimer $[(bpy)_2(py)Ru^{III}\text{-}O\text{-}Ru^{III}(bpy)_2(py)]^{4+}$ (λ_{max} = 640 nm, ε = 23,400, approximately 0.02 mM).[6,8] This μ-oxo-dimer has been observed as a decomposition product formed from **Ru=O^{2+}** in CH_3CN over extended time periods.[6] This decomposition process is a possible source of trace acid in the reaction solution.

Ru=O^{2+} also reacts with α-methylstyrene slowly (hours) to give acetophenone, α-methylstyrene oxide, 2-phenylpropenal and 2-phenylpropionaldehyde as the main products (eq 3.2). The epoxidation of olefins by **Ru=O^{2+}** has been observed before in the oxidations of *cis*- and *trans*- stilbene, norbornene, and styrene.[9] The final Ru-product (by UV-vis after several hours) is consistent with **Ru-CH_3CN^{2+}**. At 1 mM **Ru=O^{2+}** and 2 mM α-methylstyrene, 0.02mM acetophenone and 0.25 mM 2-phenylpropionaldehyde are produced as the major products. Upon standing for several days under N_2, the only observed product was acetophenone (0.17 mM).

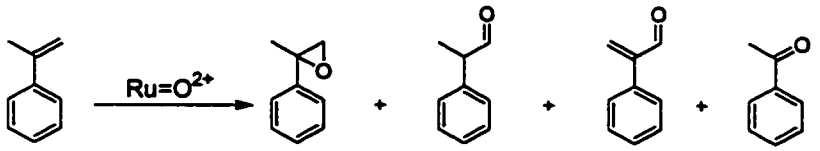

(3.2)

The reaction of **Ru=O^{2+}** with 2-phenylpropionaldehyde is quite rapid (done within seconds at 2 mM **Ru=O^{2+}**:4 mM 2-phenylpropionaldehyde). The products of this reaction were identified by GC/MS as acetophenone and 2-phenylpropenal. Also detected were trace amounts of 1-phenylethanol, 2,3-diphenylbutane, and 1-phenylethyl

acetamide (eq 3.3). Acetophenone was the major product (0.14 mM). The yield of 2-phenylpropenal was not determined quantitatively (due to the absence of an authentic sample), but can be crudely estimated at ~0.01 mM.

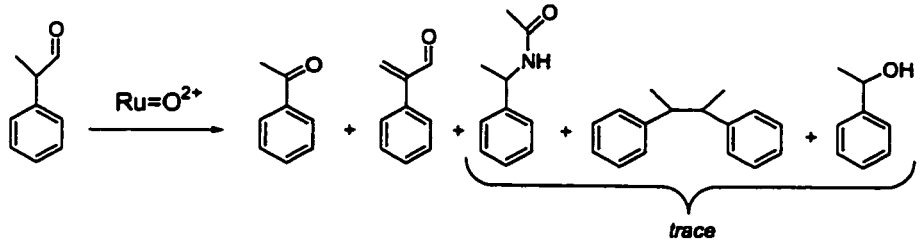

(3.3)

The oxidation of *meso*-2,3-diphenylbutane was also examined. The reaction of 1 mM **Ru=O**$^{2+}$ and 2 mM diphenylbutane gave 0.08 mM acetophenone and a mixture of unidentified products. These other products were produced in small amounts relative to acetophenone. Three of the products give *m/z* 121, 105, 91, 77, 43. The fourth product gives *m/z* 135, 105, 91, 77, 43. The source of these products is unknown.

Kinetics. The kinetics of the oxidation of cumene by **Ru=O**$^{2+}$ were measured under a variety of conditions. Most reactions were performed at 0.2 mM **Ru=O**$^{2+}$ with cumene concentrations varying from 0.08 to 0.5 M. Reaction solutions were made up in the dry box under N_2, transferred via syringe to sealable cuvettes fitted with Teflon Kontes valves and transported to the spectrophotometer. Kinetics were also measured with air-saturated solutions (see below). Due to the complex nature of the reaction, kinetics data were analyzed using SPECFIT, a global analysis software package.

Despite the various Ru complexes in this system, kinetic data can be fit with a biexponential model A $\rightarrow$ B, B $\rightarrow$ C. This model most accurately describes the initial

rise in absorbance around 380 nm followed by a subsequent decrease at this same wavelength. An overlay plot and calculated spectra returned by SPECFIT are given in Figure 3.3a and b. Calculated spectra agree well with the known spectra for these Ru complexes (Figure 3.4) and are consistent with the process $Ru{=}O^{2+} \rightarrow Ru^{III} \rightarrow Ru^{II}$.

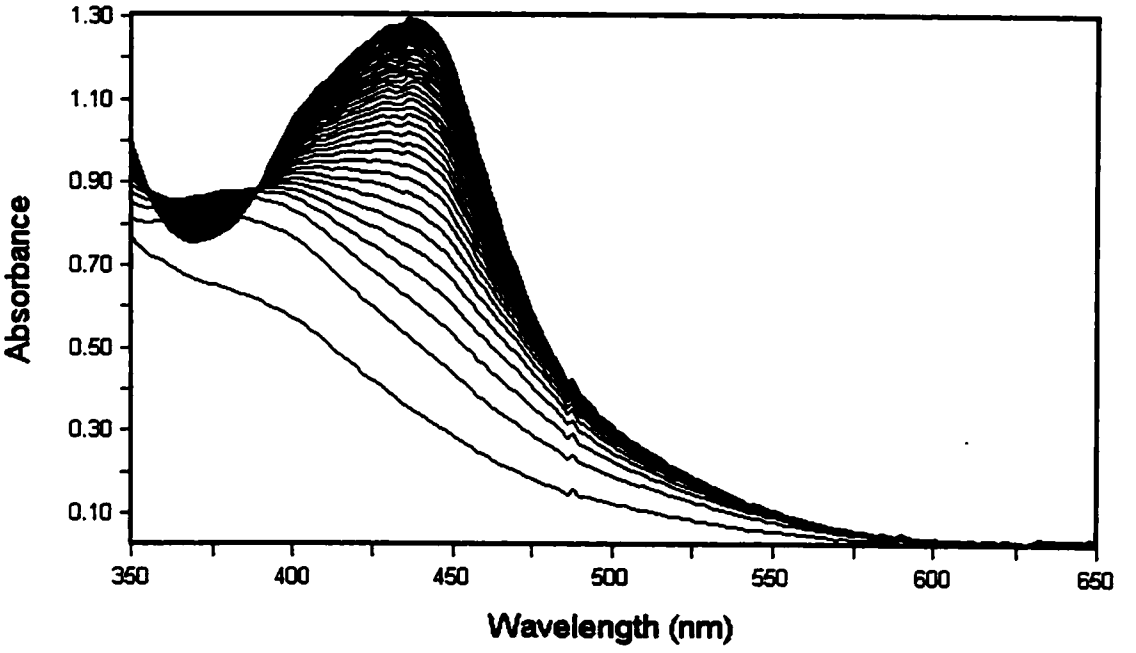

Figure 3.3a. Overlay plot for the reaction of 0.2 mM $Ru{=}O^{2+}$ with 80 mM cumene in acetonitrile. The reaction was monitored every 30 s for ~8200 s.

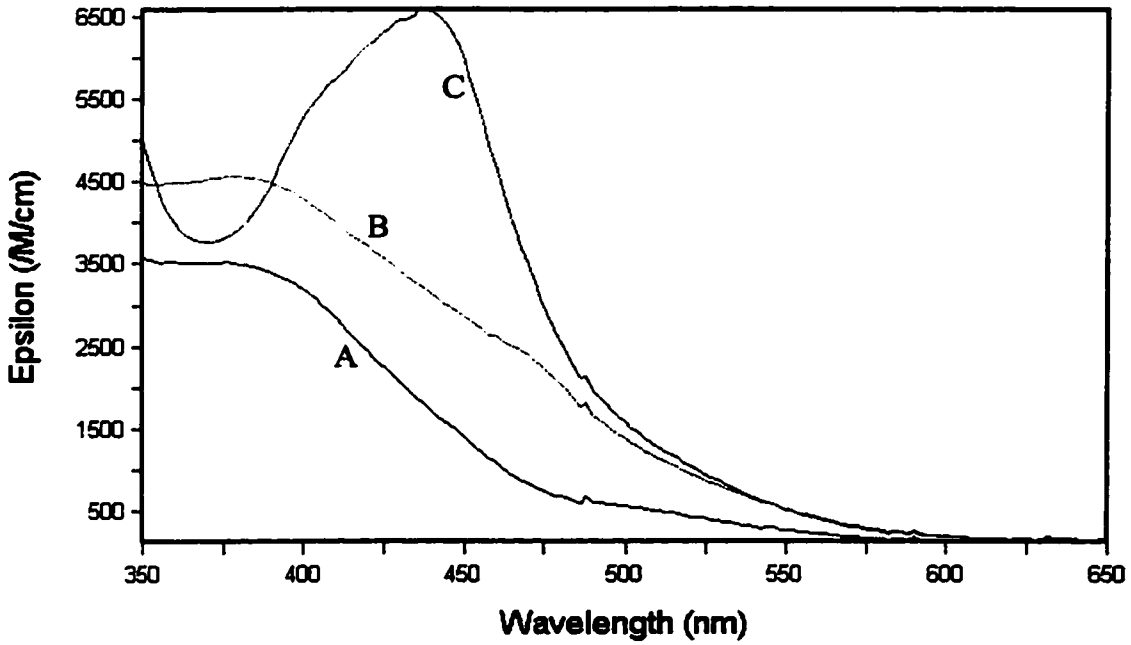

Figure 3.3b. Calculated spectra returned by SPECFIT for the reaction of 0.2 mM **Ru=O**$^{2+}$ with 80 mM cumene in acetonitrile.

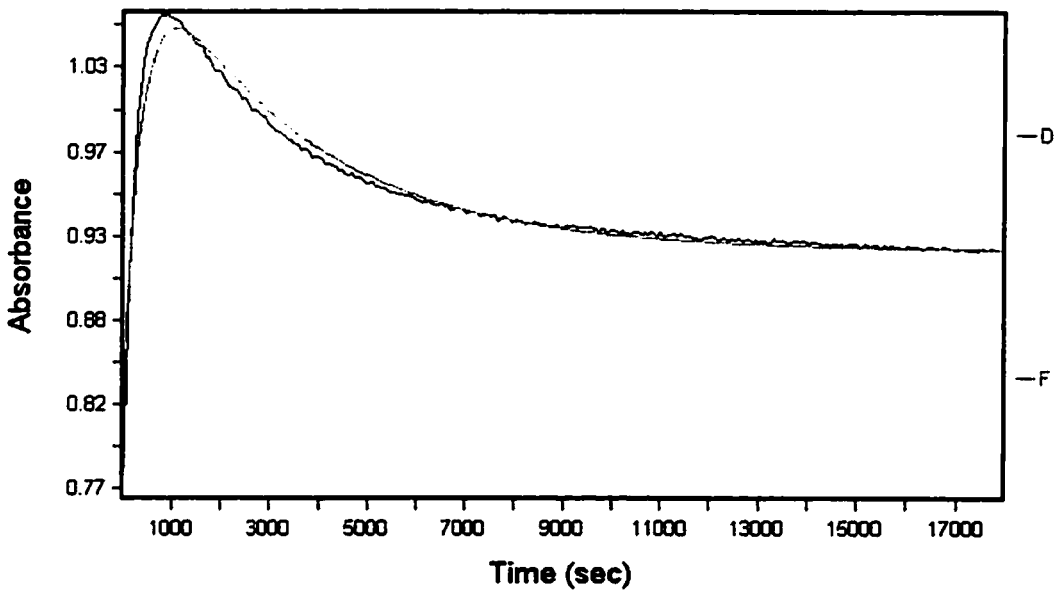

Figure 3.3c. Single wavelength trace at 370nm and SPECFIT fit for the reaction with cumene.

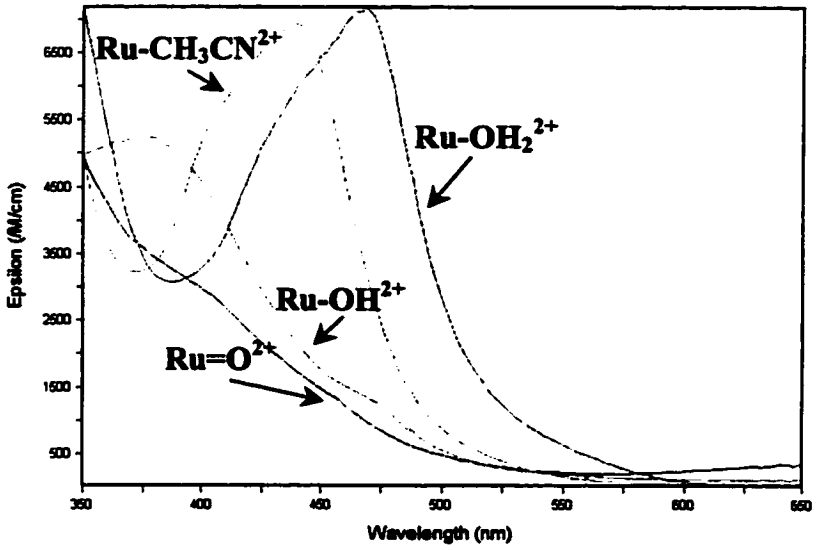

Figure 3.4. Observed spectra for **Ru=O**$^{2+}$, **Ru-OH**$^{2+}$, **Ru-OH$_2$**$^{2+}$, and **Ru-CH$_3$CN**$^{2+}$. **Ru-OH**$^{2+}$ is produced by mixing a 1:1 ratio of **Ru=O**$^{2+}$ with **Ru-OH$_2$**$^{2+}$. A small amount of **Ru-OH$_2$**$^{2+}$ is present in the spectrum.

The final Ru^{II} spectrum is consistent with **Ru-CH$_3$CN**$^{2+}$ as the predominant product. Over long time periods (several hours), the final product is solely **Ru-CH$_3$CN**$^{2+}$ due to acetonitrile solvolysis of **Ru-OH$_2$**$^{2+}$. A plot of k_{obs}(A→B) vs. cumene concentration yields a straight line indicating first order dependence of the rate on cumene concentration (Figure 3.5). The slope gives a second-order rate constant k'(A→B) = $(3.4 \pm 0.3) \times 10^{-2}$ M^{-1} s^{-1}. This is similar to the value previously reported by Meyer of $(2.6 \pm 0.3) \times 10^{-2}$ M^{-1} s^{-1}.[1] The k_{obs}(B→C) values do not correlate well with cumene

concentration and most likely represent multiple processes – reactions of the substrate with **Ru=O**$^{2+}$ and/or **Ru-OH**$^{2+}$ and solvolysis of products. The average value for k_{obs}(B→C) is 1.2×10^{-3} s^{-1}.

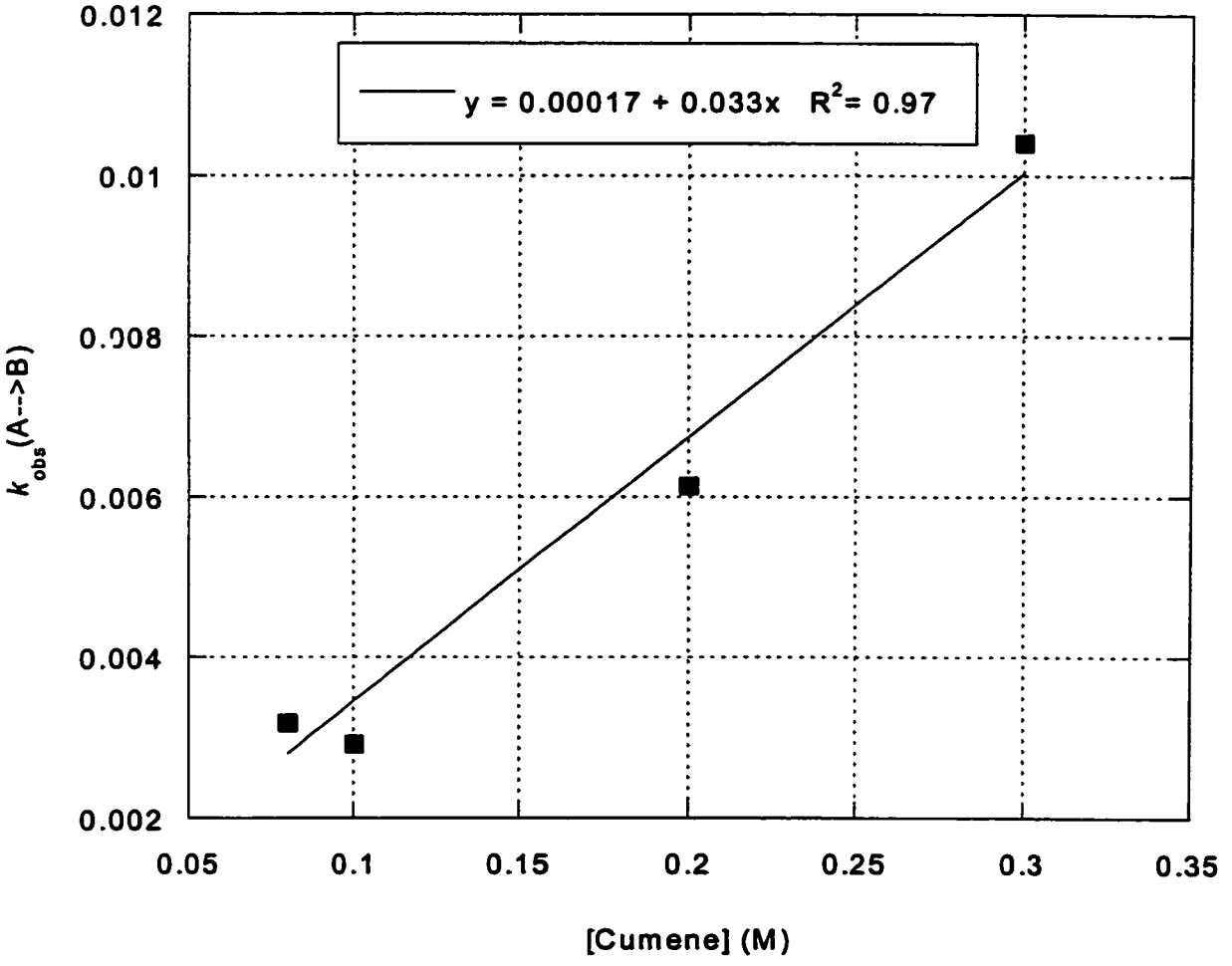

Figure 3.5. Graph of k_{obs} vs. cumene concentration for the kinetic step A→B.

The kinetics of the reaction of 0.2 mM **Ru=O**$^{2+}$ with cumene was also investigated in air-saturated solutions over a range of cumene concentrations (4 – 240

mM). The data were analyzed as described above to give a second-order rate constant of $k_{cumene,O2} = 0.479 \pm 0.011\ M^{-1}\ s^{-1}$. This is almost 15 times faster than the rate constant under nitrogen.

As described earlier (see Chapter 2), **Ru=O^{2+}** can accept a net hydrogen atom to give $[(bpy)_2(py)Ru^{III}\text{-}OH]^{2+}$ (**Ru-OH^{2+}**). **Ru-OH^{2+}** can accept a further hydrogen atom to give the aquo complex $[(bpy)_2(py)Ru^{II}\text{-}OH_2]^{2+}$ (**Ru-OH$_2^{2+}$**). **Ru=O^{2+}** and **Ru-OH^{2+}** undergo a rapid comproportionation reaction to give two equivalents of **Ru-OH^{2+}** species (eq 3.4).[6]

$$Ru{=}O^{2+} + Ru\text{-}OH_2^{2+} \rightleftharpoons 2Ru\text{-}OH^{2+} \qquad \begin{matrix} k_f = 4.07 \times 10^3\ M^{-1}\ s^{-1} \\ k_r = 80.6\ M^{-1}\ s^{-1} \end{matrix} \qquad (3.4)$$

This comproportionation reaction is likely a kinetically important source of **Ru-OH^{2+}**. On the time-scale of these reactions, it is difficult to differentiate the source of **Ru-OH^{2+}** – comproportionation or one-electron oxidation of the substrate. The aquo complex is also known to undergo solvolysis readily in acetonitrile to give $[(bpy)_2(py)Ru^{II}\text{-}CH_3CN]^{2+}$ (**Ru-CH$_3$CN^{2+}**) ($k_{solv} = 1.66 \times 10^{-3}\ s^{-1}$).[6]

The oxidation of α-methylstyrene has similar spectroscopic features to that of the oxidation of cumene. The kinetics data were analyzed in an identical manner to give second-order rate constants $k'_{MS}(A \rightarrow B) = (2.7 \pm 0.4) \times 10^{-2}\ M^{-1}\ s^{-1}$ and $k_{obs(MS)}(B \rightarrow C) = (3.0 \pm 0.3) \times 10^{-4}\ s^{-1}$.

Kinetics With Added Nucleophiles. In an attempt to reproduce the reported dependence of the reaction rates for the oxidation of cumene by **Ru=O^{2+}** in the presence of nucleophiles,[1] kinetic measurements were obtained in the presence of added LiBr,

tert-butanol, and H_2O. Reaction rates were measured in acetonitrile at room temperature as described above, except that stock solutions of the nucleophile in acetonitrile were used as the solvent. **Ru=O**$^{2+}$ concentration was kept constant at 0.2 mM and cumene concentration was typically 4 mM. Nucleophile concentrations were varied over the range of 1 mM to 1.6 M (except for reactions with LiBr, which were saturated at concentrations near 0.7 M). Similar experiments were conducted side by side using KPF_6 and 1,2-dichloroethane as non-nucleophilic analogs – these were done to test for variations in rates due to ionic strength and changes in solvent polarity. In all cases except for reactions with LiBr, no variations from the oxidation rate without added nucleophiles were observed. At high LiBr concentrations (0.6 M) a rapid disappearance of **Ru=O**$^{2+}$ was observed *even in the absence of added oxidizable substrate* (Figure 3.6). The final UV-vis spectrum of this reaction is consistent with $[(bpy)_2(py)RuBr]^+$ – confirmed by comparison with the UV-vis spectrum obtained from the addition of LiBr to **Ru-OH**$_2^{2+}$ in CH_3CN.

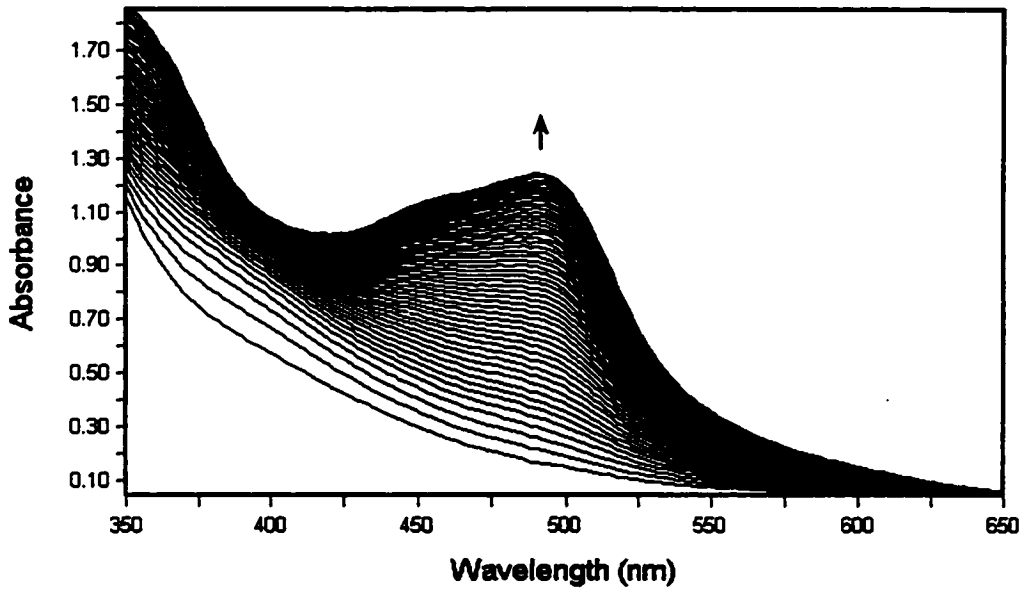

Figure 3.6. Overlay plot of 0.2 mM **Ru=O**$^{2+}$ with 0.6 M LiBr in acetonitrile. Kinetics measurements were recorded every 100s for 5000 s.

Discussion

In the study of the oxidation of cumene by **Ru=O**$^{2+}$ previously reported by Meyer and co-workers, a mechanism of hydride transfer was proposed. This mechanism was proposed primarily due to the linear dependence of oxidation rate constants on the concentration of added nucleophile (water, lithium bromide and *tert*-butanol). This mechanism would have been the first example of hydride transfer reported for the oxidation of a C-H bond by **Ru=O**$^{2+}$, possibly extending the range of mechanistic pathways available to this oxidant. Studies in our laboratory, with results later confirmed by the Meyer group, however, indicate that the dependence on

nucleophile concentration cannot be reproduced. Furthermore, the original study made no effort to identify products. In a nucleophilic substitution mechanism with lithium bromide or *t*-butanol added, one would expect substituted products – i.e., 2-bromo-2-phenyl propane or *tert*-butyl 2-(2-phenylpropyl) ether. None of these products were detected by GC/MS or ^{1}H NMR in the study reported here.

The products from the oxidation of cumene (α-methylstyrene, cumyl alcohol, and acetophenone) are a mixture of oxygenated and non-oxygenated compounds. $H_2{}^{18}O$ labeling studies indicate that the source of the oxygen is not water in the solvent, but from the oxidant. The change in product ratios in the presence of O_2 is indicative of radical intermediates. As discussed in the previous chapter, the only mechanism that adequately accounts for all the experimental evidence is one of initial hydrogen-atom abstraction followed by trapping of the radical by the oxidant to give the oxygenated product, cumyl alcohol, or further oxidation of the radical intermediate to give the olefin, α-methylstyrene (this product is also the result of dehydration of cumyl alcohol). The additional products observed are products of further oxidation of α-methylstyrene (Figure 3.7).

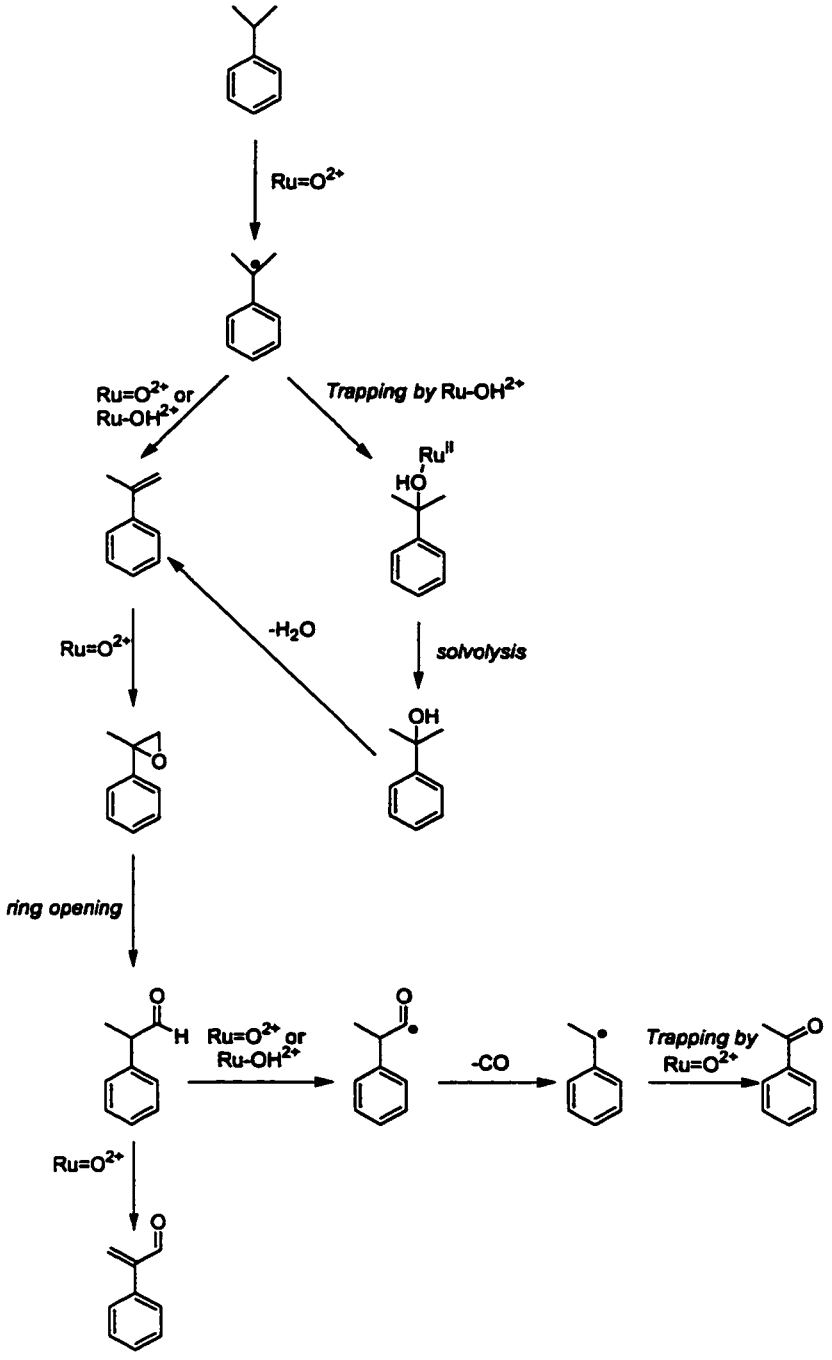

Figure 3.7. Proposed mechanism for the oxidation of cumene by $\mathbf{Ru{=}O^{2+}}$.

While the oxidation of α-methylstyrene is slow, SPECFIT simulations of the oxidation of cumene by **Ru=O**$^{2+}$ indicate that α-methylstyrene is a competent intermediate for the production of acetophenone (Figure 3.8). This is further supported by the quite rapid oxidation of 2-phenylpropionaldehyde to give acetophenone, 2-phenylpropenal, and trace amounts of benzyl-radical and -cation trapped products – acetamide and 2,3-diphenylbutane. This is further confirmed by the detection of trace amounts of 2-phenylpropionaldehyde at short reaction times in the oxidation of cumene. It is interesting that 2-phenylpropenal is not seen in greater yields, but this may be due to its further reactivity with **Ru=O**$^{2+}$ or **Ru-OH**$^{2+}$ (with the possible loss of CO_2 to eventually give more acetophenone). The reaction of **Ru=O**$^{2+}$ with 2-phenylpropenal was not performed due to lack of a readily available commercial source.

A SPECFIT model of the reaction of **Ru=O**$^{2+}$ with cumene is shown in Figure 3.8. Rate constants k_1, k_3 and k_6 correspond to the experimental values determined in the oxidation of cumene and α-methylstyrene ($k_1 \equiv k'(A \rightarrow B)$, $k_3 \equiv k'(B \rightarrow C)$, $k_6 \equiv k'_{MS}(A \rightarrow B)$). Rate constants involving radical trapping have been known to be between 10^6-10^9 M^{-1} s^{-1} and are simply assigned a value of 10^8 (k_2, k_4, k_9, k_{10}).[10] The rate constants for the acid-catalyzed dehydration of cumyl alcohol and epoxide ring-opening were chosen to give a reasonable correlation with observed product concentrations. The rate constant for the oxidation of 2-phenylpropionaldehyde (k_8) was also chosen to give good agreement with the experimental results based on the observation that this

oxidation is rapid. Initial concentrations were put into the model as 1 mM **Ru=O^{2+}** and 2 mM cumene.

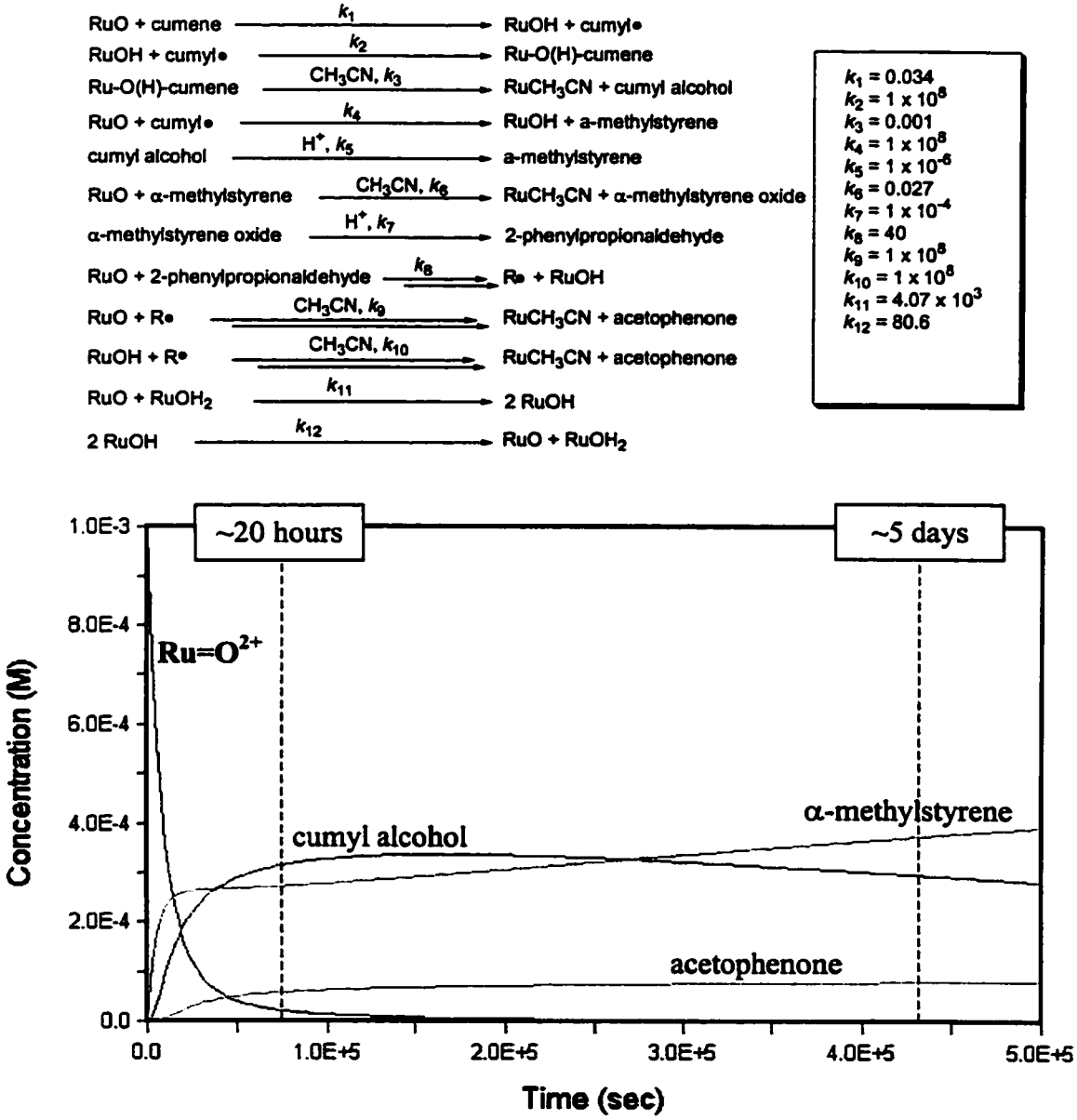

Figure 3.8. Mechanistic model for the oxidation of 2 mM cumene by 1 mM **Ru=O^{2+}** and calculated concentration profiles from the SPECFIT simulation of the model (rate constants are given in M^{-1} s^{-1}.

The model is consistent with the observed changes in product distribution even after all the oxidant has been consumed. The organic rearrangements of products subsequent to oxidant consumption lead to a complex reaction mixture over time.

The rate constant for the initial step in the oxidation of cumene $k'(A \rightarrow B) = (3.4 \pm 0.3) \times 10^{-2}\ M^{-1}\ s^{-1}$ (k_1 in the model above) is consistent with the relatively large bond dissociation energy (compared to the substrates studied in the previous chapter) of cumene (84.8 kcal/mol).[11] Adding cumene to the graph of oxidation rate vs. bond dissociation energy for reactions with $\mathbf{Ru{=}O^{2+}}$ gives a good correlation (Figure 3.9), consistent with initial hydrogen-atom abstraction.

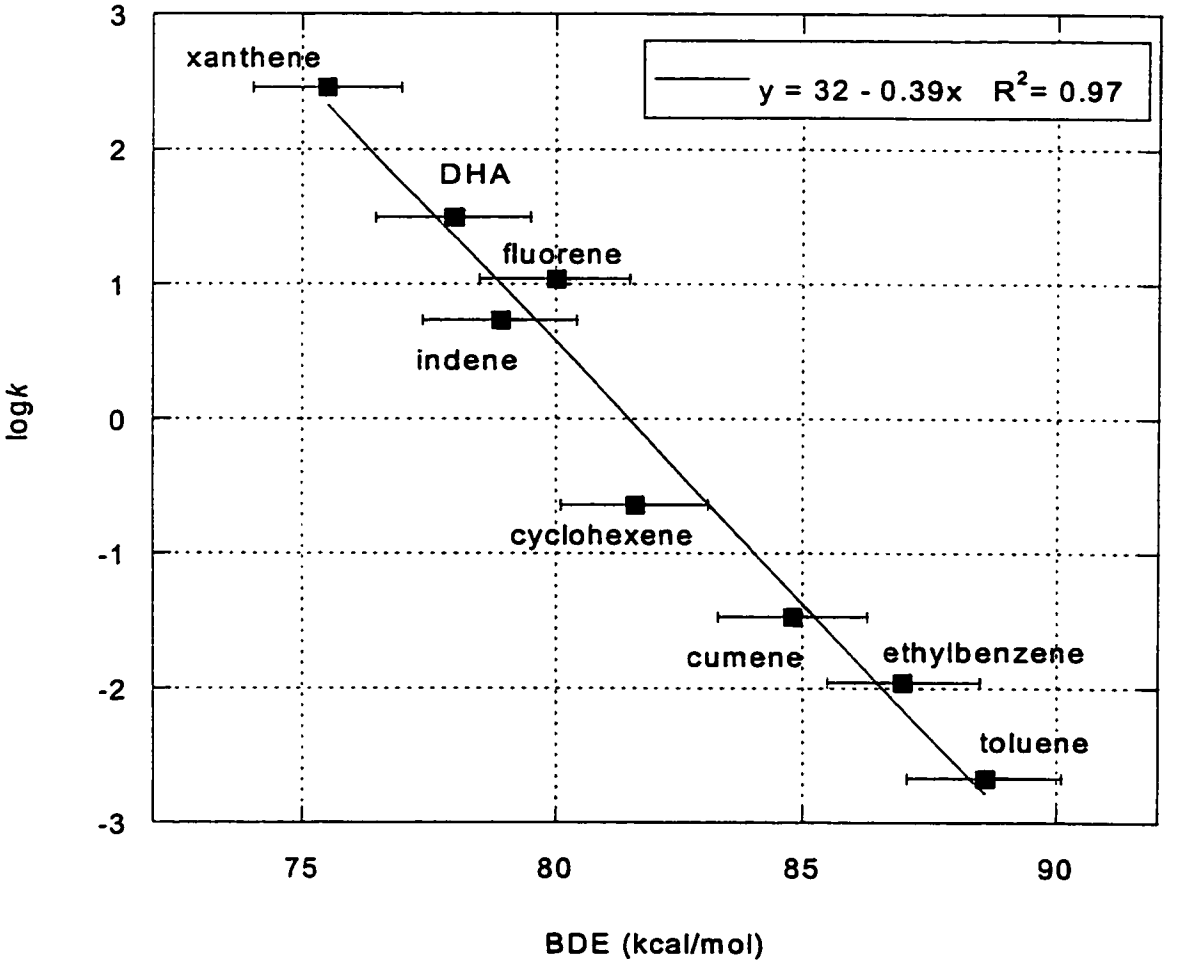

Figure 3.9. Graph of log *k* (per hydrogen atom) vs. substrate C-H bond dissociation energy for a variety of organic substrates studied.

Following initial hydrogen-atom abstraction from cumene by **Ru=O**$^{2+}$ to give the cumyl radical, the radical intermediate may go on to be oxidized further – giving α-methylstyrene, or it may be trapped by the oxidant (**Ru=O**$^{2+}$ or **Ru-OH**$^{2+}$) to give the alcohol product, cumyl alcohol. Further oxidation of cumyl alcohol is unlikely due to the lack of oxidizable hydrogens. It appears, however, that cumyl alcohol undergoes an

acid-catalyzed dehydration over time to give more α-methylstyrene. This is evidenced by the decrease in cumyl alcohol yields with concomitant increases in α-methylstyrene and acetophenone over time.

The oxidation of α-methylstyrene is the source of all remaining organic products observed. These products appear to form from initial epoxide formation upon oxidation of the olefin by $\mathbf{Ru{=}O^{2+}}$. This is followed by ring-opening to give readily oxidized aldehyde products. These eventually lead to the appearance of acetophenone through facile losses of CO and/or CO_2. Carbocation intermediates – most likely from trace acid in the solvent catalyzing the epoxide ring opening – are implicated by the appearance of trace amounts of *N*-(1-phenylethyl)acetamide, the acetonitrile-trapped benzyl cation product.[12] The mechanism of formation of these cations is unclear, but may result from trace acid in the reaction solutions – possibly from the slow decomposition of $\mathbf{Ru{=}O^{2+}}$ in CH_3CN.[6]

A mechanism of hydride transfer is not adequate to explain the evidence presented in this study. The more plausible explanation is a one-electron process to give an organic radical intermediate. This one-electron process is best explained by a mechanism of initial hydrogen-atom abstraction as it accounts for the organic products observed and is supported by the excellent correlation of oxidation rate with substrate C-H bond dissociation energy. It is possible that other C-H bond oxidations by $\mathbf{Ru{=}O^{2+}}$ may proceed by initial hydrogen-atom transfer rather than the proposed oxygen-atom insertion. For example, when the rate constants given for cyclohexene[13] and

ethylbenzene[5] were measured again under inert atmosphere (Chapter 2) and plotted versus their respective bond dissociation energies[11], a good correlation is observed (Figure 3.9). Furthermore, the proposed mechanism provides a plausible explanation for the observation of benzophenone and diphenylacetaldehyde in the oxidations of *cis*- and *trans*- stilbene via oxidation of the ring-opened products (eq 3.5).[9]

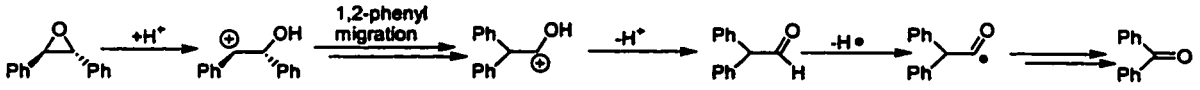

(3.5)

Experimental Section

General Considerations. All experiments were performed under an N_2 atmosphere using standard techniques unless otherwise noted. Solvents (including deuterated solvents from Cambridge Isotope) were degassed and dried according to standard procedures.[14] Acetonitrile (low-water brand) was purchased from Burdick and Jackson and dispensed from a keg plumbed directly into the dry box. Deuterated acetonitrile (CD_3CN) was stirred over CaH_2 for two days, vacuum transferred to P_2O_5 and stirred for four hours. It was then transferred back to CaH_2, stirred for 30 minutes, and transferred to a sealable flask prior to use. Cumene was purified via standard procedures.[14] Other reagents were purchased from Aldrich and used as received unless otherwise noted. $Ru(bpy)_2Cl_2$ and $[Ru(bpy)_2(py)Cl](PF_6)$ were synthesized according to literature methods.[15,16] $[Ru(bpy)_2(py)(OH_2)](PF_6)_2$ and $[Ru(bpy)_2(py)O](PF_6)_2$ were synthesized by modified literature procedures. The same procedure for the synthesis of $[Ru(bpy)_2(py)(OH_2)](ClO_4)_2$ was followed,[17] except that a saturated solution of KPF_6 in

water was used to precipitate the product. A procedure similar to the literature synthesis of $[Ru(bpy)_2(py)^{18}O](ClO_4)_2$ was used[18] to produce $[Ru(bpy)_2(py)O](PF_6)_2$. Liquid Br_2 was added in a very small amount to the dissolved **Ru-OH$_2^{2+}$** and the resulting solution was purged with N_2 for several minutes. The solution was cooled and 1-2 mL of saturated KPF_6 in water was added to precipitate the product. **Ru=O^{2+}**, **Ru-OH^{2+}**, **Ru-OH$_2^{2+}$**, and **Ru-CH$_3$CN^{2+}** were characterized by NMR and UV-vis spectroscopies.[16,17]

NMR spectra were recorded on Bruker AC-200, AF-300, and DRX-500 spectrometers at ambient temperatures and are reported in ppm relative to TMS (^{1}H). UV-vis spectra were recorded on a Hewlett Packard 8453 diode array spectrophotometer and are reported as λ_{max} (nm), (ε, M^{-1} cm^{-1}). GC/MS spectra were obtained on a Hewlett Packard 5971 instrument equipped with a non-polar capillary column and a mass spectral analyzer. GC/FID data were collected on a Hewlett Packard 5890 Series II equipped with an HP DB1 (methyl silicone, 5m × 0.53mm × 0.25μm). Yields of organic products were quantified using response factors and confirmed by the addition of authentic samples.

Typical Procedure for Organic Oxidations. A solution of **cumene** (1.7 μL, 12 μmol) and **Ru=O^{2+}** (6 μmol) in 6 mL acetonitrile turned orange in several hours. Cumyl alcohol, acetophenone, and α-methylstyrene were observed by GC/MS and confirmed by the addition of authentic samples. Products were quantified by GC/FID response factors. Reactions with α-methylstyrene, cumyl alcohol, 2-phenylpropionaldehyde, and *meso*-2,3-diphenylbutane were carried out under similar conditions. Oxidations were also monitored by ^{1}H NMR. Solutions were made up with hexamethyldisiloxane as an internal standard.

^{18}O-labeling studies were conducted under the same conditions as above, but with 10 mM and 200 mM added $H_2{}^{18}O$. The amount of ^{18}O incorporation was measured by comparing the M^+ : $(M+2)^+$ peak intensity ratios for products formed in the presence of $H_2{}^{18}O$ to those formed in the absence of $H_2{}^{18}O$.

Kinetic Studies. Kinetic data were typically gathered over several hours every 30-180s. Solutions were made up in an N_2-filled dry box immediately prior to use in sealable cuvettes with Teflon Kontes valves. Kinetic data were analyzed using the global analysis software package SPECFIT (Spectrum Software Associates, Marlborough, MA). In reactions with added nucleophiles (*t*-butanol, water, and LiBr), kinetics data were acquired simultaneously with control reactions containing no added nucleophile.

Notes to Chapter 3

(1) Thompson, M. S.; Meyer, T. J. *J. Am. Chem. Soc.* **1982**, *104*, 5070-5076.

(2) Gardner, K. A.; Mayer, J. M. *Science* **1995**, *269*, 1849-1851.

(3) March, J. *Advanced Organic Chemistry*, 4th ed.; Wiley-Interscience: New York, 1992, pp. 340-341.

(4) March, J. *Advanced Organic Chemistry*, 4th ed.; Wiley-Interscience: New York, 1992, pp. 350-351.

(5) Curry, M.; Huynh, M. H. V.; Stultz, L. K.; Binstead, R. A.; Meyer, T. J.; Bryant, J. R.; Mayer, J. M. *manuscript in preparation.*

(6) Binstead, R. A.; Stultz, L. K.; Meyer, T. J. *Inorg. Chem.* **1995**, *34*, 546-551.

(7) Gilbert, J.; Roecker, L.; Meyer, T. J. *Inorg. Chem.* **1987**, *26*, 1126-1132.

(8) Doppelt, P.; Meyer, T. J. *Inorg. Chem.* **1987**, *26*, 2027-2034.

(9) Stultz, L. K.; Binstead, R. A.; Reynolds, M. S.; Meyer, T. J. *J. Am. Chem. Soc.* **1995**, *117*, 2520-2532.

(10) Arends, I. W. C. E.; Mulder, P.; Clark, K. B.; Wayner, D. D. *J. Phys. Chem.*. **1995**, *99*, 8182-8189.

(11) Denisov, E. T.; Denisova, T. G. *Handbook of Antioxidants*, 2nd Ed., CRC Press: Boca Raton, 2000, pp. 21-36.

(12) Ritter, J. J.; Minieri, P. P. *J. Am. Chem. Soc.* **1948**, *70*, 4045-4058.

(13) Stultz, L. K.; Huynh, M. H. V.; Binstead, R. A.; Curry, M.; Meyer, T. J. *J. Am. Chem. Soc.* **2000**, *122*, 5984-5996.

(14) Perrin, D. D.; Armarego, W. L. F. *Purification of Laboratory Chemicals*, 3rd Ed., Pergamon Press: New York, 1988.

(15) Sullivan, B. P.; Salmon, D. J.; Meyer, T. J. *Inorg.Chem.* **1978**, *17*, 3334-3341.

(16) Moyer, B. A.; Meyer, T. J. *Inorg. Chem.* **1981**, *20*, 436-444.

(17) Dobson, J. C.; Helms, J. H.; Doppelt, P.; Sullivan, B. P.; Hatfield, W. E.; Meyer, T. J. *Inorg. Chem.* **1989**, *28*, 2200-2204.

(18) Thompson, M. S.; Meyer, T. J. *J. Am. Chem. Soc.* **1982**, *104*, 4106-4115.

Bibliography

(1) Andrulis, P. J.. Jr.; Dewar, M. J. S.; Dietz, R.; Hunt, R. L. *J. Am. Chem. Soc.* **1966**, *88*, 5473-5478.

(2) Arends, I. W. C. E.; Mulder, P.; Clark, K. B.; Wayner, D. D. M. *J. Phys. Chem.* **1995**, *99*, 8182-8189.

(3) Arndt, D. *Manganese Compounds as Oxidizing Agents in Organic Chemistry* Open Court: La Salle, 1981.

(4) Baciocchi, E.; Bietti, M.; Lanzalunga, O. *Acc. Chem. Res.* **2000**, *33*, 243-251.

(5) Baciocchi, E.; Bietti, M.; Putignani, L.; Steenken, S. *J. Am. Chem. Soc.* **1996**, *118*, 5952-5960.

(6) Bailey, R. J.; Card, P. J.; Schechter, H. *J. Am. Chem. Soc.* **1983**, *105*, 6096-6103.

(7) Banci, L.; Ciofi-Baffoni, S.; Tien, M. *Biochemistry* **1999**, *38*, 3205-3210.

(8) Barckholtz, C.; Barckholtz, T. A.; Hadad, C. M. *J. Am. Chem. Soc.* **1999**, *121*, 491-500.

(9) Bell, F. A.; Ledwith, A.; Sherrington, D. C. *J. Chem. Soc. (C)* **1969**, *19*, 2719-2720.

(10) Berkowitz, J.; Ellison, G. B.; Gutman, D. *J. Phys. Chem.* **1994**, *98*, 2744-2765.

(11) Bierbaum, V.; DePuy, C.; Davico, G.; Ellison, B. *Int. J. Mass Spectrom. Ion Phys.* **1996**, *156*, 109-131.

(12) Binstead, R. A.; McGuire, M. E.; Dovletoglou, A.; Seok, W. K.; Roecker, L. E.; Meyer, T. J. *J. Am. Chem. Soc.* **1992**, *114*, 173-186.

(13) Binstead, R. A.; Meyer, T. J. *J. Am. Chem. Soc.* **1987**, *109*, 3287-3297.

(14) Binstead, R. A.; Stultz, L. K.; Meyer, T. J. *Inorg. Chem.* **1995**, *34*, 546-551.

(15) Bordwell, F. G. *Acc. Chem. Res.* **1988**, *21*, 456-463.

(16) Bordwell, F. G.; Cheng, J. P.; Ji, G.; Satish, A. V.; Zhang, X. *J. Am. Chem. Soc.* **1991**, *113*, 9790-9795.

(17) Bordwell, F. G.; Cheng, J.-P.; Harrelson, J. A., Jr. *J. Am. Chem. Soc.* **1988**, *110*, 1229-1231.

(18) Bouwman, E.; Caulton, K. G.; Christou, G.; Folting, K.; Gasser, C.; Hendrickson, D. N.; Huffman, J. C.; Lobkovsky, E. B.; Martin, J. D.; Michel, P.; Tsai, H.; Xue, Z. *Inorg. Chem.* **1993**, *32*, 3463-3470.

(19) Bryant, J. R.; Taves, J. E; Mayer, J. M. *Inorg. Chem.* **2002**, *41*, 2769-2776.

(20) Burkey, T. J.; Majewski, M.; Griller, D. *J. Am. Chem. Soc.* **1986**, *108*, 2218-2221.

(21) Cheng, J. -P.; Handoo, K. L.; Parker, V. D. *J. Am. Chem. Soc.* **1993**,*115*, 2655-2660.

(22) Chiswell, B.; McKensie, E. D.; Lindoy, L. F. in *Comprehensive Coordination Chemistry*; Wilkinson, G.; Gillard, R. D.; McCleverty, J. A., Eds.; Pergamon Press: Oxford, 1987: Vol. 1.

(23) Citterio, A.; Santi, R.; Fiorani, T.; Strologo, S. *J. Org. Chem.* **1989**, *54*, 2703-2712.

(24) Coellen, M.; Rüchardt, C. *Chem. Eur. J.* **1995**, *1*, 564-567.

(25) Connelly, N. G.; Geiger, W. E. *Chem. Rev.* **1996**, *96*, 877-910.

(26) Cotton, F. A.; Wilkinson, G.; Murillo, C. A.; Bochmann, M. *Advanced Inorganic Chemistry*, 6th ed.; Wiley: New York, 1999.

(27) Cox, J. D.; Pilcher, G. *Thermochemistry of Organic and Organometallic Compounds*; Academic Press: New York, 1970.

(28) Darbeau, R. W.; White, E. H.; Song, F.; Darbeau, N. R.; Chou J. *J. Org. Chem.* **1999**, *64*, 5966-5978.

(29) De Klein, W. J. *Organic Syntheses By Oxidation With Metal Compounds* Mijs, W. J.; de Jonge, C. R. H. I., Eds., Plenum Press: New York, 1986.

(30) Denisov, E. T.; Denisova, T. G. *Handbook of Antioxidants*, 2nd Ed., CRC Press: Boca Raton, 2000.

(31) Dickman, M. H. *Acta Cryst.* **1997**, *C53*, 402-404.

(32) Dobson, J. C.; Helms, J. H.; Doppelt, P.; Sullivan, B. P.; Hatfield, W. E.; Meyer, T. J. *Inorg. Chem.* **1989**, *28*, 2200-2204.

(33) Donnelly, K. D.; Fristad, W. E.; Gellerman, B. J.; Peterson, J. R.; Selle, B. J. *Tetrahedron Lett.* **1984**, *25*, 607-610.

(34) Doppelt, P.; Meyer, T. J. *Inorg. Chem.* **1987**, *26*, 2027-2034.

(35) Eberson, L. *Electron Transfer Reactions in Organic Chemistry*; Springer-Verlag: Berlin, 1987.

(36) Eberson, L. *J. Am. Chem. Soc.* **1983**, *105*, 3192-3199.

(37) Espenson, J. H. *Chemical Kinetics and Reaction Mechanisms*, 2nd ed.; McGraw-Hill: New York, 1995.

(38) Evans, S.; Hamnett, A.; Orchard, A. F.; Lloyd, D. R. *Faraday Discuss. Chem. Soc.* **1972**, *54*, 227-250.

(39) Fox, T.; Kollman, P. A. *J. Phys. Chem.* **1996**, *100*, 2950-2956.

(40) Fristad, W. E.; Peterson, J. R.; Ernst, A. B.; Urbi, G. B. *Tetrahedron*, **1986**, *42*, 3429-3442.

(41) Gardner, K. A.; Kuehnert, L. L.; Mayer, J. M.; *Inorg. Chem.* **1997**, *36*, 2069-2078.

(42) Gardner, K. A.; Mayer, J. M. *Science* **1995**, *269*, 1849-1851.

(43) Geiger, W. E. in *Organometallic Radical Processes*; Trogler, W. C., Ed.; Elsevier Science Pub.: Amsterdam, 1990.

(44) Gilbert, J. A.; Gersten, S. W.; Meyer, T. J. *J. Am. Chem. Soc.* **1982**, *104*, 6872-6873.

(45) Gilbert, J.; Roecker, L.; Meyer, T. J. *Inorg. Chem.* **1987**, *26*, 1126-1132.

(46) Handoo, K. L.; Cheng, J. -P.; Parker, V. D. *J. Am. Chem. Soc.* **1993**,*115*, 5067-5072.

(47) Heiba, E. I.; Dessau, R. M.; Koehl, W. J., Jr. *J. Am. Chem. Soc.* **1969**, *91*, 138-145.

(48) Howard, J. A.; Chenier, J. H. B. *J. Am. Chem. Soc.* **1973**, *95*, 3054-3055.

(49) http://webbook.nist.gov/chemistry.

(50) Izutsu, K. *Acid-Base Dissociation Constants in Dipolar Aprotic Solvents*, Blackwell Scientific Publications: Oxford, 1990, 21, 28.

(51) Jiao, X. D.; Metelski, P. D.; Espenson, J. H. *Inorg. Chem.* **2001**, *40*, 3228-3233.

(52) Joshi, D. K.; Gold, M. H. *Biochemistry* **1994**, *33*, 10969-10976.

(53) King, B. T.; Noll, B. C.; McKinley, A. J.; Michl, J. *J. Am. Chem. Soc.* **1996**, *118*, 10902-10903.

(54) King, S. T. *J. Catal.* **1991**, *131*, 215-225.

(55) Kishi, K.; Wariishi, H.; Marquez, L.; Dunford, H. B.; Gold, M. H. *Biochemistry* **1994**, *33*, 8694-8701.

(56) Kochi, J. K. in *Comprehensive Organic Synthesis*; Trost, B. M., Fleming, I., Eds. Pergamon: New York, 1991, Vol. 7.

(57) Laarhoven, L. J.; Mulder, P.; Wayner, D. D. M. *Acc. Chem. Res.* **1999**, *32*, 342-349.

(58) Larsen, A. S.; Wang, K.; Lockwood, M. A.; Rice, G. L.; Won, T.-J.; Lovell, S.; Sadilek, M.; Turecek, F.; Mayer, J. M *J. Am. Chem. Soc.* **2002**, *124*, 10112-10123.

(59) Lebeau, E. L.; Binstead, R. A.; Meyer, T. J. *J. Am. Chem. Soc.*, **2001**, *123*, 10535-10544.

(60) Lockwood, M. A.; Blubaugh, T. J.; Collier, A. M.; Lovell, S.; Mayer, J. M. *Angew. Chem. Int. Ed.* **1999**, *38*, 225-227.

(61) Lockwood, M. A; Wang, K.; Mayer, J. M. *J. Am. Chem. Soc.* **1999**, *121*, 11894-11895.

(62) Lowry, T. H.; Richardson, K. S. *Mechanism and Theory in Organic Chemistry*, 3rd ed.; HarperCollins: New York, 1987.

(63) March, J. *Advanced Organic Chemistry*, 4th ed.; Wiley-Interscience: New York, 1992.

(64) Marcus, R. A.; Sutin, N. *Biochim. Biophys. Acta* **1985**, *811*, 265-322.

(65) Mayer, J. M. *Acc. Chem. Res.* **1998**, *31*, 441-450.

(66) Mayer, J. M. Chapter 1 in *Biomimetic Oxidations Catalyzed by Transition Metal Complexes*, B. Meunier, Ed., Imperial College Press: London, 2000.

(67) Mayo, D. W.; Pike, R. M.; Butcher, S. S. *Microscale Organic Laboratory*, Wiley: New York, 2nd ed.

(68) McKillop, A.; Turrell, A. G.; Young, D. W.; Taylor, E. C. *J. Am. Chem. Soc.* **1980**, *102*, 6504-6512.

(69) Moyer, B. A.; Meyer, T. J. *Inorg. Chem.* **1981**, *20*, 436-444.

(70) Moyer, B. A.; Meyer, T. J. *J. Am. Chem. Soc.* **1978**, *100*, 3601-3603.

(71) Moyer, B. A.; Sipe, K.; Meyer, T. J. *Inorg. Chem.* **1981**, *20*, 1475-1480.

(72) Necsoiu, I.; Ghenciulescu, A.; Rentea, M.; Rentea, C. N.; Nenitzescu, C. D. *Rev. Roum. Chim.* **1967**, *12*, 1503-1510.

(73) Nelsen, S. F.; Ismagilov, R. F.; Chem, L.-J.; Brandt, J. L.; Chen, X.; Pladziewicz, J. R. *J. Am. Chem. Soc.* **1996**, *118*, 1555-1556.

(74) Nishino, H. *Bull. Chem. Soc. Jpn.* **1986**, *59*, 1733-1739.

(75) Olah, G. A.; Molnár, Á. *Hydrocarbon Chemistry* Wiley: New York, 1995.

(76) Parker, V. D. *J. Am. Chem. Soc.* **1992**, *114*, 7458-7462.

(77) Parker, V. D. *J. Am. Chem. Soc.* **1993**, *115*, 1201.

(78) Partenheimer, W. *Catal. Today* **1995**, *23*, 69.

(79) Perrin, D. D.; Armarego, W. L. F. *Purification of Laboratory Chemicals 3rd Ed.*, Pergamon Press: New York, 1988.

(80) Pratt, D. A.; Wright, J. S.; Ingold, K. U. *J. Am. Chem. Soc.* **1999**, *20*, 4877-4882.

(81) Reddy, G. V. B.; Gelpke, M. D. S.; Gold, M. H. *J. Bacteriol.* **1998**, *180*, 5159-5164.

(82) Reichert, C.; Bancroft, G. M.; Westmore, J. B. *Can. Jour. Chem.* **1970**, *48*, 1362-1370.

(83) Ritter, J. J.; Minieri, P. P. *J. Am. Chem. Soc.* **1948**, *70*, 4045-4058.

(84) Roecker, L.; Dobson, J. C.; Vining, W. J.; Meyer, T. J. *Inorg. Chem.* **1987**, *26*, 779-781.

(85) Roecker, L.; Meyer, T. J. *J. Am. Chem. Soc.* **1987**, *109*, 746-754.

(86) Roth, J. P.; Lovell, S.; Mayer, J. M. *J. Am. Chem. Soc.* **2000**, *122*, 5486-5498.

(87) Roth, J. P.; Mayer, J. M.; *Inorg. Chem.* **1999**, *38*, 2760-2761.

(88) Roth, J. P.; Yoder, J. C.; Won, T.-J.; Mayer, J. M. *Science* **2001**, *294*, 2524-2526.

(89) Salah, N. B.; Mhalla, F. M. *J. Electroanal. Chem.* **2000**, *485*, 42-48.

(90) Sandström, J. *Dynamic NMR Spectroscopy*; Academic Press: New York, 1982.

(91) Schlesener, C. J.; Kochi, J. K. *J. Org. Chem.* **1984**, *49*, 3142-3150.

(92) Schmidt, W.; Steckhan, E. *Chem. Ber.* **1980**, *113*, 577-585.

(93) Schwink, L.; Knochel, P. *Chem. Eur. J.* **1998**, *4*, 950-968.

(94) Seok, W. K.; Dobson, J. C.; Meyer, T. J. *Inorg. Chem.* **1988**, *27*, 3-5.

(95) Sharpe, P.; Eyler, J. R.; Richardson, D. E. *Inorg. Chem.* **1990**, *29*, 2779-2787.

(96) Snider, B. B. *Chem. Rev.* **1996**, *96*, 339-363.

(97) Sorokin, A.; Robert, A.; Meunier B. *J. Am. Chem. Soc.* **1993**, *115*, 7293-7299.

(98) Stultz, L. K.; Binstead, R. A.; Reynolds, M. S.; Meyer, T. J. *J. Am. Chem. Soc.* **1995**, *117*, 2520-2532.

(99) Stultz, L. K.; Huynh, M. H. V.; Binstead, R. A.; Curry, M; Meyer, T. J. *J. Am. Chem. Soc.* **2000**, *122*, 5984-5996.

(100) Sullivan, B. P.; Salmon, D. J.; Meyer, T. J. *Inorg. Chem.* **1978**, *17*, 3334-3341.

(101) Thompson, M. S.; Meyer, T. J. *J. Am. Chem. Soc.* **1982**, *104*, 4106-4115.

(102) Thompson, M. S.; Meyer, T. J. *J. Am. Chem. Soc.* **1982**, *104*, 5070-5076.

(103) Uemura, S.; Ikeda, T.; Tanaka, S.; Okano, M. *J. Chem. Soc. Perkin Trans. 1*, **1979**, 2574-2576.

(104) Uemura, S.; Tanaka, S.; Okano, M. *J. Chem. Soc. Perkin Trans. 1* **1976**, 1966-1969.

(105) Valli, K.; Gold, M. H. *J. Bacteriol.* **1991**, *173*, 345-352.

(106) van der Ploeg, R. E.; de Korte, R. W.; Kooyman, E. C. *J. Catal.* **1968**, *10*, 52-59.

(107) Wang, K.; Mayer, J. M. *J. Am. Chem. Soc.* **1997**, *119*, 1470-1471.

(108) Wariishi, H.; Akileswaran, L.; Gold, M. H. *Biochemistry* **1988**, *27*, 5365-5370.

(109) Wariishi, H.; Valli, K.; Gold, M. H. *Biochemistry* **1989**, *28*, 6017-6023.

(110) Wayner, D. D. M.; Parker, V. D. *Acc. Chem. Res.* **1993**, *26*, 287-294.

(111) Yamaguchi, K.; Sawyer, D. T. *Inorg. Chem.* **1985**, *24*, 971-976.

(112) Yonemura, H.; Nishino, H.; Kurosawa, K. *Bull. Chem. Soc. Jpn.* **1986**, *59*, 3153-3159.

(113) Zhang, X.-M.; Bordwell, F. G.; *J. Am. Chem. Soc.* **1992**, *114*, 7458-7462.

Appendix A – GC/FID Response Factors

Compound	Response Factor vs. 2 mM Naphthalene	Error
DHA	860	± 40.8
Anthracene	575	± 54.4
Anthraquinone	565	± 68.11
Xanthene	585	± 21.7
Xanthone	701	± 45.4
Bixanthene	1255	± 107
Fluorene	621	± 22.9
Fluorenone	806	± 42.1
Bifluorene	1332	± 107
Cumyl Alcohol	510	± 10.3
Acetophenone	373	± 1.5
α-Methylstyrene	452	± 4.8
2-Phenylpropionaldehyde	247	± 38.9

Concentrations are found by multiplying the ratio of compound to naphthalene by the response factor.

Vita

Jasmine Bryant was born in Los Angeles, California and graduated from North Hollywood High School. She went on to earn her Bachelor of Science degree in chemistry from the California Institute of Technology in Pasadena, CA. She performed undergraduate research there with Prof. Andrew Myers and Prof. Jacqueline Barton before graduating in 1995. After moving to Seattle, she earned her Masters in Teaching from Seattle University and spent a year teaching science at Kamiakin Junior High School. In 1998, she enrolled at the University of Washington and joined Prof. James Mayer's group. She earned a Doctor of Philosophy in Inorganic Chemistry in December, 2002.